AD

USAAVLABS TECHNICAL REPORT 70-58

WIND-TUNNEL INVESTIGATION OF A QUARTER-SCALE TWO-BLADED HIGH-PERFORMANCE ROTOR IN A FREON ATMOSPHERE

By

Charles Lee
Bruce Charles
David Kidd

February 1971

EUSTIS DIRECTORATE
U. S. ARMY AIR MOBILITY RESEARCH AND DEVELOPMENT LABORATORY
FORT EUSTIS, VIRGINIA

CONTRACT DA 44-177-AMC-292(T)
BELL HELICOPTER COMPANY
FORT WORTH, TEXAS

DISCLAIMERS

The findings in this report are not to be construed as an official Department of the Army position unless so designated by other authorized documents.

When Government drawings, specifications, or other data are used for any purpose other than in connection with a definitely related Government procurement operation, the United States Government thereby incurs no responsibility nor any obligation whatsoever; and the fact that the Government may have formulated, furnished, or in any way supplied the said drawings, specifications, or other data is not to be regarded by implication or otherwise as in any manner licensing the holder or any other person or corporation, or conveying any rights or permission, to manufacture, use, or sell any patented invention that may in any way be related thereto.

DISPOSITION INSTRUCTIONS

Destroy this report when no longer needed. Do not return it to the originator.

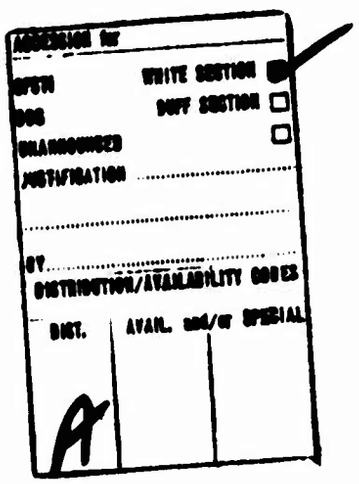

DEPARTMENT OF THE ARMY
U. S. ARMY AIR MOBILITY RESEARCH & DEVELOPMENT LABORATORY
EUSTIS DIRECTORATE
FORT EUSTIS, VIRGINIA 23604

This report has been reviewed by the Eustis Directorate, U. S. Army Air Mobility Research and Development Laboratory and is considered to be technically sound. It is published to disseminate information that will provide a stimulant for technical exchange.

Task 1F162204A13903
Contract DA 44-177-AMC-292(T)
USAAVLABS Technical Report 70-58
February 1971

WIND-TUNNEL INVESTIGATION OF A QUARTER-SCALE TWO-BLADED HIGH-PERFORMANCE ROTOR IN A FREON ATMOSPHERE

Bell Helicopter Report 575-099-004

By

Charles Lee
Bruce Charles
David Kidd

Prepared by

Bell Helicopter Company
Fort Worth, Texas

for

EUSTIS DIRECTORATE
U. S. ARMY
AIR MOBILITY RESEARCH AND DEVELOPMENT LABORATORY
FORT EUSTIS, VIRGINIA

SUMMARY

This report presents the results of a wind-tunnel investigation of a one-quarter-scale two-bladed teetering rotor system tested in a Freon atmosphere. The objectives of the tests were to determine the rotor aerodynamic characteristics at combinations of high advance ratio and high advancing-tip Mach number, to establish the feasibility of obtaining aerodynamic and rotor structural loads from a scaled model operating in a Freon atmosphere, and to compare model and full-scale data.

Two 11-foot-diameter rotors were tested: one having -10-degree twist and a constant thickness and planform, and the other having 0-degree twist, constant planform, and a thickness taper in the outboard 20 percent of span. Rotor aerodynamic data and blade structural loads data were obtained for both rotors. Scaling parameters were established by maintaining the model rotor advance ratio and advancing-tip Mach number numerically equal to an equivalent full-scale rotor. Rotor dynamics were preserved in the model on a "per-rev" basis by maintaining the full-scale ratio of the blade natural frequency divided by the rotor rotational frequency. Data were obtained at advance ratios from 0.30 to 0.72 in combination with advancing-tip Mach numbers varying from 0.70 to 0.96.

In general, the aerodynamic test data followed predicted trends and correlated well with full-scale tunnel data in the areas of low blade loading at low advance ratios and advancing-tip Mach numbers. The blade loads data followed the expected trends, but their magnitude could not be readily compared to existing flight test data due to the differences between the flight test conditions, model test conditions attained, and hub impedance differences.

FOREWORD

This program was sponsored by the Eustis Directorate, U. S. Army Air Mobility Research and Development Laboratory under Contract DA 44-177-AMC-292(T), Task 1F162204A13903. The work was performed under the technical cognizance of Patrick Cancro, U. S. Army Project Engineer. The program at Bell Helicopter Company was under the technical direction of Charles D. Lee, Project Engineer.

The assistance, cooperation, and active participation of Robert Huston, Charles Morris, and Matthew Winston of the NASA-Langley Research Center, in organizing and conducting the tests, are gratefully acknowledged. Appreciation is expressed to the personnel of the NASA-Langley Transonic Dynamics Tunnel for their support throughout this program.

TABLE OF CONTENTS

LIST OF ILLUSTRATIONS

LIST OF ILLUSTRATIONS - Continued

LIST OF ILLUSTRATIONS - Continued

LIST OF ILLUSTRATIONS - Continued

LIST OF TABLES

LIST OF SYMBOLS

a	speed of sound, ft/sec
a_{1_s}	longitudinal flapping angle with respect to rotor shaft, deg
b	number of blades
B_1	longitudinal cyclic pitch, deg
c_d	section drag coefficient
C_D	rotor drag coefficient, $D = \rho \pi R^2 (\Omega R)^2$
C_D/σ	rotor drag coefficient/solidity
c_l	section lift coefficient
C_L	rotor lift coefficient, $C_L = L/\rho \pi R^2 (\Omega R)^2$
C_L/σ	rotor lift coefficient/solidity
C_Q	rotor torque coefficient, $C_Q = Q/\rho \pi R^2 (\Omega R)^2 R$
C_Q/σ	rotor torque coefficient/solidity
C_R/σ	resultant force coefficient/solidity $C_R/\sigma = \left[(C_L/\sigma)^2 + (C_D/\sigma)^2\right]^{1/2}$
D	drag, the resultant force parallel to the relative wind direction, positive in downwind direction, lb
E	modulus of elasticity, lb/in^2
f	unit stress, load/area, lb/in^2
hp	rotor power required, horsepower
L	lift, the component of rotor resultant force perpendicular to the relative wind direction in the plane of the relative wind and the shaft, positive up, lb
ℓ	characteristic length as used in model geometric scaling, in.
M	Mach number, $M = V/a$

LIST OF SYMBOLS - Continued

$M_{(1.0,90.)}$	advancing-tip Mach number, $M_{(1.0,90.)} = (V + \Omega R)/a$
$M_{\Omega R}$	rotational Mach number, $M_{\Omega R} = \Omega R/A$
P	power, ft-lb/sec
q	dynamic pressure, lb/ft^2
Q	shaft torque, the moment about the shaft z axis, positive when torque tends to accelerate the rotor, ft-lb
R	rotor radius, ft
S_g	geometric scaling factor, $\ell_{model}/\ell_{full\text{-}scale}$
V	forward speed, ft/sec
α	fuselage pitch angle, deg
α_s	shaft angle of attack, the angle between the relative wind and a plane normal to the shaft axis, positive in no-up direction, deg
α_c	control axis angle of attack, the angle between the relative wind, the shaft axis, and the projection of the control axis on the plane of the relative wind axis, positive in nose-up direction, deg
γ	Lock number, air forces/mass forces
θ_o	blade collective pitch angle measured at blade root, deg
θ_1	blade root to tip twist, deg
μ	advance ratios, $\mu = V/\Omega R$
μ'	dynamic viscosity, $lb\text{-}sec/ft^2$
ρ	density, $slugs/ft^3$
σ	rotor solidity, $\sigma = \frac{\text{blade area}}{\text{rotor disc area}}$

Ω	rotor shaft angular velocity, rad/sec
ω	natural frequency, cycles/sec
ψ	blade azimuth position measured from downwind position in the direction of rotation, deg

(Note: In the Appendix CLP and CDP are used to denote C_L and C_D.)

Subscripts

b	blade
F	full scale
M	model
s	shaft

INTRODUCTION

The operational speeds of present-day helicopters are far in excess of those believed feasible only a few years ago. Helicopters are presently flying at advance ratios approaching 0.50 and at advancing-tip Mach numbers nearing 1.00. (The U. S. Army AH-56A Cheyenne reportedly has flown at an advance ratio of approximately 0.54 and advancing-tip Mach numbers of 0.90.) Experimental rotorcraft have flown at advance ratios exceeding 0.70, and future helicopters or their derivatives will operate in, and probably beyond, this range of advance ratios and advancing-tip Mach numbers.

Theory has been extended to encompass the projected speed capabilities of these future machines. Until recently, very little data have been available from which the theory could be verified or modified. The conditions at which flight-test data are taken are usually not accurately enough determined nor sufficiently controlled for theoretical verification. Small-scale model tests in wind tunnels meet with the common scaling problem of simulating the significant parameters simultaneously. Full-scale testing of normal-sized rotors is restricted to about 200 knots due to available tunnel limitations. The use of Freon as a test medium for testing scaled rotors is one approach to obtaining the necessary data.

The use of Freon as a test medium, with its characteristic low speed of sound (≈510 ft/sec) and high density (≈0.008 slug/ft^2), permits closer simulation of the significant rotor parameters when testing a scaled-rotor system. Also, model design requirements such as stiffness and mass are easier to satisfy. However, the validity of data obtained in Freon is questioned, because the ratio of specific heats of Freon is about 1.13 as compared to 1.40 for the same ratio in air. This implies that the boundary layer and pressure distribution may not be scaled when incipient blade stall occurs. The questions relating to the specific heat of Freon cannot be answered satisfactorily without obtaining sufficient data under comparable controlled conditions in both Freon and air. Using such data, valid comparisons may be made.

This program was undertaken to provide data to assess:

- The aerodynamic characteristics of rotors operating at combinations of high advance ratio and advancing-tip Mach number
- The feasibility of obtaining rotor and aerodynamic structural loads from a dynamically similar scaled model
- The validity of data obtained in a Freon atmosphere

TEST EQUIPMENT

MODEL DESCRIPTION

The model, as shown installed in the tunnel in Figure 1, has an 11-foot-diameter main rotor and no tail rotor. The body is torpedo-shaped and is the minimum size (20-inch diameter) that will enclose the mechanical components. A fixed-incidence horizontal stabilizer is installed to minimize the fuselage pitching moment.

Figure 2 is a schematic of the model and shows the relationship of the various component parts. Figure 3 gives the dimensional envelope for the model installation. The support frame of the model is constructed of heavy aluminum alloy plate. This frame attaches to the pitch plate and provides the model pitch axis. Model pitch change is effected by a remotely controlled linear actuator attached to the frame at one end and to the pitch plate at the other. The pitch plate is bolted to the NASA-Langley 6-component balance (SPO3R).

The model pylon assembly is attached to the support frame through four Lord mounts (see Figure 2). The spring rate of these mounts was selected to establish the desired pylon frequency. The pylon assembly consists of the power train, transmission, rotor shaft, controls system, hub, and rotor. The fact that the model motors were installed as a part of the pylon assembly resulted in a higher-than-scale pylon inertia; thus the hub impedance of the model is not scaled to that of the flight tested hub.

The rotor is powered by two variable-frequency, water-cooled model motors each rated 30 horsepower at 12,000 rpm. The motors are belted to a common input to the transmission assembly that drives the rotor. An overall motor rpm reduction of 18:1 is accomplished ahead of the rotor shaft by a 6.9:1 belt reduction and a 2.6:1 gear reduction. This reduction is compatible with the requirement to maintain the full-scale advance ratio and advancing-tip Mach number during the model tests.

The rotor controls consist of a "rise-and-fall" swashplate, driven by a pylon-based actuator, to vary the blade collective pitch, and two swashplate-mounted actuators to input the lateral and longitudinal (fore and aft) cyclic requirements. All controls are actuated from a remotely located control console (see Figure 4). The rotor control rates are each designed to one-quarter of a degree per second for the rated 28-volt input to the control motors. These rates can be changed by varying the voltage to the motors. Incorporated in the fore and aft cyclic control system is the capability of introducing a rapid control input to the rotor (1 degree in 1/100-second) at a preselected rotor azimuth position. The rapid cyclic control

input is initiated by an electrical signal triggered at a fixed rotor azimuth position. This signal can be delayed electronically, and thus the rotor azimuth at which the cyclic input occurs can be varied over a range of approximately 90 degrees.

A tubular steel truss-type tail boom structure attaches to the aft support frame and provides the structural support for the horizontal stabilizer and the tail boom fairing. The nose, pylon, and center-body fairings are attached directly to the support frame. Approximately 250 pounds of lead are attached to the frame and tail boom in the appropriate locations to produce a fuselage that is free of resonant frequencies throughout the rotor operating range.

ROTOR SYSTEM

The model has a two-bladed semirigid rotor system. Three rotors were fabricated for testing on the model; however, time permitted testing only rotors 1 and 3 (-10-degree twist and 0-degree twist). The geometric parameters of the rotors are presented in Table I.

TABLE I. ROTOR GEOMETRIC PARAMETERS

Rotor	Diameter (ft)	Chord (in.)	Twist (deg)	Tapered Tips
1	11	6.75	-10	No
2	11	6.75	- 5	Yes
3	11	6.75	0	Yes

Rotor 1 is geometrically and dynamically similar to the Bell "door-hinge" (540) rotor system used on the UH-1C and AH-1G series helicopters. This is a symmetrical airfoil section about 9-percent thick. All three rotors have the same constant-thickness airfoil section except for the tapered-tip portion. The airfoil coordinates for the constant section are given in Table II, and typical rotor cross sections are shown in Figure 5. Rotors 2 and 3 are tapered in thickness only from 80 percent of radius to the tip. Starting at 80 percent of radius, rotors 2 and 3 taper linearly to an NACA 0006 airfoil section at the tip.

TABLE II. BELL 540 AIRFOIL COORDINATES

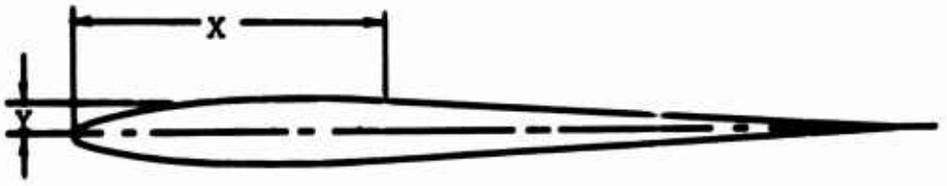

X	Y
.007	.032
.014	.046
.026	.064
.052	.084
.079	.108
.105	.124
.131	.137
.158	.149
.210	.169
.262	.187
.315	.202
.446	.232
.630	.262
.735	.275
.840	.286
1.050	.301
1.312	.312
1.575	.315
2.100	.304
2.694	.274
6.750	.007
LER	.083

SCALING CRITERIA

Scaling parameters were determined by maintaining the model rotor advance ratio and advancing-tip Mach number numerically equal to the full-scale rotor values, or

$$\mu_M = \mu_F \text{ and } M_{(1.0,90.)_M} = M_{(1.0,90.)_F}$$

Rotor dynamics are simulated on a "per-rev" basis by maintaining the ratio of the model rotor natural frequency divided by the model rotor rotational frequency equal to the same full-scale rotor ratio. In order to meet this blade frequency scaling and to maintain rotor behavior simulation, the blade Lock number is numerically scaled. Table III, taken from Reference 1, shows some of the more important scaling relationships.

Rotor 1 (-10-degree twist blades) is a dynamically similar, one-quarter scale model of the Bell Model 540 rotor system. The scaling parameters of Table III, flapwise and chordwise stiffness and mass distributions, were followed in designing this rotor. It should be noted that no attempt was made to scale the torsional stiffness of the blade. However, subsequent shake tests of the rotor system showed the first-symmetric torsional mode to be reasonably close to the scaled frequency (see Table IV). Due to the high frequencies involved, the other torsional modes could not be defined during the shake test and do not necessarily correspond with the full-scale blade frequencies.

Two hub assemblies were fabricated of 17-4 PH steel. Both hubs have stiffness and mass distributions that are equivalent to the full-scale hub assembly. The basic difference between the two hubs is the amount of underslinging. Hubs 1 and 2 have 1.20 and 1.08 inches of underslinging, respectively. The underslinging of hub 1 is scaled from the full-scale 540 hub. This hub was used throughout the test program and is shown in Figure 6.

The geometric blade design for each of the three rotors is essentially the same. Rotors 2 and 3 are not scaled to a particular configuration, but they are designed to avoid resonant frequencies within the proposed operating rpm. Figures 7 through 12 show the blade natural frequencies versus rpm for the full-scale 540 rotor system and for the quarter-scale model rotors. Collective mode as referred to in Figures 7 through 12 are those blade bending modes excited by collective pitch inputs; these are the flapwise symmetric modes and chordwise asymmetric modes. Cyclic mode refers to the blade bending modes excited by cyclic pitch inputs; these modes are the asymmetric flapwise and symmetric chordwise modes. Scaled rotor rpm and frequencies are equal to 1.88 times the equivalent full-scale value. Figures 11 and 12 are representative of both rotors 2 and 3 (-5-degree twist and 0-degree twist). Twist is the only difference between these blades, and it does not significantly affect the blade frequencies.

TABLE III. SCALED DIMENSIONLESS RATIOS

(1) Stiffness Ratio for $(\omega/\Omega)_M \; (\omega/\Omega)_F = 1$	$\frac{(EI)_M}{(EI)_F} :: Sg^4 \times \frac{(\rho_b)_M}{(\rho_b)_F} \times \frac{(M_{\Omega R})^2_M}{(M_{\Omega R})^2_F} \times \left[\frac{a_M}{a_F}\right]^2$
(2) Rotor Power	$\frac{P_M}{P_F} :: \frac{\rho_M}{\rho_F} \times \left[\frac{a_M}{a_F}\right]^3 \times Sg^2$
(3) Stress Level (Air Loads)	$\frac{f_M}{f_F} :: \frac{\rho_M}{\rho_F} \times \frac{(M_{\Omega R})^2_M}{(M_{\Omega F})^2_F} \times \left[\frac{a_M}{a_F}\right]^2$
(4) Aerodynamic Force	$\frac{F'_M}{F'_F} :: \frac{\rho_M}{\rho_F} \times \left[\frac{a_M}{a_F}\right]^2 \times Sg^2$
(5) Centrifugal Force	$\frac{(C.F.)_M}{(C.F.)_F} :: \frac{(\rho\Omega^2)_M}{(\rho\Omega^2)_F} \times Sg^4$
(6) Rotational Mach No.	$\frac{(M_{\Omega R})_M}{(M_{\Omega R})_F} :: \frac{\Omega_M}{\Omega_F} \times Sg \times \frac{a_F}{a_M}$
(7) Lock No.	$\frac{\gamma_M}{\gamma_F} :: \frac{(\rho/\rho_b)_M}{(\rho/\rho_b)_F}$
(8) Reynolds No.	$\frac{R_M}{R_F} :: \frac{(\rho a/\mu')_M}{(\rho a/\mu')_F} \times Sg \times \frac{(M_{\Omega R})_M}{(M_{\Omega R})_F}$
(9) Froude No.	$\frac{F_M}{F_F} :: \left[\frac{a_M}{a_F}\right]^2 \times \frac{1}{Sg}$

TABLE IV. SHAKE TEST DYNAMIC-SIMILARITY VERIFICATION OF 1/4-SCALE MODEL 540 ROTOR SYSTEM

(Based on comparison of static natural frequencies of primary modes through 7/rev, and at a collective pitch setting of zero degrees)

Model Rotor Parameters:

Rotor diameter	-	11 ft
Number of blades	-	2
Blade chord	-	6.75 in.
Blade twist	-	-10 deg
Taper tips	-	No
Hub geometry	-	"Door hinge"
"Normal" rpm	-	600

Model Scaling Factors

Model test medium	-Freon
$\frac{\text{Model length}}{\text{Full-scale length}}$	- .25
$\frac{\text{Model Mach no.}}{\text{Full-scale Mach no.}}$	- 1.00
$\frac{\text{Model nat. freq.}}{\text{Full-scale nat. freq.}}$	- 1.88

Mode Identification	Mode Shape	Full-Scale 540 x Scale Factor Calc'd. (cps)	Full-Scale 540 x Scale Factor Shake (cps)	1/4 Scale Rotor (2) Shake Test (cps)	Error %
Inplane					
1st Sym.(1)		21.4	13.7	21.0 (3)	-1.9
1st Asym.	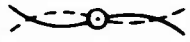	62.0	54.3	71.0 (4)	+30.8
Out-of-Plane					
1st Sym.(1)		1.7	1.7	-	-
2nd Sym.(1)		10.0	12.4	13.0	+4.8
3rd Sym.(1)		28.2	32.6	35.5	+8.9
4th Sym.(1)		61.3	69.6	70.0	+0.6
1st Asym.		7.5	7.3	8.5	+16.4
2nd Asym.		24.6	25.2	24.0	- 4.8
3rd Asym.		55.1	53.3	55.0	+ 3.2
Torsion (Blade)					
1st Sym.			53.2	57.0	+7.2

See next page for notes.

TABLE IV - Continued

NOTES

(1) Calculated - $\frac{\text{Hub Restraint}}{\text{Cantilevered}}$

Shaken - Free-Free

(2) $\text{Error} = \frac{\text{Full-Scale Shake - Model Shake}}{\text{Full-Scale Shake}} \times 100$

(3) When shaking statically, the feathering bearings are unloaded (no centrifugal force), resulting in a softer effective hub stiffness and thus a lower-than-realistic frequency. Excitation of this mode during flight shows this inplane frequency to be higher than the extrapolated shake-test value and better represented by the calculated value. This effect is not expected to apply significantly to the model.

(4) This error is attributed to:

- calculated full-scale frequency (model target value) was actually 15 percent higher than subsequent full-scale shake-test data.
- chordwise stiffening due to bonded mid-weights.

INSTRUMENTATION SYSTEM

Instrumentation is installed on the model to provide the model aerodynamic parameters, rotor and control loads, rotor rpm, and various position data. Table V is a list of the instrumentation available on the model.

The forces and moments of the entire model (rotor and fuselage) are measured by means of a 6-component balance provided and calibrated by NASA-Langley. Individual component loads are obtained from foil-type strain gages wired into four active arm bridges and excited by a DC voltage. Strain-gage sensitivities were determined by direct calibration using known loadings through the expected operating range. The load-equivalent electrical output was obtained using a precision resistor shunt on one leg of the bridge.

Flapping and pylon positions are measured using strain-gaged flexures to sense position. Positions were calibrated by moving the hardware incrementally through the full operating range and plotting electrical output versus mechanical position. All control positions are obtained from potentiometers used as one arm of a four-arm bridge circuit. Each control position is equipped with dual sensing circuits for monitoring and recording, as discussed later. Control positions were calibrated as described above.

A single accelerometer is mounted to the pylon support structure to sense the pylon vibration. These data were monitored during the test to prevent exceeding safe structural limits of the basic model. Additionally, a microphone is installed within the model fairing, in the vicinity of the transmission and drive motors, to aurally monitor unusual sounds. Various loads data were monitored by direct digital readout during the test. The hub flexure flapwise- and chordwise-bending moments were continuously monitored on a dual-beam oscilloscope. Motor, transmission, and drive-system bearing temperature were monitored on a Brown recorder.

All data, except the 6-component balance and tunnel information, were recorded on magnetic tape using a contractor-supplied data acquisition system. The data acquisition system included a monitoring station where up to 13 channels of data could be displayed digitally, in engineering units, by selecting the desired channel. A direct-write oscillograph was used to record these data simultaneously. All control positions were continuously displayed on calibrated meters at the model-operator's control console. As a precaution, the potentiometers powering these meters are electrically independent of those being recorded.

TABLE V. MODEL INSTRUMENTATION LIST

Item	Transducer Location	Transducer Type
Lift	Model Mount	SP03R Balance
Drag	Model Mount	SP03R Balance
Side Force	Model Mount	SP03R Balance
Pitch Moment	Model Mount	SP03R Balance
Roll Moment	Model Mount	SP03R Balance
Yaw Moment	Model Mount	SP03R Balance
F/A Cyclic Position	Control Sys.	Potentiometer
Lateral Cyclic Position	Control Sys.	Potentiometer
Collective Position	Control Sys.	Potentiometer
Mast Pitch Position	Pitch Act.	Potentiometer
Mast Torque	Rotor Mast	Strain Gage
Rotor Rotational Speed	Rotor Mast	Magnetic P/U
Flapwise Bending Moment *	Blade Sta.15	Strain Gage
Flapwise Bending Moment	Blade Sta.30	Strain Gage
Flapwise Bending Moment	Blade Sta.47	Strain Gage
Chordwise Bending Moment	Blade Sta.30	Strain Gage
Chordwise Bending Moment	Blade Sta.47	Strain Gage
Torsional Bending Moment	Blade Sta.30	Strain Gage
Torsional Bending Moment	Blade Sta.47	Strain Gage
Flapwise Bending Moment	Hub Sta.3.2	Strain Gage
Chordwise Bending Moment	Hub Sta.2.0	Strain Gage
Pitch Link Load	Pitch Link	Strain Gage
F/A Cyclic Load	Control Sys.	Strain Gage
Lateral Cyclic Load	Control Sys.	Strain Gage
Fuselage Pitch-Plate Load	Pitch Plate	Strain Gage
Flapping Position	Rotor Hub	Strain Gage
Pylon Pitch Position	Pylon	Strain Gage
Pylon Roll Position	Pylon	Strain Gage
Pylon Accelerations	Pylon	Accelerometer
Model Internal Noise	Model Body	Microphone
Drive Train Temperatures **	Power Train	Thermocouples

* All blades had identical instrumentation.
** Motors, drive train bearings, and transmission temperatures were monitored on a Brown Temperature Recorder.

All information relative to the tunnel conditions and the model aerodynamic data (balance data, control positions, mast torque, and rpm) were recorded and reduced by NASA-Langley. The balance data were resolved such that all forces were in the relative wind-axis system, and all moments were transferred from the balance-resolving center to the center-of-rotation of the hub and referenced to the shaft-axis system. It should be noted that the collective pitch shown in the appendix and used throughout this report are approximate values. Due to the kinematics of the rotor system, collective pitch is affected by the rotor coning angle. The instrumentation system was calibrated for a static rotor and the recorded data were theoretically corrected to account for the delta collective pitch induced by the coning angle. The pertinent aerodynamic data are presented in nondimensional form in the appendix.

TESTING PROCEDURES

Model tares were obtained by operating the model without the rotor blades installed at two velocities and recording the balance data throughout the model pitch range. The tares were found to be a function of dynamic pressure and fuselage pitch attitude only and, within the range of interest, were not influenced by the rotational speed of the hub. These tares are presented in the appendix and were applied to the test data to obtain the rotor coefficients presented therein.

For each rotor and each test condition, the rotor rotational speed and tunnel conditions (speed, Freon purity, and pressure) were adjusted to maintain constant values of rotor advance ratio and advancing-tip Mach number. At each test condition, the rotor-shaft angle (fuselage-body attitude) was incrementally varied. For each shaft angle, rotor lift (collective pitch) was varied incrementally to map the test envelope. The rotor cyclic pitch was adjusted to minimize the first-harmonic flapping with respect to the rotor shaft, and data were recorded at each combination of shaft angle and rotor lift. The maximum lift obtained at each condition was limited by one or more of the following restraints: rotor stall, excessive loads, excessive vibration, maximum cyclic pitch, available rotor power, or maximum motor temperature. In most all cases, the motor power or temperature limit was reached first.

At each test condition (advance ratio and advancing-tip Mach number combination), the rapid cyclic control input was applied at two lift values at a shaft angle of -5 degrees. Transient rotor data were recorded for each cyclic input.

TEST PROGRAM

The test program was arranged to map combinations of advance ratio and advancing-tip Mach number covering the operating range of present-day helicopters up to that of future high-speed helicopters. Combinations tested are defined under Test Results (see Figure 13). The use of Freon as a test medium allows higher combinations of advance ratio and advancing-tip Mach number than are easily attainable in conventional air tunnels. The test as conducted was designed to provide data that were comparable to existing full-scale tunnel data and full-scale flight test data.

Two rotors were tested, -10-degree twist and 0-degree twist. The third rotor (-5-degree twist) was not tested in order to permit more time to be devoted to testing the other two rotors.

The -10-degree twist rotor was tested at an advance ratio of 0.30 for advancing-tip Mach numbers varying from 0.72 to 0.96. These test conditions were repeated for the 0-degree twist rotor to permit an evaluation of twist effects. The 0-degree twist rotor was tested at advance ratios varying from 0.30 to 0.83 and advancing-tip Mach numbers from 0.47 to 0.96. Due to the many variables associated with testing in Freon (temperature, pressure, purity, and velocity), exact duplication of the conditions was impracticable.

TEST RESULTS

The model test results are discussed under two categories in this report. The first category discussed is the aerodynamic data which cover the rotor aerodynamic characteristics and performance. The dynamic category presents the rotor loads and dynamic response characteristics. Figure 13 shows the advance ratio and advancing-tip Mach number combinations that were tested.

AERODYNAMIC TEST RESULTS

Method of Presentation

The model performance data obtained for several conditions shown in Figure 13 have been graphed and crossplotted to show rotor power variation as a function of advance ratio and advancing-tip Mach number. Full-scale wind-tunnel rotor data and theoretical performance are also included for comparison. This method of presentation shows rotor behavior trends with varying advance ratio at constant advancing-tip Mach number and at constant advance ratio with varying Mach number.

It was desirable to present the performance in coefficient form for comparison purposes. However, to obtain the horsepower required from a standard torque coefficient over solidity, C_Q/σ, it is necessary to multiply C_Q/σ by a different dimensionalizing factor at each rpm. For this reason, a new factor $[M_{(1.0,90)}/1 + \mu]^3 C_Q/\sigma$ is used since it is directly proportional to horsepower per square foot of rotor blade area. When the power variation is graphed in this form versus advance ratio or Mach number, a given ordinate increment represents a constant horsepower difference for any μ-$M_{(1.0,90)}$ combination.

Theoretical Performance Method

Classical blade-element strip theory is used in calculating the model rotor performance. It embodies a rigid blade operating in a quasi-steady, two-dimensional flow field. In this method, airfoil pitching and plunging velocities are assumed to have no influence on the aerodynamic force coefficients which are therefore taken from static two-dimensional data. Further, in calculating blade-element angle of attack, the wake-induced inflow is replaced by a uniform distribution, and spanwise-flow effects, due to advance ratio and the vortex field, are neglected.

Additional calculations have been made for the Freon model data under another contract to determine the effects of nonuniform inflow and local unsteady aerodynamics. The results of these

calculations will be compared with the Freon model performance and published in a later report.

Section aerodynamic characteristics (c_l and c_d) for the theoretical performance method are taken from two-dimensional wind-tunnel tests (in air) of the Bell 540 airfoil section defined in Table II. These tests provide data at Mach numbers from 0.30 to 0.30 at corresponding Reynolds numbers from 3 to 6 million.

Airfoil properties outside the range of data available have been estimated from NACA 0012 airfoil data. In some instances 0012 data were used directly. The curves above stall for all Mach numbers are faired into 0012 data, extending the angle-of-attack range to 30 degrees. A 0.10 Mach number 0012 curve is used to provide a 180-degree angle-of-attack range. Approximate curves for 0.20 and 0.90 Mach numbers have been estimated from corresponding 0012 curves.

The basic theoretical method, using NACA 0012 airfoil data, has been correlated with full-scale (two-bladed, semirigid) rotor wind-tunnel performance at various advancing-tip Mach number and advance ratio conditions (see References 2 and 3). In general, below rotor stall the theory predicts Mach number effects well (see Reference 2). However, Reference 3 indicates that at low Mach number and high advance ratio ($\mu > 0.40$ $M_{(1.0,90)} \simeq 0.50$) conditions, it gives larger propulsive force values than test results show.

Performance Comparisons

Comparisons of Freon model data with full-scale wind-tunnel rotor data are made to determine if the Freon model performance represents full-scale behavior. Full-scale 540 rotor wind-tunnel data are unavailable; therefore, the comparisons are made using data from rotors that are not geometrically similar. The -10-degree twist and 0-degree twist rotors are compared, respectively, with standard UH-1D and modified UH-1B rotors. (Geometric differences between the rotor systems are illustrated in Table VI.) Due to differences in rotor geometry, the comparisons are intended only to show if the model and full-scale rotors exhibit the same performance trends.

Analytical performance calculations are also correlated with the test results to determine the ability to predict small-scale performance. These results can be compared directly to the Freon data since all calculations were made using the reduced scale geometry and Freon atmospheric properties.

Both Freon and theoretical performance are presented and compared with the full-scale rotor data on a "full-size" basis. Thus, Freon and theory coefficients are assumed to be valid for a full-scale version of the model rotor operating in a standard

air atmosphere. All dimensional values obtained from these coefficients use the standard air density, speed of sound in air, and the full-scale blade area. For these conditions, an ordinate increment, $\Delta[M_{(1,0,90)}/1+\mu]^3\ C_Q/\sigma = 0.001$, corresponds (approximately) to a six-horsepower-per-square-foot of blade area power increment for the three sets of data.

TABLE VI. COMPARISON OF ROTOR GEOMETRIES

Parameters	Twisted Freon Rotor	UH-1D* Rotor	Untwisted Freon Rotor	UH-1B Modified* Rotor
Twist	-10 deg	-10.9 deg	0 deg	-1.83 deg
Solidity	0.0651	0.0464	0.0651	0.0506
Full-Scale Blade Area	99 ft^2	84 ft^2	99 ft^2	77 ft^2
Airfoil Section	0009.3 mod (see Table II)	NACA 0012	0009.3 mod NACA 0006 tip	NACA 0012 NACA 0006 mod tip

* UH-1D and UH-1B data are taken from References 2 and 3.

-10-Degree Twist Rotor

The -10-degree twist Freon rotor performance is shown in Figure 14 with full-scale UH-1D and theory comparisons. An analysis of the experimental results will be given first, followed by the theoretical comparisons. The data are presented at 0.30 advance ratio using the advancing-tip Mach number as the primary variable. Solidity corrections were applied, using the method of Reference 4, to reduce both model and theoretical results to the solidity base of the UH-1D.

In all cases where sufficient data are available, the experimental comparisons indicate a crossover point occurring between 0.80 and 0.90 Mach number. Above this point, the model power requirements are lower (by approximately two-horsepower-per-square-foot at $M_{(1,0,90)} = 0.95$) than those of the UH-1D rotor, while the opposite is true at the low Mach conditions.

This behavior may be attributed to thickness ratio differences between profile sections of the two rotors (see Table VI). Figure 15 compares the model and UH-1D results with thin-tip UH-1D performance. The thin-tip rotor is a standard UH-1D

rotor having a linear thickness taper, from 12-percent to 6-percent thickness, over the last 20 percent of the radius. By varying the thickness ratio at the tip, a substantial power saving over standard blade performance is shown between $M_{(1.0,90)} = 0.85$ and 0.95. However, the taper penalizes performance at lower Mach numbers. The thickness ratio of the Freon rotor (9.30 percent) is smaller than the UH-1D rotor, but it is not tapered. Despite these differences, the model shows Mach number trends similar to the thin-tip rotor.

Classical rotor theory calculations to match the -10-degree twist Freon performance are shown in Figure 14. The calculated power generally correlates within 60 horsepower of the actual performance except above 0.90 tip Mach number. At these Mach numbers, theory considerably overestimates the required power. The differences may be caused by the use of NACA 0012 airfoil data above 0.80 local Mach number where 540 airfoil data were not available. This is examined again for the 0-degree twist rotor.

0-Degree Twist Rotor

The 0-degree twist rotor data and theoretical calculations are shown in Figures 16 and 17 as functions of advance ratio and advancing-tip Mach number, respectively. Full-scale wind-tunnel performance of a modified UH-1B rotor (see Reference 3) is superimposed on the figures as a standard of comparison. The airfoils of both model and full-scale blades are linearly tapered in thickness, beginning approximately at the 80-percent radius station and extending to the tip. Airfoil data in the calculations were not available for the tapered portion of the rotor. However, the improved supercritical Mach number performance of the thinner sections is accounted for by increasing the local drag divergence Mach number as a function of the thickness ratio. (The method is shown in Figure 18 of Reference 2.) Corrections to the test data for solidity differences (see Table VI) were found to be small and were not applied in this instance.

Advance Ratio Trends

Comparison of the model and full-scale experimental performance with varying advance ratio is shown in Figure 16. For unknown reasons, the model test data appear to show erratic behavior at 0.34 and 0.36 advance ratios for 0.80 and 0.90 Mach numbers respectively. The model data curves for 0.85 and 0.95 Mach numbers appear to be much smoother; however, at these Mach numbers, no data were taken near 0.35 advance ratio and the faired curve may be misleading. Insufficient full-scale data are available to verify this trend. It should be noted that

on Figures 16 and 17, for various conditions, only one full-scale data point is available, as indicated by the absence of the large dashed line. Where only a single full-scale data point is available, that point is indicated by a symbol. Likewise, where only a single theoretical point could be obtained, due to analytical rotor stall, that point is indicated by a symbol.

Despite irregularities in the Freon data, this model and full-scale performance show reasonable agreement. Generally, the model performance lies above the full-scale data except at higher advance ratios where the Freon data levels off. More full-scale data would be required to show any significant differences in the high advance ratio trends. Since the model rotor has 29 percent more solidity than the full-scale rotor, it will have (on a full-size basis) a correspondingly larger horsepower requirement at points where the curves intersect. Similarly, the force values represented by the lift and drag coefficients will be higher for the model rotor.

Calculation of the Freon model performance using a uniform inflow theory is shown by the small-dashed lines in Figure 16. The theory was calculated only at the Mach number and advance ratio conditions where model data were taken. The resulting curves do not indicate the erratic behavior shown by the data.

Theoretical advance ratio trends at 0.80, 0.85, and 0.90 Mach numbers for the lowest lift values show that theory underestimates high advance ratio power requirements ($\mu > 0.45$). Test-theory comparisons in References 3 and 7 also reveal this behavior. The data of Reference 3 were obtained at low tip-Mach numbers [$M_{(1.0,90)} \approx 0.50$] and show small horsepower differences. Since small differences could be attributed to error, it was uncertain that these trends would exist at higher Mach numbers. However, the differences at higher Mach numbers are significant. For example, at 0.55 advance ratio and 0.85 Mach number, the model power required corrected to full-scale magnitude is approximately 238 more horsepower than theory predicts for $C_L/\sigma = 0.04$ and $C_D/\sigma = 0.00$.

Theory predictions at higher lift values do not show underestimation at high advance ratios because of rotor stall. The 0.80 Mach number comparisons for $C_L/\sigma = 0.08$ indicate that theory has stalled between 0.30 and 0.34 advance ratio, while the data remain unstalled to approximately 0.45 advance ratio. It will be shown later that theory stalls at lift coefficients much below the model experimental values.

Theoretical advance ratio trends at 0.95 Mach number are similar to those at lower Mach numbers, but the curves lie well above the model data. This behavior will be examined in the Mach number trend section.

Mach Number Trends

The display of power requirements as a function of advancing-tip Mach number is presented in Figure 17. This figure is the result of crossplotting the data of Figure 16 at advance ratios of 0.31, 0.36, 0.41, and 0.45.

Only the 0.36 and 0.41 advance ratio cases have enough full-scale data to show comparative trend. The Freon data again show irregular curves, and it is believed that the 0.80 and 0.90 Mach number values are high at 0.36 advance ratio. Full-scale data at 0.41 advance ratio are available to 0.95 Mach number for the lowest lift. No significant differences between the model and full-scale high Mach number performance trends are shown in this case. It is interesting to note that despite the difference in their thickness ratios, which extends over 80 percent of the radius, the comparisons do not show a significant thickness ratio effect. Unlike the -10-degree twist rotors compared in Figure 15, both model and full-scale rotors have similarly tapered-thickness tips and equal thickness ratios at the tip. Therefore, the thickness ratio at the tip stations appears to be the important factor causing the differences in Figure 15.

Theoretical model performance at low advance ratios shows reasonable agreement with the test data below 0.90 Mach number. At 0.31 advance ratio and 0.95 Mach number, it considerably overestimates the power required. Since the Freon calculations use NACA 0012 airfoil data above 0.80 local Mach numbers, a comparison with theoretical UH-1B(modified) rotor performance was made to determine if this airfoil data might cause the high Mach number differences. Figure 18 shows that the full-scale rotor theory predicts less power at 0.95 Mach number than is calculated for the model rotor. In both instances, NACA 0012 airfoil data are used, indicating that the behavior is not caused by improper airfoil data. Twist differences were also considered, but Figure 18 shows that the effects are small. Due to the differences in test media, the possibility exists that supercritical flow may have less severe effects on a rotating airfoil operating in Freon than it does in air. To answer this question it will be necessary to test a Freon model rotor having an NACA 0012 or other airfoil whose characteristics are well known.

The Mach number curves at higher advance ratios show trends similar to those at lower advance ratios. As the advance ratio is increased, the theory curves shift downward with respect to the data, giving an appearance of better agreement at higher Mach numbers.

Test-Theory Comparison at $\mu = 0.44$, $M_{(1.0,90.)} = 0.77$

A broader comparison of model and theoretical performance including control positions is presented in Figure 19 for 0.44 advance ratio and 0.77 advancing-tip Mach number. These conditions were chosen so that dependence on high Mach number NACA 0012 airfoil data would be eliminated from the calculations, thereby allowing a better representation of high advance ratio test-theory correlation.

In Figure 19(a), theoretically calculated performance has been superimposed upon a graph of the experimental data showing the variation of lift coefficient with control axis angle of attack for various control positions. The lines having symbols indicate experimental Freon data measured at constant shaft angles. Since collective pitch was not varied in even increments during the test, the pitch lines shown are crossplotted from other graphs.

Generally, the theoretical and experimental shaft angle lines correlate to within a 1-degree control plane, a_c, increment of each other. At low shaft angles for a given a_c, the theory shows higher lift coefficients than the test data, but the trend is reversed above $a_s = -10$ degrees. Correlation of the three-quarter-radius collective pitch shows similar agreement. However, at low pitch values, theory underestimates the lift for a given $\theta_{.75R}$ and a_c. Above $\theta_{.75R} = 10$ degrees, the test-theory agreement is very close.

The major problem encountered in calculating the model performance is the prediction of rotor stall. Figure 19(a) shows that the theoretical maximum lift coefficients at stall occur far below the test data. Further, the character of the theoretical stall break is much more abrupt than the gradual behavior of the model data. This behavior has been shown before (Reference 3) and is characteristic of an analysis that does not consider unsteady aerodynamic effects.

A comparison of the test and calculated performance at equal resultant force coefficients over solidity, $(C_R/\sigma)^2 = (C_L/\sigma)^2 + (C_D/\sigma)^2$, is presented in Figure 19(b). For these μ-M conditions, an increment, $C_Q/\sigma = 0.001$, represents approximately 91 horsepower on a full-scale version of the model rotor. The test-theory correlation below theoretical stall is reasonable. However, the theory shows stall at $C_D/\sigma \approx -0.003$ for a $C_L/\sigma = 0.06$. This is noted as a change in slope of the theoretical C_L/σ curve in Figure 19(b). For all practical purposes, the entire theoretical curve for $C_L/\sigma = 0.07$ is above stall.

DYNAMIC TEST RESULTS

One of the purposes of the Freon tunnel tests of the quarter-scale dynamic model of the Model 540 rotor system was to gather data for assessing the feasibility of obtaining rotor loads from such models.

During the tests, rotor and control system forces and moments were recorded at 39 advance ratio-Mach number coordinates, Figure 20, with μ ranging from 0.29 to 0.83 and with Mach number ranging from 0.47 to 0.96. Ten channels of rotor and control system instrumentation, Table V, produced approximately 7500 data points, most of which have been reviewed in one or more of the following forms: peak loads read from meters during the tests, tabulated average of 24 cycles of one-half peak-to-peak loads, Brush Recorder strip-out from tape, and digital harmonic-analysis. Detailed examination of this vast quantity of data is beyond the scope of the present effort; however, the data have been considered in enough detail to determine major trends.

The effort to establish the feasibility of using the Freon tunnel for loads determination was based more on trend rather than on quantitative-correlation since most of the data were recorded using the zero-twist blades for which there are no flight-measured data. This paucity of flight data is indicated in Figure 20 by the dashed frame which contains all of the tunnel data for which corresponding (-10-degree twist) flight data exist. The solid frame bounds the runs receiving most attention and the ones from which all of the data presented were taken.

Where possible, the plotting follows the convention established in previous USAAVLABS reports dealing with the results of wind-tunnel loads tests of full-scale and model rotors. This facilitates comparing the present results with those of previous tests. Reference 5 is suitable for trend correlation; accordingly, its format is followed closely for presenting moment trends produced by the following:

- sweeps of α and θ_o at $M_{(1.0,90.)}$, μ coordinates
- variation of drag at constant lift at $M_{(1.0,90.)}$, μ coordinates
- variation of blade twist/tip thickness
- sweeps of $M_{(1.0,90.)}$ at constant μ
- sweeps of μ at constant $M_{(1.0,90.)}$

Quantitative comparisons between flight-measured, Freon tunnel-measured, and calculated rotor moments for cases enclosed in the dashed frame in Figure 20 were made, and sample data are presented. Finally, plots of transient flapping induced by pulsing the cyclic control system are given to indicate rotor stability.

Basic Data

Figures 21 and 22 present rotor bending and twisting moment data directly in terms of model parameters; that is, moments are presented as a function of collective pitch for constant values of shaft angle, or rotor angle of attack when flapping is trimmed to zero. These graphs are of the same type as Figure 59 of Reference 5, except for a rearrangement necessitated by the testing procedure used. In Reference 5, vibratory stress is graphed as a function of rotor angle of attack for constant values of collective pitch.

This type graph stems directly from the method of recording aerodynamic data in the tunnel, and it is not without value. However, caution must be used in interpreting tunnel dynamic results and in making loads and vibration extrapolations to flight. These points are discussed in greater detail in a later section.

Some merits of this type graph are:

- If made on-site at the tunnel, it would give a very good running account of loads for test-safety purposes, and it could pin-point areas for special loads investigations.

- It reveals whether the data are well or badly behaved.

- It gives an overview of the total domain of the loads for a given rotor if the test-point grid is fine enough to reveal all significant dynamic and unsteady aerodynamic effects.

Tunnel data tend to be well behaved. When such data are not well behaved, it is usually because of an instrumentation malfunction or dynamic or unsteady aerodynamic phenomena. Relatively little attention has been given to these phenomena because most wind-tunnel tests of rotors have been for aerodynamic performance purposes with rotor instrumentation being used primarily for test-safety purposes.

A cursory look at Figures 21 and 23 reveals that the data are well behaved, with all gages showing the general trends of (1) increasing load with increasing collective pitch at constant values of shaft angle and (2) increasing loads with increasing shaft angle of attack for constant values of collective pitch. The same trends are shown in Figure 59 of Reference 5. In addition, the expected trend of increasing loads with increasing μ is seen in comparing Figures 21 and 22.

The Effect of Lift and Drag on Rotor Oscillatory Loads

The data of the previous section are replotted here as a function of drag coefficient over solidity for constant values of lift coefficient over solidity to reveal more clearly the dependence of the loads on these parameters.

In Figure 23, it is seen that all loads vary uniformly with lift and drag. For the flapwise and torsional loads, the dependence is primarily on lift since the intensity of the oscillatory airloads causing both are predominantly functions of lift. The loads at flapwise station 0.23R appear to be an exception; however, the increase, with propulsive force (negative C_D/σ), shown is due to increased coupling with the inplane moment caused by the increase of blade angle and moment toward the root.

The chordwise loads are strongly a function of both lift and drag. For positive drag coefficient over solidity values in the range 0.002 to 0.006, the chord loads vary little with increasing lift because of the low collective and cyclic pitch values used near autorotation. The increase in loads with propulsive force and the increased sensitivity to lift in the propulsive force domain are due to both increased oscillatory airloads and an increase in response amplification associated with the downward shift of the first chordwise mode toward one-per-rev and the upward shift of the first asymmetric flapwise mode toward three-per-rev.

The trends shown in Figure 23 are similar to those of Figure 24 with the exception of the tendency of the flapwise and torsional moments to peak and fall off as propulsive force increases. The reason for this is not known.

The loads data of these figures show good overall trends for one-half peak-to-peak data plotted versus lift coefficient over solidity and drag coefficient over solidity. A full explanation of the curve characteristics would require a much closer look at the harmonic content of the waveform.

The above trends are corroborated by the results of the high performance helicopter research studies, such as References 6, 7, and 8, which show reduction in flapwise and chordwise loads by unloading the rotor of both lift and propulsive force. In addition, the full-scale rotor tests of Reference 5, Figure 86, for $\mu = 0.40$ and $M(1.0,90.) = 0.83$ show similar trends with the exception that flapwise loads for that rotor are more drag dependent.

The Combined Effect of Twist and Tip Thickness on Rotor Oscillatory Loads

A considerable amount of data are presented in Reference 5 comparing the oscillatory stress values for blade twists of -8 and 0-degrees. For the Freon tunnel tests, a comparison of twist alone cannot be made since both tip thickness and twist were changed in going from the standard-tip, -10-degree twist blades to the thin-tip, 0-degree twist blades. However, it is believed that a useful trend comparison can be made.

Figure 25, showing the combined effect of tip thickness and twist on flapwise moments at $\mu = 0.30$ and $M(1.0,90.) = 0.72$, can be compared with Figure 67 of Reference 5. Plots are presented showing flapwise moments as a function of lift and drag for three radial stations. Comparison shows that the trends of Figure 25 match the trends of Reference 5 very closely, demonstrating clearly the first-order reduction in flapwise loads over the mid-portion of the blade.

As discussed in Reference 5, this reduction probably results from a reduction of an impulsive loading whose shape favors excitation of the first pinned mode of the hinged blade and the first asymmetric mode of the teetering rotor. The excitation results from negative lift at the tip of the advancing blade and at the root of the retreating blade in the reversed flow region. Reduction of twist delays the development of this pattern of excitation probably by making the blade angle more positive in both of these regions.

Figure 26 presents similar data at the same advance ratio but at a higher Mach number, $M(1.0,90.) = 0.96$. The presentation is the same as for Figure 25, but instead of three radial stations, one each of flapwise, chordwise, and torsion at radial station 0.45R is presented.

The principal result--a first-order reduction in loads with reduced twist--is shown for flapwise, chordwise, and torsion. This deviates somewhat from the results of Reference 5 which show considerably less effect for chordwise and torsional loads. This difference is possibly associated with the beneficial effect of thin tips at the higher Mach numbers.

The Effect of Advancing-Tip Mach Number on Oscillatory Rotor Moments

Figure 27 is taken from Reference 5 and is typical of a large amount of data presented to show the effect of advancing-tip Mach number on blade stresses. Almost all of the plots showed this "U-shaped" characteristic of high loads at low and high Mach numbers which was reasonably attributed to stall at the low Mach numbers and compressibility at the high Mach numbers. Attempts to plot the Freon tunnel data in the same way for a direct comparison produced badly behaved plots. Other methods of plotting, such as a Mach number sweep at constant rotor angle of attack, showed well-behaved plots in which loads continued to decrease with increasing Mach number for moderate to high lift values. A modification of the plot of Reference 5 reveals a clearer picture of the variation in loads with Mach number.

In Figure 28, blade loads are plotted as a function of drag for one value of disc loading at several values of Mach number. Figure 28(a), for a disc loading of 1 lb/ft^2, shows relatively little variation in moment with Mach number in any drag plane. Figure 28(b), at a disc loading of 2 lb/ft^2, shows considerable variation with Mach number in each drag plane, with the loads also varying considerably from one drag plane to another. The strong peak is due to three-per-rev resonance of the first flapwise asymmetric mode, which is passed through as rpm and collective pitch vary in holding a constant μ and disc loading while sweeping Mach number. Finally, Figure 28(c), at a disc loading of 4 lb/ft^2, shows what is likely a general up lifting of the previous surface associated with increased oscillatory force amplitude, which may indicate stall at low rpm and high collective pitch. However, even this surface shows decreasing loads at the highest Mach numbers tested.

In no case examined was the characteristic "U-shaped" curve of Reference 5 revealed. The indications of stall are obscured at low Mach numbers by a rotor three-per-rev resonance in Figure 29(b); however, the lift surface for 4 lb/ft^2, Figure 28(c), shows either or both stall and dynamic amplification. It appears that the increase in loads at high Mach numbers is absent through $M(1.0,90.) = 0.95$. This result is in agreement with the results of tests of a 48-foot UH-1D rotor in the Ames 40 by 80-foot tunnel which show relatively little increase in loads below $M(1.0,90.) = 0.95$.

This example shows the caution which must be exercised in interpreting rotor loads data plotted in terms of advance ratio, Mach number, C_L, and C_D. In many cases the primary variables, rpm, collective pitch, cyclic pitch, pylon angle of attack, and flapping, are of more direct importance. In the present case,

collective pitch and rpm are dominant because of their direct relation to the rotor natural frequency spectrum.

The Effect of Advance Ratio on Rotor Oscillatory Moments

The effect of advance ratio on flapwise, chordwise, and torsional oscillatory moments at radial station 0.45R is shown in Figure 29. Oscillatory moment is presented as a function of μ over the range 0.30 to 0.54 for three values of disc loading and three values of drag.

The flapwise, chordwise, and torsional moments show similar trends of increasing with μ, lift, and propulsive force, with the upward break in loads occurring at lower μ's for increasing lift. The flapwise and torsional moment behavior is similar, showing a rather gradual increase with μ. The chord moments show significantly larger gradients with lift, drag, and advance ratio. These trends are all in close agreement with the results of the Bell-AVLABS High Performance Helicopter flight research programs reported in Reference 7.

Comparison of Flight-Measured, Freon Tunnel-Measured, and Calculated Rotor Loads

Comparisons were made between flapwise and chordwise moments obtained by calculation, by measurement of the quarter-scale model in Freon, and by measurement of a full-scale UH-1B in flight. The Freon tunnel tests in which comparable data were recorded are shown in the dashed frame of Figure 20. Flight test data were obtained from the load level survey of the UH-1B with the Model 540 rotor, Reference 9.

Comparisons were made for several closely corresponding test conditions, and the bending moment correlation was about the same in each case. The flight and tunnel conditions for the comparison presented are given in Table VII. Calculations were made for the free flight case.

TABLE VII. PRINCIPAL FLIGHT PARAMETERS FOR LOADS COMPARISON BETWEEN FULL-SCALE FLIGHT TEST AND QUARTER-SCALE FREON TUNNEL TESTS OF THE MODEL 540 ROTOR

	M(1.0,90.)	μ	C_L/σ	C_D/σ	θ_o Degrees	a_c Degrees
Flight	.89	.29	.068	.0084	19.9	-17.6
Tunnel	.92	.30	.066	.0120	15.9	-16.0
Flight: UH-1B Serial Number 63-8636, Flight 98B, Record No. 354						
Tunnel: Data Point 216						

Sample bending moment data are presented in Figures 30 and 31, which show waveforms and harmonic content, respectively.

In Figure 30(a) are shown calculated, flight-measured, and Freon tunnel-measured waveforms of flapwise bending moments at four spanwise stations. The plots show fair to good agreement in overall amplitude, with the greatest discrepancy occurring at the most inboard station. A comparison of the overall amplitudes and the amplitudes of the first three harmonics of these waveforms is made in Figure 31(a). A cursory look at these plots reveals a reasonably good distribution of harmonic amplitudes; however, there is a significant percentage variation between the amplitudes of corresponding harmonics.

In Figure 30(b), a comparison is made between chordwise waveforms at three radial stations. The agreement in overall amplitudes is fair to good; however, as in the flapwise case, there is some difference in the harmonic content. The amplitudes of the overall waves and the first three harmonics are compared in Figure 31(b). Again, a fair distribution of harmonics is shown with considerable percentage variation in amplitude between corresponding harmonics. The free-flight and calculated values agree fairly well, while significant deviation is noted for the model case.

An overall assessment of these figures shows that the comparison between calculated and flight-measured bending moments is reasonably good except for the flapwise moment at station 0.05R. The tunnel measured moments agree reasonably well with theory except for the flapwise moments at station 0.05R and the chordwise moments at stations 0.03R and 0.45R. Probably the largest source of error is associated with the vertical and in-plane hub impedances which are difficult to quantify for both the model and the analysis.

The lack of definition of hub impedance and other factors discussed later renders the above comparison inconclusive regarding the feasibility of using a dynamic model in the Freon tunnel to determine full-scale rotor loads.

Rotor Stability

Rotor stability was assessed during each collective-pitch sweep at mid- and high-pitch settings by transiently exciting flapping with a 1-degree step input in cyclic pitch and observing the resulting motion. Figures 32, 33, and 34 present samples of flapping and loads transients for μ values of 0.30, 0.49, and 0.72. Following excitation, the flapping assumes a new stable position within a fraction of a rotor cycle. In no case did the rotor exhibit marginal stability.

Discussion of Results

The principal objective of the loads study was to establish the feasibility of using a dynamically scaled model in the Freon tunnel for determining full-scale rotor loads in free flight. Trend comparisons with published data and general experience, comparison of calculated and measured loads, and the visual assessment of a large amount of the Freon tunnel data lead to the judgment that it is feasible to determine full-scale, free-flight loads with a dynamically scaled rotor in the Freon tunnel.

The above is the strongest statement that can be made in view of several basic problem areas which were defined in the course of this effort. These problems have more to do with the concepts and methods for dynamics testing than with the Freon medium itself. It would have been desirable to have resolved these problems before executing the subject tests. This may have been possible within the available state of the art; however, even recent published literature reveals a gereral lack of appreciation of these fundamentals. A reasonable explanation for this is that most wind-tunnel testing to date has been for aerodynamic performance purposes. It is true that most of the rotors tested in recent years have been instrumented with strain gages; however, these gages were primarily used for safety of test purposes and in most instances were used only casually for loads correlation. The problems defined are briefly discussed in this section along with some general comments on salient features of the set of very well behaved data obtained during the subject tests.

The best introduction to the problems is a series of questions:

- What constitutes good loads correlation between tunnel and flight tests?
- How are corresponding conditions determined for a rotor in the wind tunnel and a rotor in free flight?
- Is it possible to obtain good correlation between loads determined in a full-scale air tunnel and loads determined in free flight?

The answers to these questions are mandatory before a stronger case can be made for the Freon tunnel.

Correlation Criteria

Correlation between tunnel and flight tests means something different in all of the following areas: performance,

stability, moments/stress, shear force, and vibration. The farther down the list, the more difficult the test concepts become. The rules for correlation can readily be established for performance and stability. The rules for shear force and vibration appear to be very complex at this stage. However, the question here deals with the rules for correlating moments, or stress; the determination of such rules is possible.

Good correlation may be defined as follows. Instrument a rotor with strain gages for testing both in the tunnel and in flight. Using the same scale factors throughout, if the output waveform from the same gage can be exactly superposed for corresponding test conditions, then good correlation has been obtained. This definition may be relaxed in various ways, for instance, it could be required that the one-half peak-to-peak loads and the amplitudes of the first n harmonics must agree within a certain percent. The main thing is to have criteria determined ahead of time.

Determination of Corresponding Test Conditions

When an attempt is made to define corresponding test conditions, the question arises as to the purpose of the test: aerodynamic performance, stability, moments, forces, or vibration. The lists of parameters will vary with each of these purposes, and they will vary between the methods: calculation, tunnel test, and flight test. Since most of the rotor tests to date have been conducted for performance reasons, there is a tendency to satisfy the lists defining the flight condition for performance correlation without recognizing the necessity to tailor the list for loads when loads correlation is wanted.

A convenient way to determine what list was used in a given case is to note the coordinates and legend in published figures to see what was thought necessary to define the test condition. An example is Figure 30 of Reference 10, wherein correlation between loads for tunnel, flight, and calculation is presented. Stress is shown at a state defined by V, L, D, and α for a rotor whose dimensional, kinematic, and dynamic properties are defined. No definition of hub impedance along and normal to the shaft is given.

For determining hinged-rotor stress, this omission may not be important since the hinges effectively decouple the blades from the pylon for moments and stress. However, even for the hinged rotor, the specification of hub impedance is important if hub shears or vibration is the object of correlation.

For the teetering, semirigid rotor, the impedances must be defined to establish corresponding test conditions between

flight and tunnel even for moment or stress correlation since the rotor couples strongly with the pylon. More will be said about this in later paragraphs.

Another example of stress data presentation is Figure 59 of Reference 5 wherein stress is related to

(a) a_c, θ_o, μ, $M_{(1.0,90.)}$, V, and $a_1 = 0$

for a defined rotor and undefined hub impedance. A cross plot of these same data presents stress as a function of

(b) C_L/σ, C_D/σ, μ, $M_{(1.0,90.)}$, V and $a_1 = 0$.

Plotting within the boundaries specified in (b) produces well-behaved stress curves which are functions of these variables if dynamic effects are absent. When dynamic effects are present, plotting stress as a function of these variables is misleading because it assigns incorrect causes. In addition, the practice of setting flapping to zero removes a variable which is important for loads correlation. A better set of variables for loads correlation is given by

(c) C_L/σ, C_D/σ, V, μ, α, B_1, a_{1s}, and θ_o

with blade dynamic and hub impedance properties defined for the case of the semirigid rotor.

The use of these coordinates does not change the aerodynamics and has the advantage of allowing the rotor natural frequency plots to be readily used to interpret dynamic effects. These effects are especially clear in the data of the subject tests as indicated in the surfaces plotted in Figure 28. A great deal can be learned from further studies of these data with respect to defining the importance of an indicated resonance shown by the frequency plot.

It is known that it is difficult to design a rotor which is completely free of resonance or near-resonance over the entire rotor speed range owing to the effects of rpm and collective pitch. It is also known that no catastrophic effects result from operating at an indicated resonance; however, the reasons for this are not known. Possible reasons include: structural damping, a self-limiting mechanism in the aeroelastic loads, cyclic detuning, or other nonlinear or unsteady effects which preclude steady-state resonance. Cyclic detuning is considered to be an especially important effective damping mechanism for rotor modes whose frequencies vary significantly with pitch. In such cases, steady-state resonance only occurs for zero cyclic feathering.

It is also desirable to be able to separate response peaks which are due to dynamic effects from those due to unsteady aerodynamic effects. The data from the subject tests appear to contain both types of peaks.

The argument that the parameters of (a), (b), and (c) of the previous page are equivalent for loads correlation must be carefully reevaluated since in presenting loads data the variables indicated are usually taken at face value, and cause and effect relations are assigned to the variables displayed. This assumption of equivalence is responsible for considerable confusion and misinterpretation whenever dynamic amplification or attenuation is appreciable.

As indicated above, the definition of hub impedance along and normal to the shaft is necessary for establishing corresponding conditions between free flight and the wind tunnel for moments, shears, and vibration in the case of the two-bladed teetering rotor, and for shears and vibration in the case of the hinged rotor. The problem can be viewed thus: The mass and elastic properties of the hub and blade can be accurately defined. The loads developed in the blade in flight depend on the aerodynamic reactions which are, among other things, functions of azimuth and frequency and the dynamic reactions at the hub which are also functions of azimuth and frequency. Much effort has been expended in determining the airload reactions, while relatively little research has been aimed at the definition of hub impedance.

On several occasions during the past 15 years, variations in hub impedance have shown appreciable effects on rotor loads. The lack of precise understanding of this problem has necessitated the use of factors of safety in rotor design and often has frustrated attempts to correlate loads determined by analysis and test. To remove these deficiencies, research toward an accurate treatment of hub impedance has accelerated during the past year, taking advantage of improvements in analytical and test methods accruing over a period of several years. Significantly improved treatments of hub impedance are now being incorporated in all rotor loads analyses.

The hub impedance problem has important implications for establishing corresponding test conditions between the Freon tunnel and the flight tests of the UH-1B used for comparison. No attempt was made to scale the impedance along the drive shaft; and, although the first pylon frequency was scaled, its inertia was not because it was not feasible to scale its weight. The magnitude of the error in loads from this source is not known.

Loads Correlation Between Full-Scale Flight and Full-Scale Tunnel Tests

The quarter-scale Freon tunnel tests show good trend correlation; however, the quantitative correlation is not as good as desired. At this time it is not possible to determine if the lack of correlation is due to the Freon medium, the nonscaled model hub impedance or some other factors. Valuable guidance in resolving this question could have been obtained from a correlation study between the full-scale rotor-pylon system in a full-scale tunnel and in free flight. Such a test was not accomplished, and it is not known to what extent full-scale correlation could be achieved primarily because of the hub impedance question. Lack of full-scale correlation would not likely be ascribed to the medium.

Summary of Loads Correlation Concepts

The preceding disucssion has been aimed at putting the loads correlation problem in perspective both for model and full-scale tunnel tests by calling attention to (1) the need for more precise correlation criteria, (2) the necessity for exercising great care in determining corresponding test conditions between tunnel and flight, and (3) the need to establish correlation between full-scale wind tunnels and free flight.

CONCLUSIONS

Small-scale rotor performance and loads data for -10-degree twist and 0-degree twist two-bladed teetering rotor systems have been obtained in a Freon wind tunnel. Comparisons of the model test results with theory and full-scale test results were made to ascertain the validity of the model test data. The significant conclusions from the program follow:

- The -10-degree twist model rotor performance shows good agreement with standard and thin-tip UH-1D Mach number trends, considering their airfoil profile and thickness ratio differences. In the 0-degree twist rotor comparisons, variations between rotor thickness ratios at inboard radius stations are shown to have little influence on the Mach number trends.

- Theoretical calculations of Mach number trends show large overestimation of power above 0.90 advancing-tip Mach number when compared with the model test data. A comparison of model and full-scale theory calculations indicates that the use of NACA 0012 airfoil data did not cause this behavior. A possible explanation for the test-theory differences is that supercritical flow effects in Freon may be less severe than in air. An experimental model test of a rotor using an NACA 0012 airfoil will be necessary to answer this question.

- The model and full-scale experimental performance as a function of advance ratio show no significant trend differences. Theoretical predictions of the advance ratio trends were made using a uniform inflow analysis. At low lift coefficients, the theory underestimates high advance ratio ($\mu > 0.45$) power requirements. This behavior is not shown at higher lift coefficients because the theory predicts rotor stall at very low lift and propulsive force coefficients in comparisons with the model data.

- Trend correlation shows that it is feasible to determine full-scale, free-flight loads using a dynamically scaled model in the Freon tunnel.

- Quantitative correlation of the oscillatory moments of the model and flight test data did not yield the accuracy desired. Sources of error large enough to account for the difference between the tunnel and flight loads probably reside in the nonscaled hub impedance and discrepancies in the original full-scale rotor stiffness values used for model scaling.

- The criteria and methods for rotor correlation studies between free-flight and tunnel tests for the categories of aerodynamic performance, stability, vibration, rotor moments, and rotor shear forces have not been adequately defined in the past. Results from the subject tests offer significant improvements in test concepts for loads correlation.

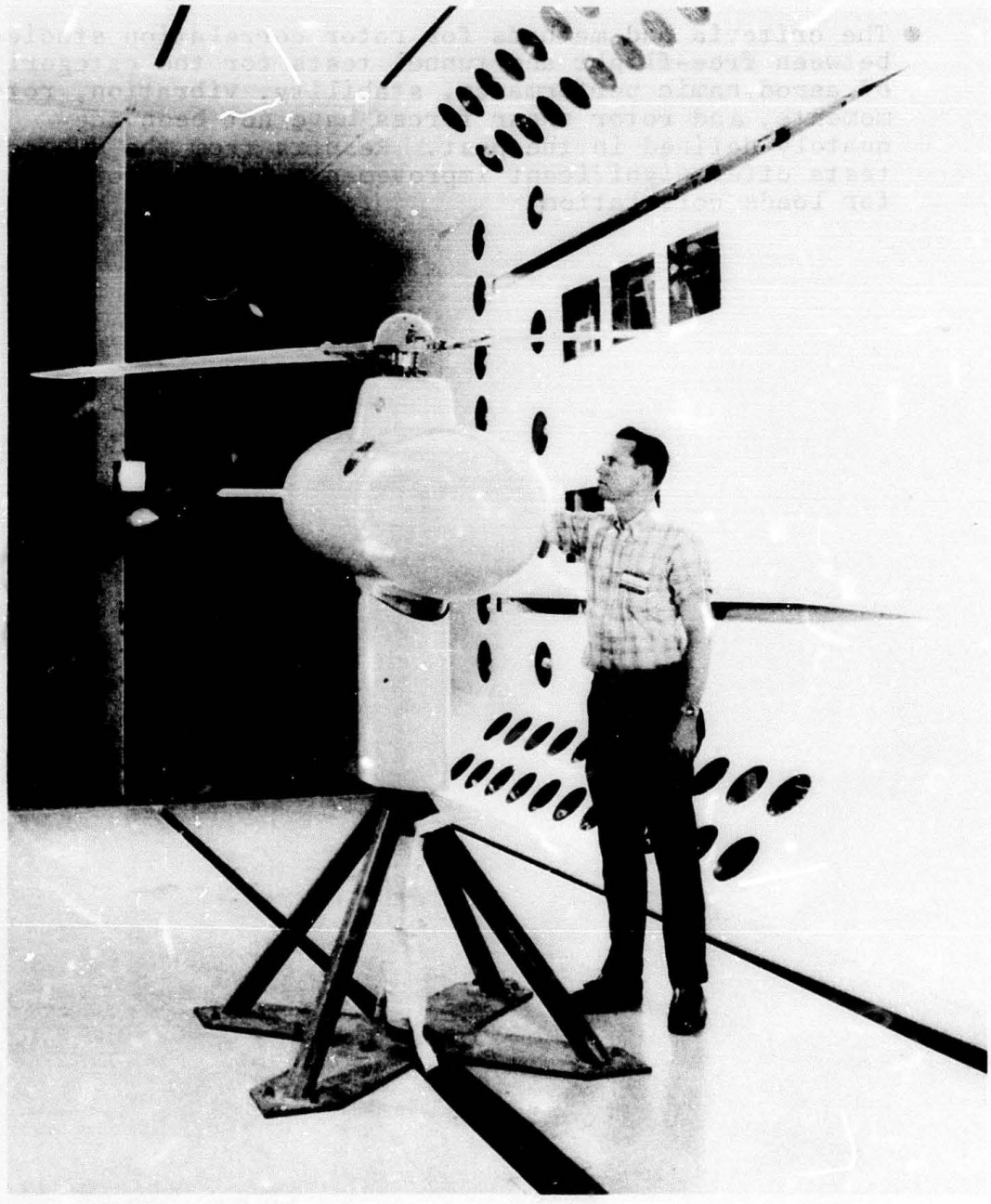

Figure 1. Model Installed in Tunnel.

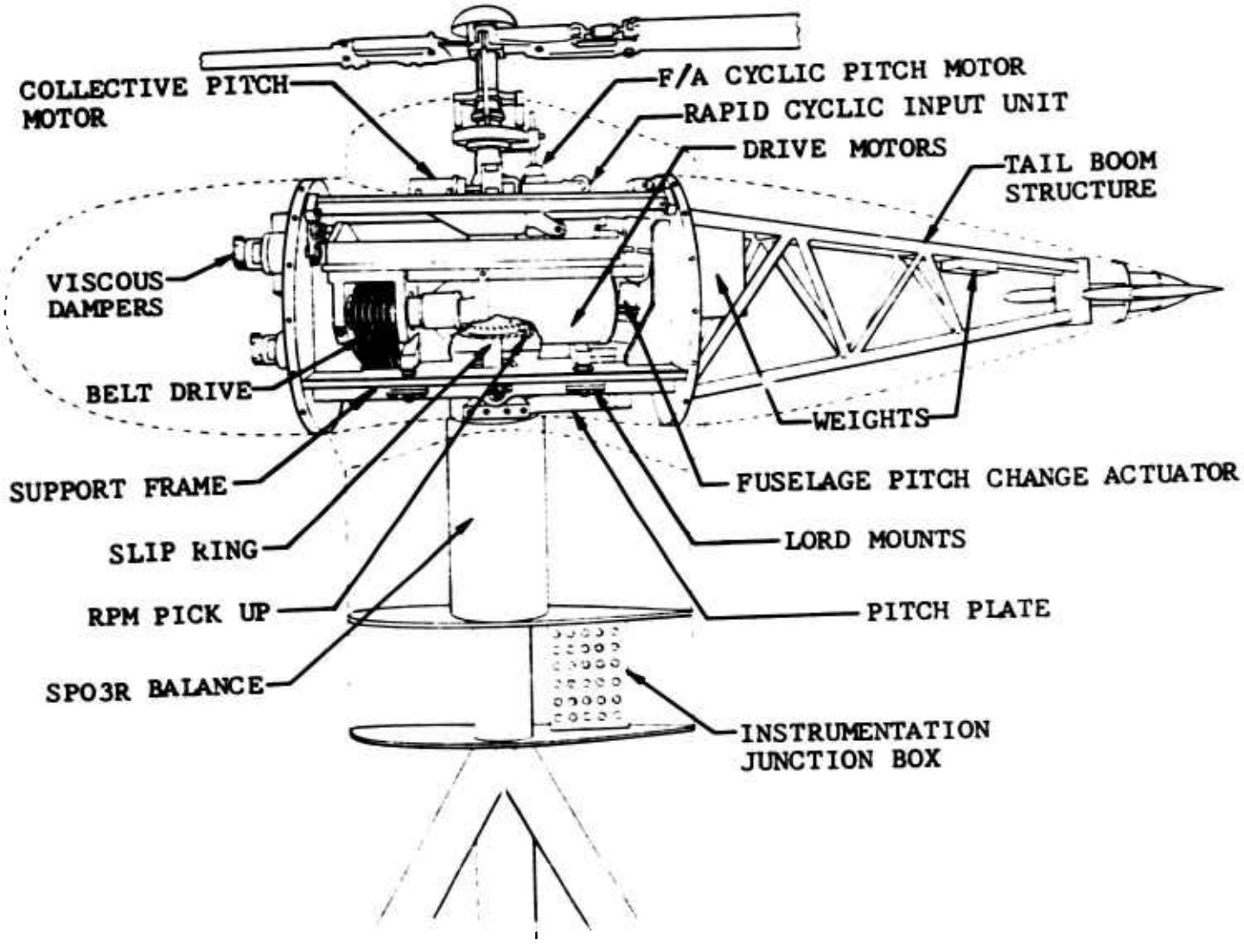

Figure 2. Model Schematic.

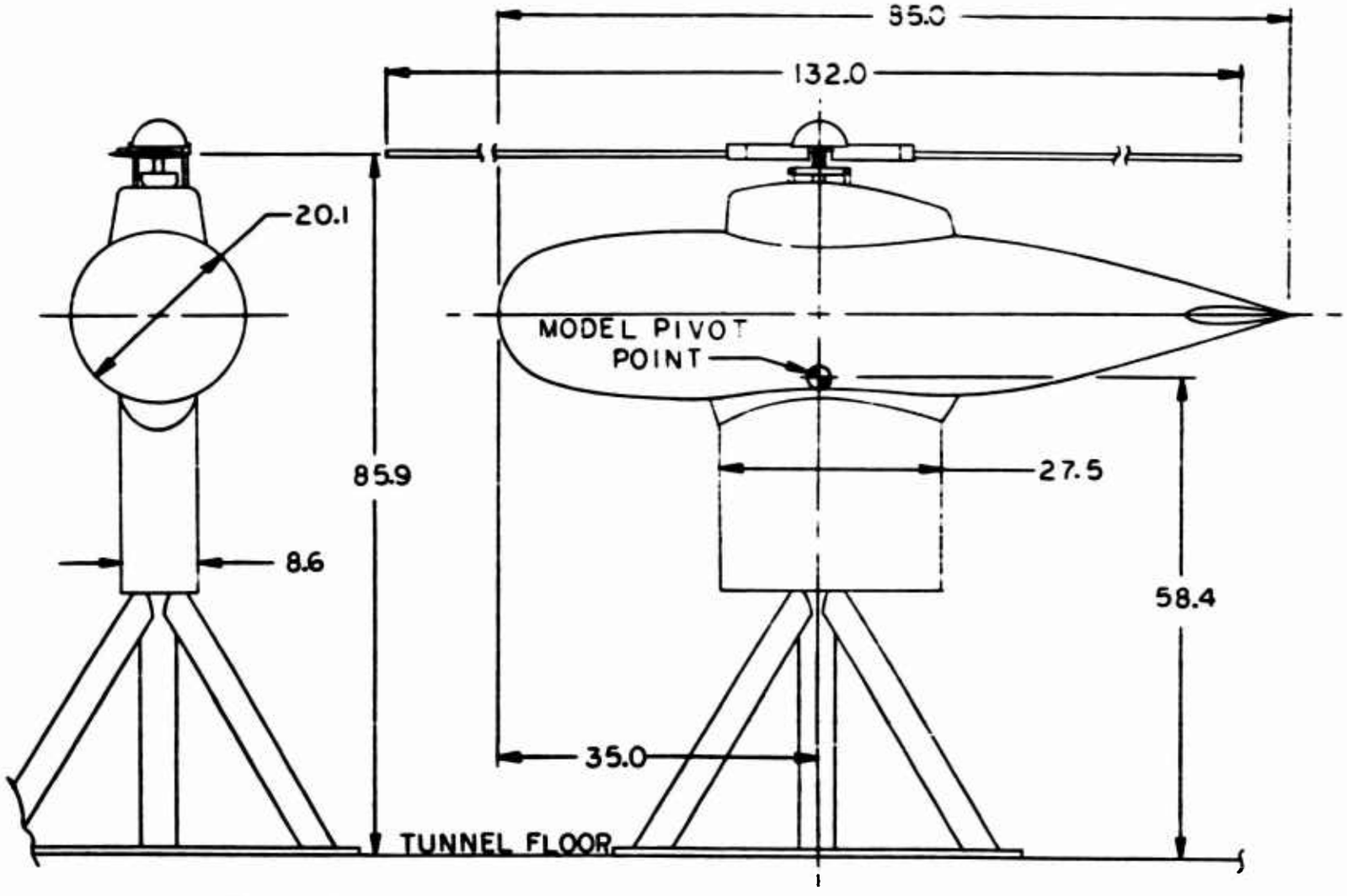

Figure 3. Model Installation Dimensional Data.
All Dimensions in Inches.

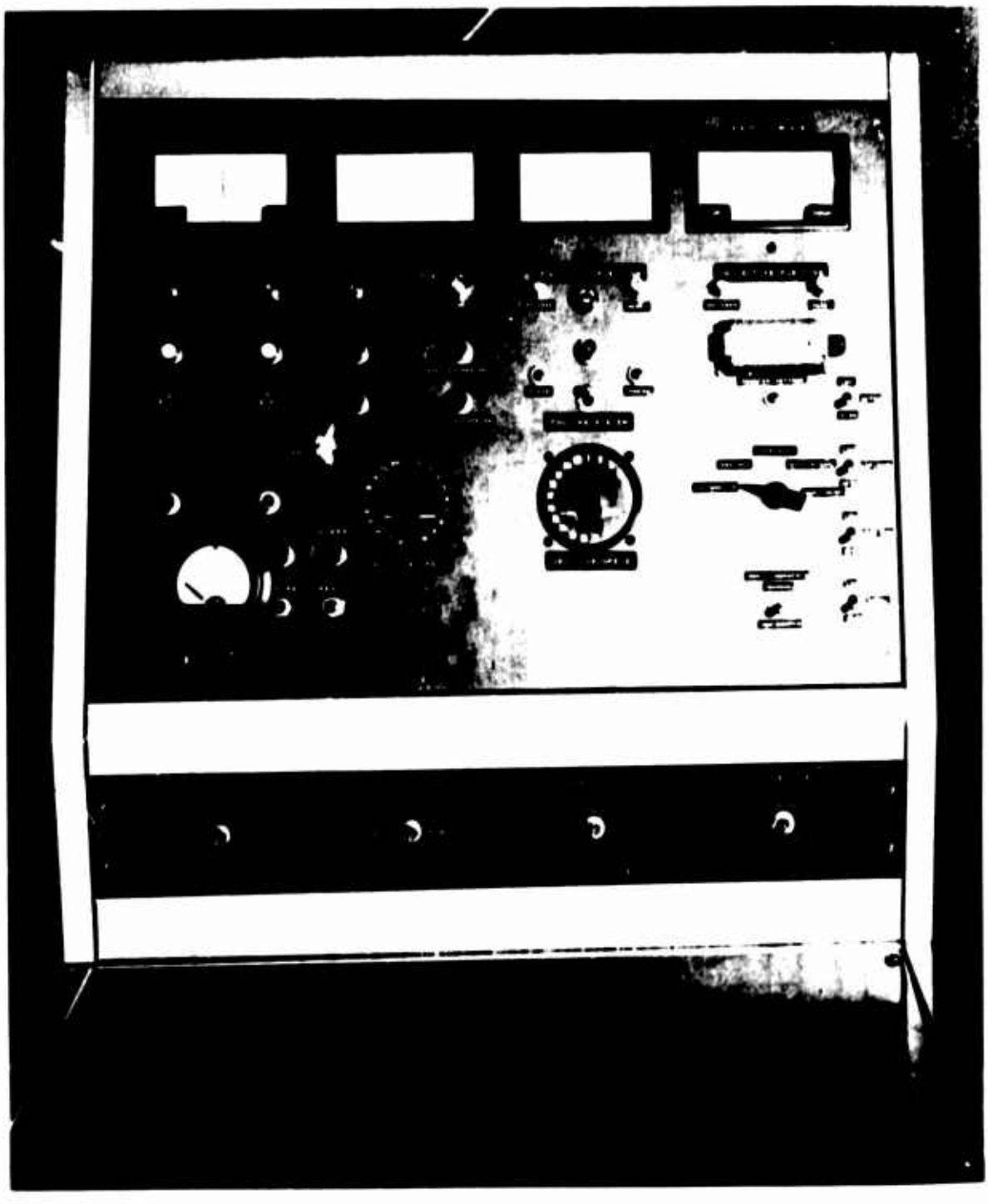

Figure 4. Control Console.

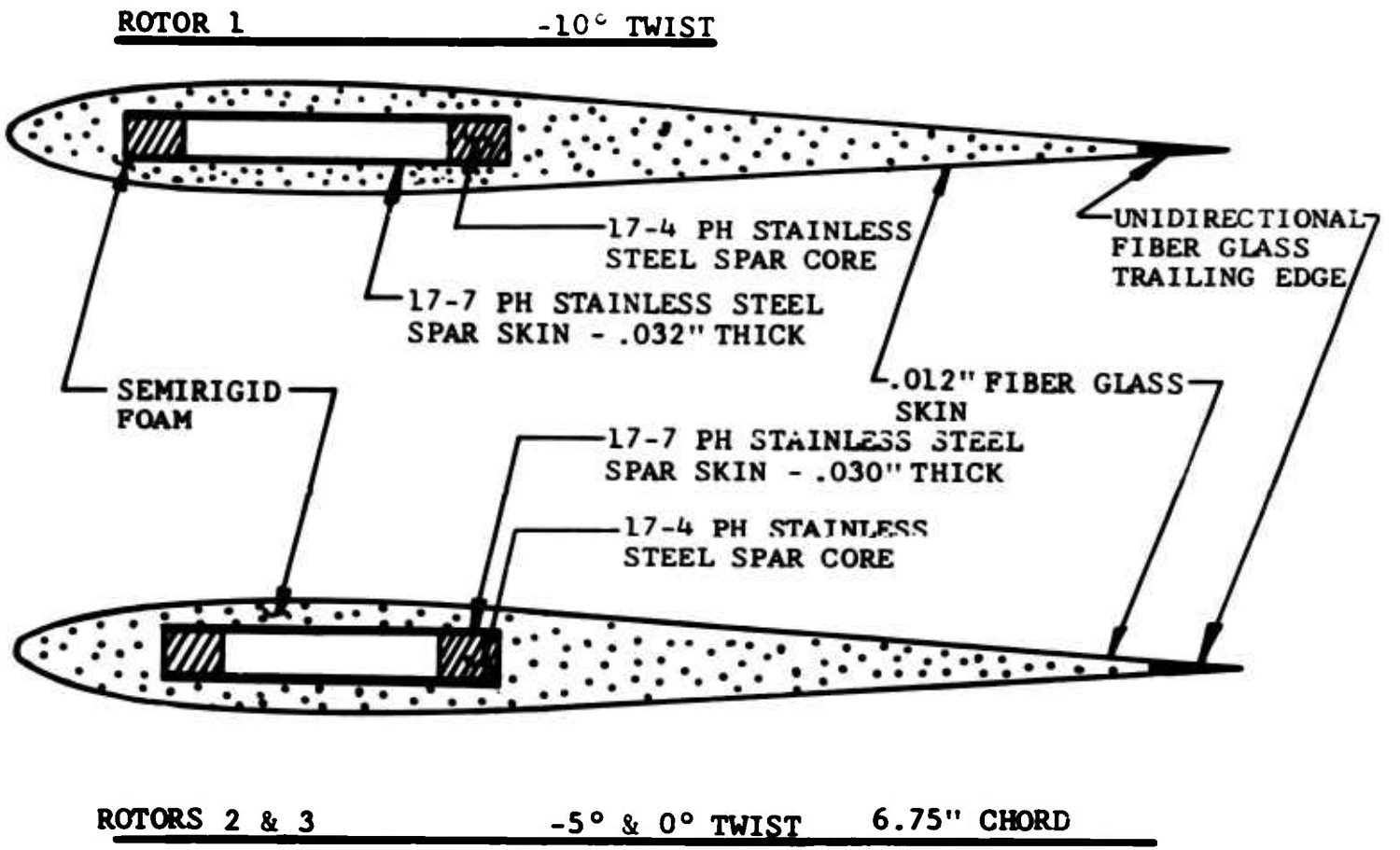

Figure 5. Typical Rotor Cross Sections.

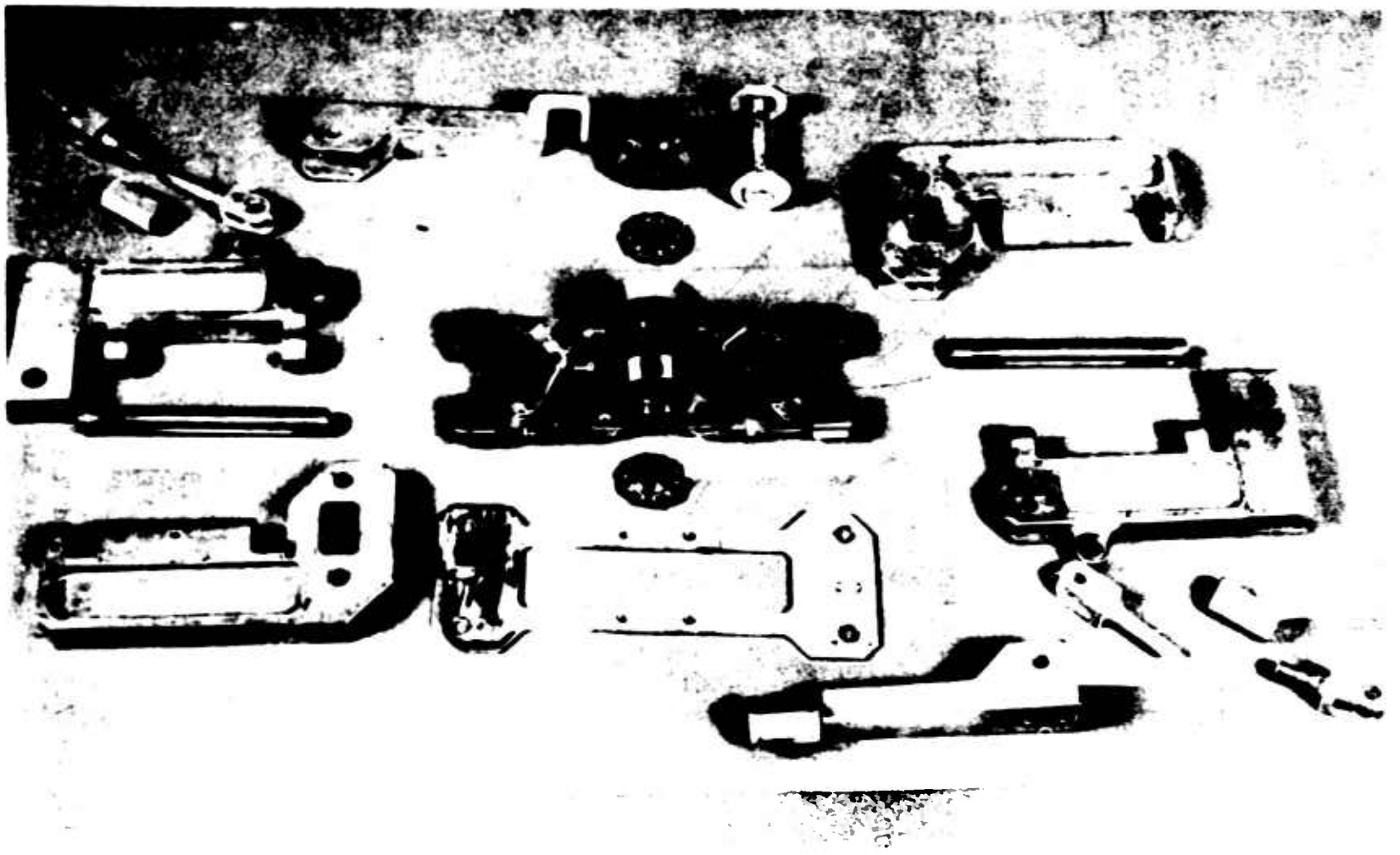

Figure 6. Model Hub Components.

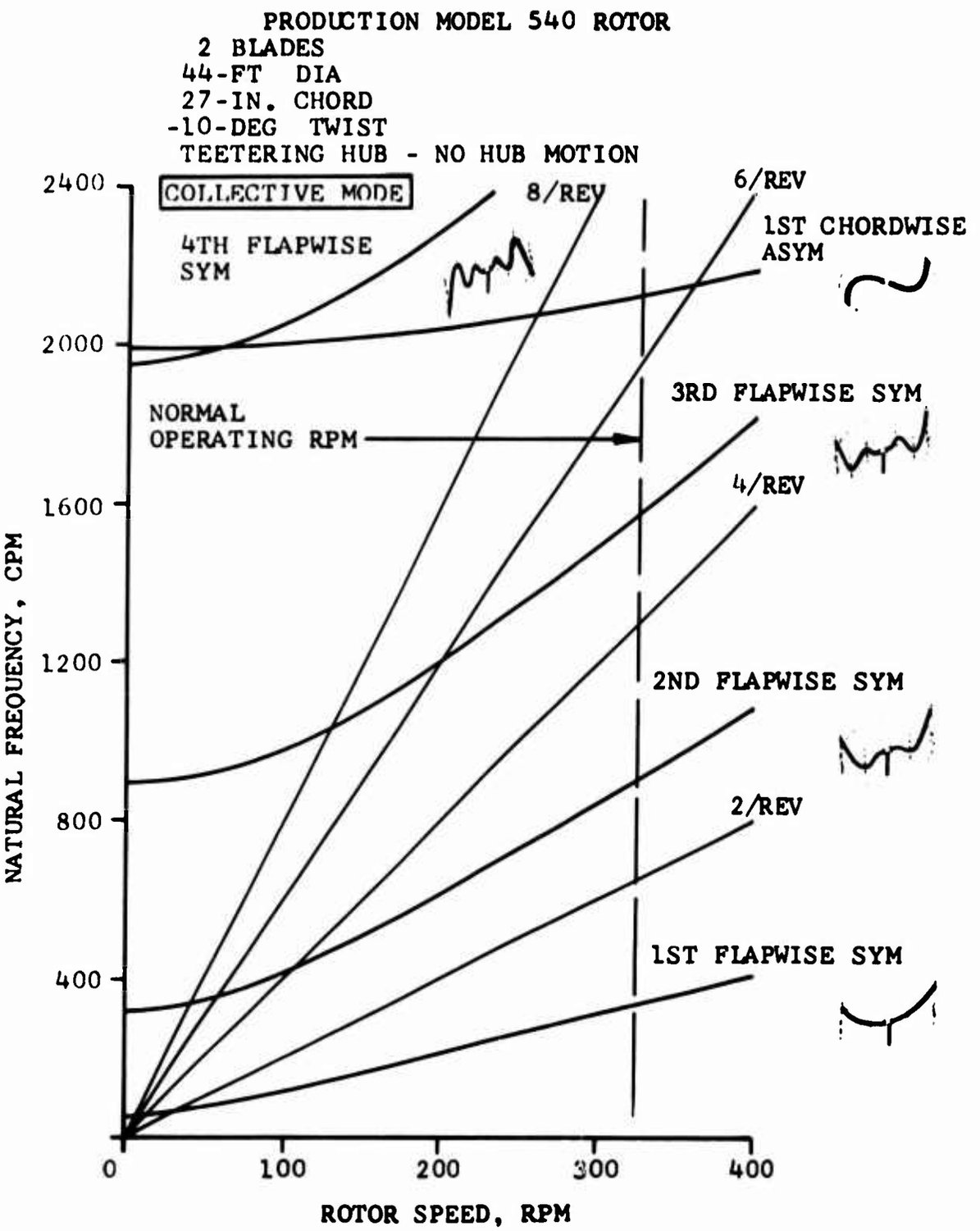

Figure 7. Uncoupled Rotor Natural Frequencies, Full-Scale Rotor (Collective Mode).

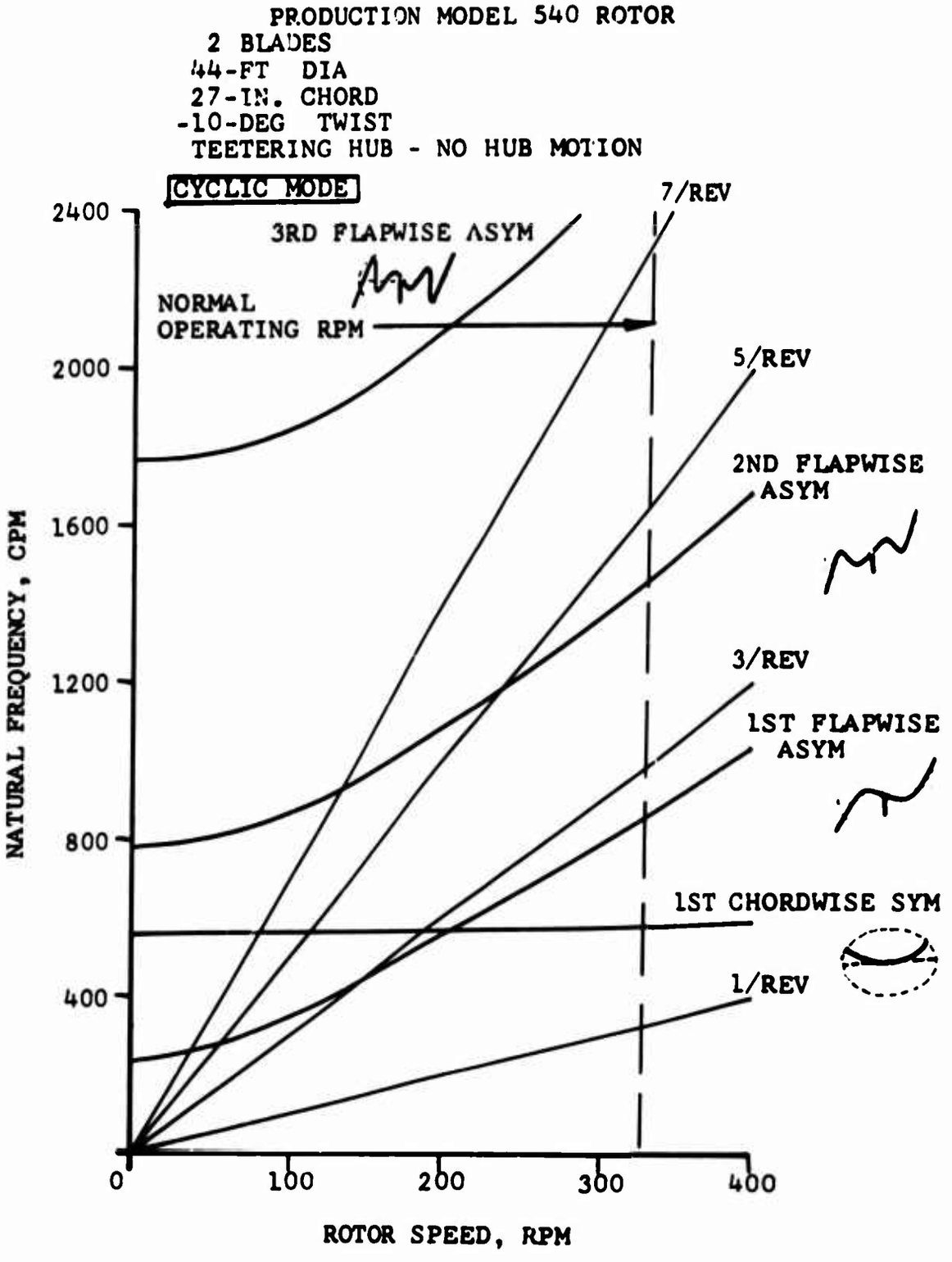

Figure 8. Uncoupled Rotor Natural Frequencies, Full-Scale Rotor (Cylic Mode).

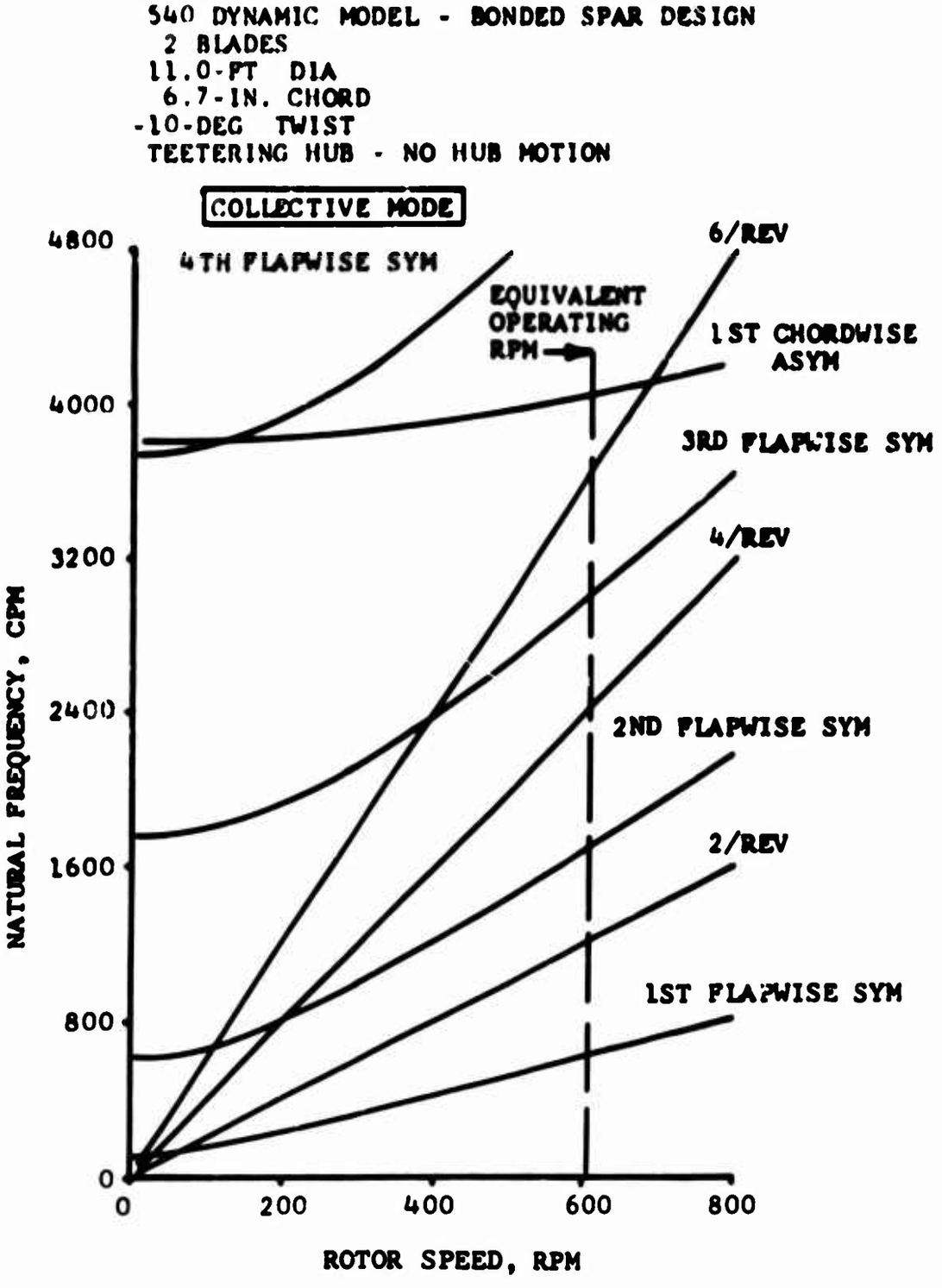

Figure 9. Uncoupled Rotor Natural Frequencies, -10-Degree-Twist Model Rotor (Collective Mode).

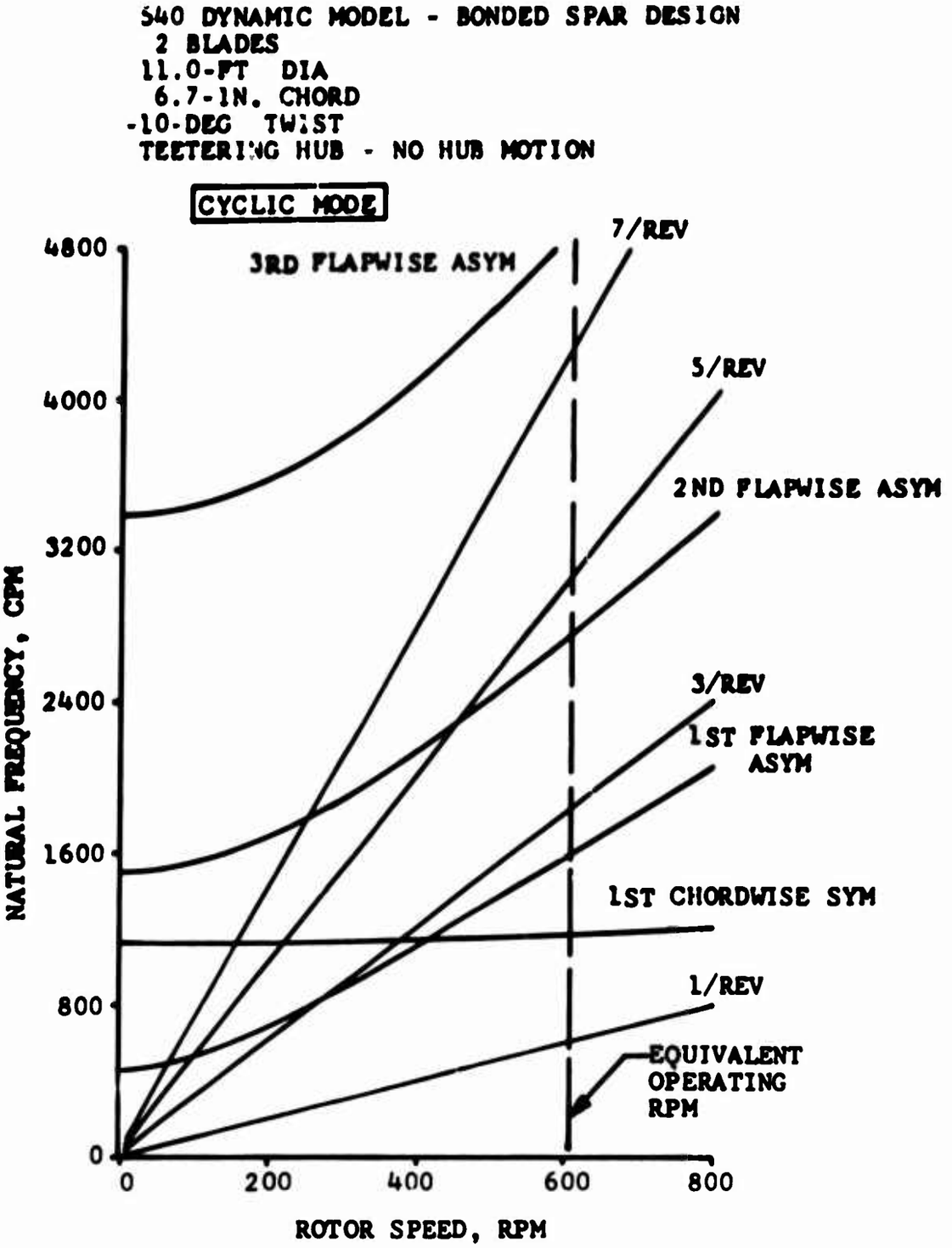

Figure 10. Uncoupled Rotor Natural Frequencies, -10-Degree-Twist Model Rotor (Cyclic Mode).

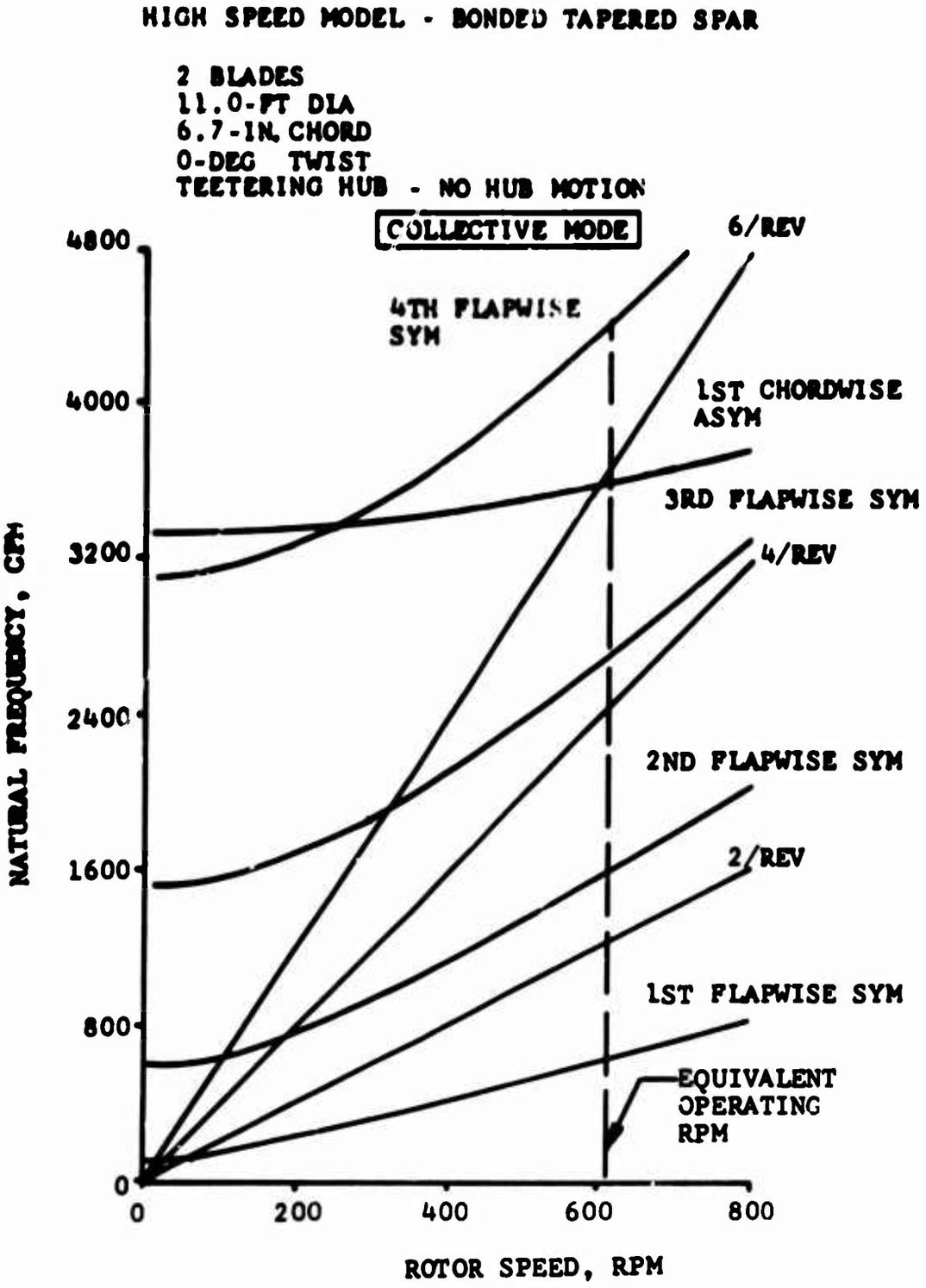

Figure 11. Uncoupled Rotor Natural Frequencies, 0-Degree-Twist Model Rotor (Collective Mode).

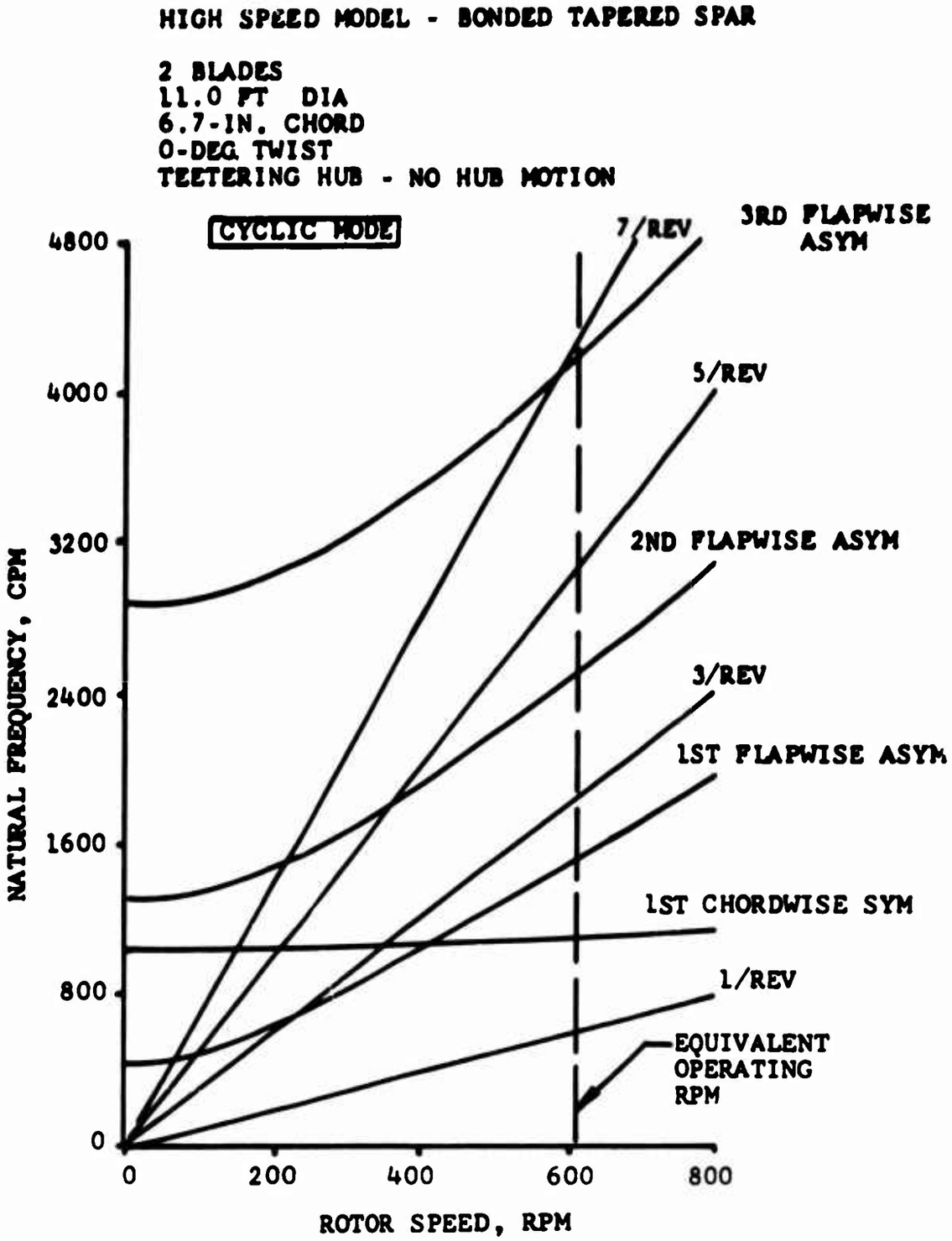

Figure 12. Uncoupled Rotor Natural Frequencies, 0-Degree-Twist Model Rotor (Cyclic Mode).

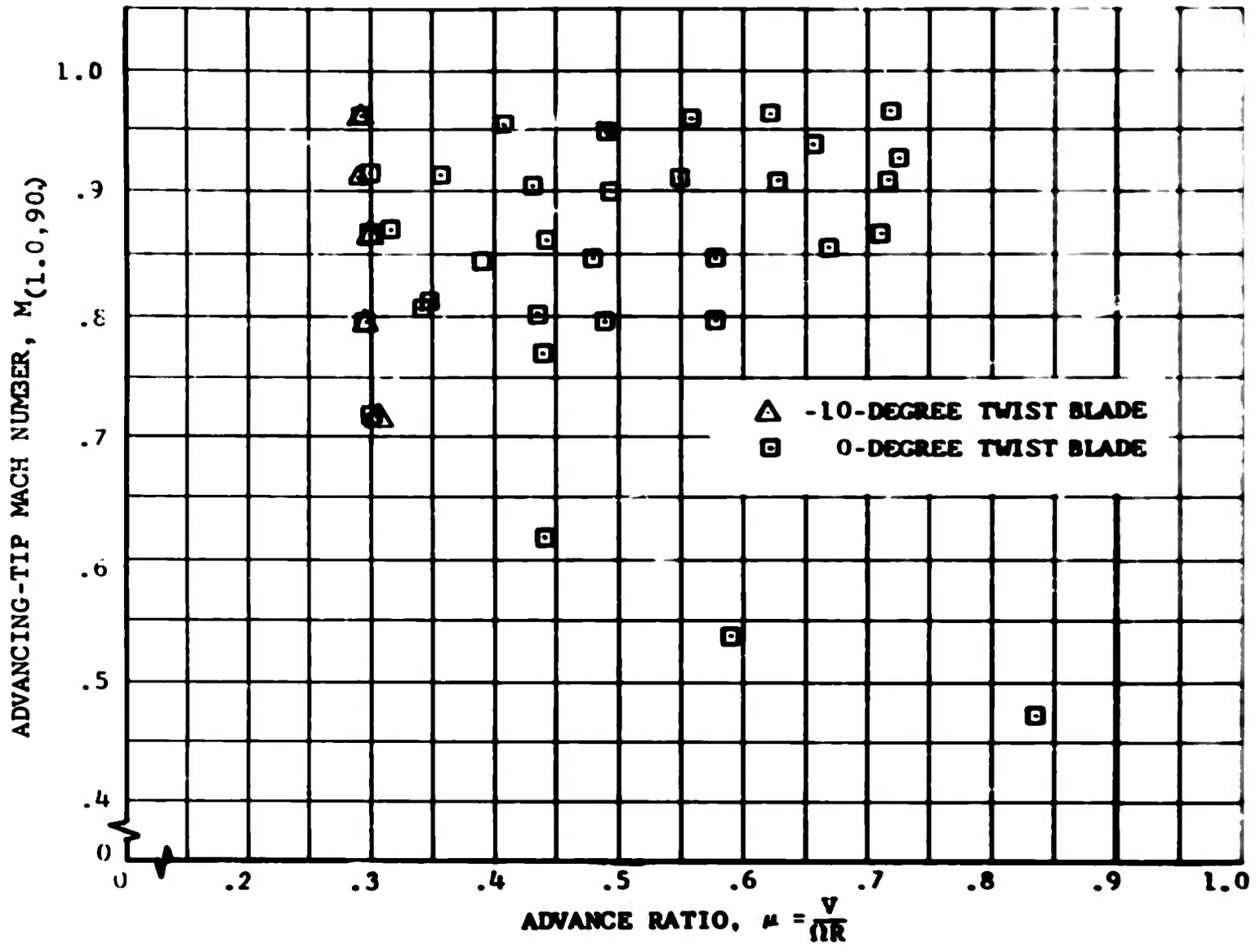

Figure 13. Model Test Conditions.

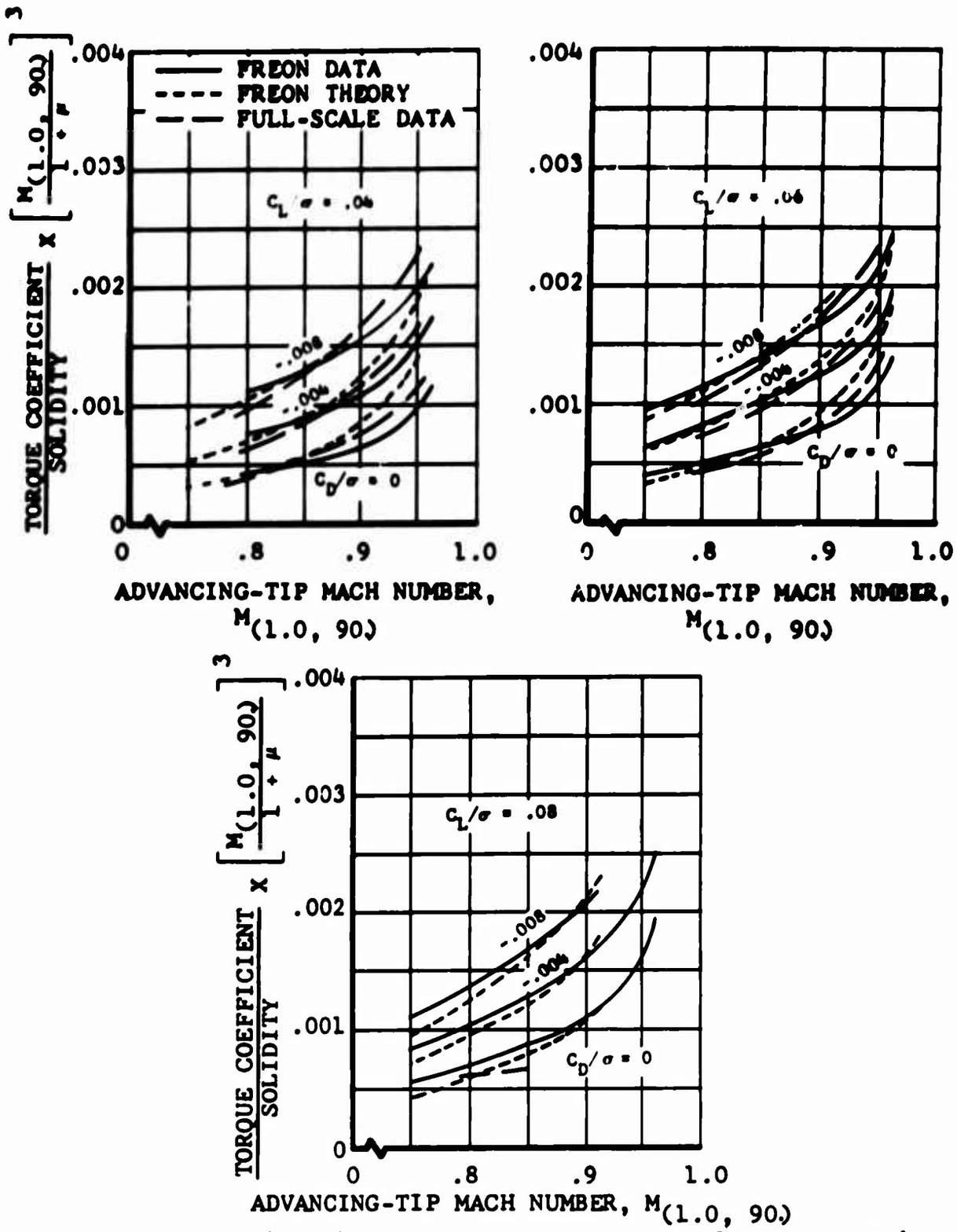

Figure 14. Nondimensional Performance of the -10-Degree-Twist Model Rotor as a Function of Advancing-Tip Mach Number at 0.30 Advance Ratio With Full-Scale UH-1D Rotor and Theory Performance Comparisons.

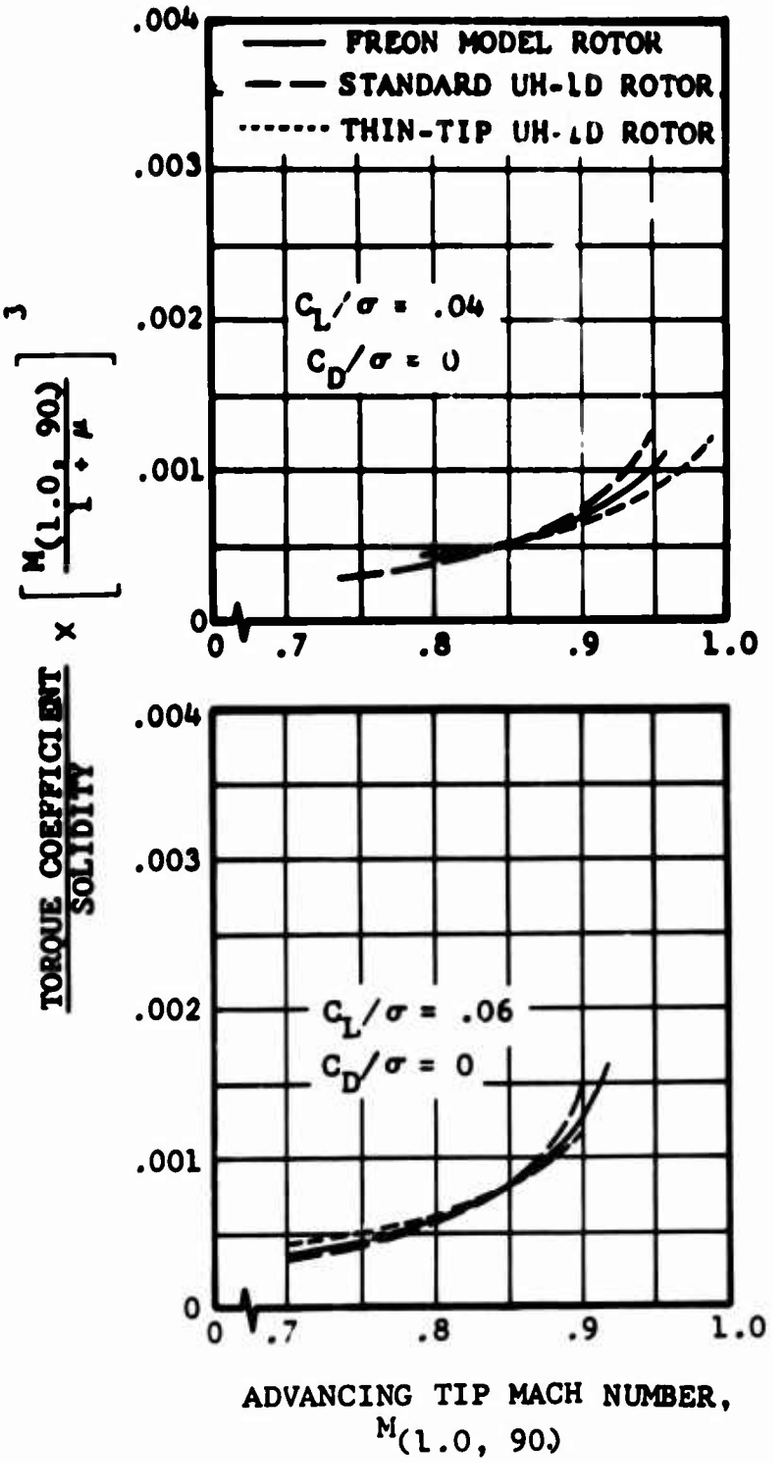

Figure 15. Nondimensional Performance of a -10-Degree-Twist Model Rotor as a Function of Advancing-Tip Mach Number at 0.30 Advance Ratio With Standard Tip and Thin Tip UH-1D Rotor Comparisons.

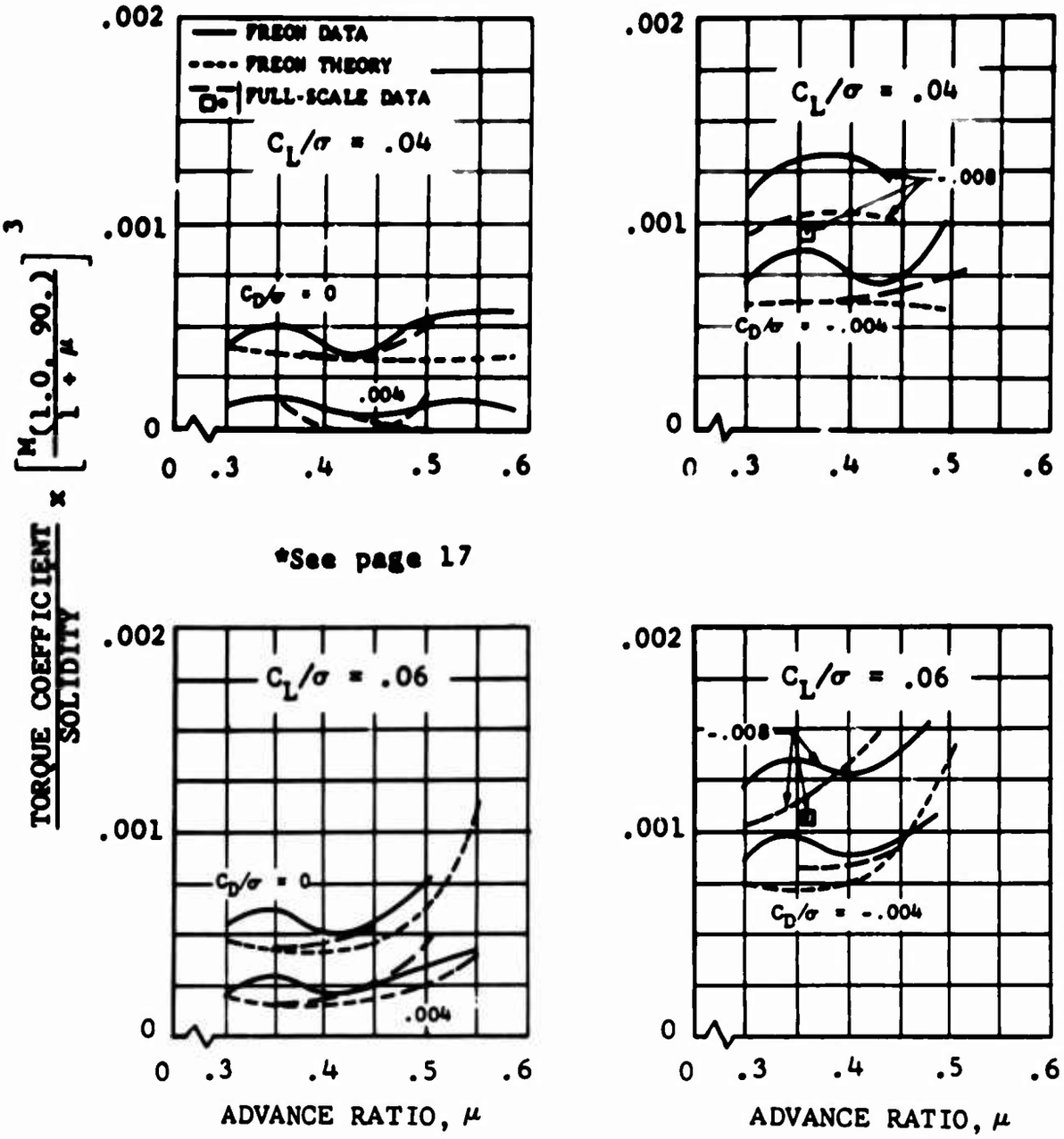

*See page 17

(a) $M_{(1.0,\ 90.)} = 0.80$

Figure 16. Nondimensional Performance of the 0-Degree-Twist Model Rotor as a Function of Advance Ratio at Various Advancing-Tip Mach Numbers With Full-Scale UH-1B (Modified) Rotor and Uniform-Inflow Theory Performance Comparisons.

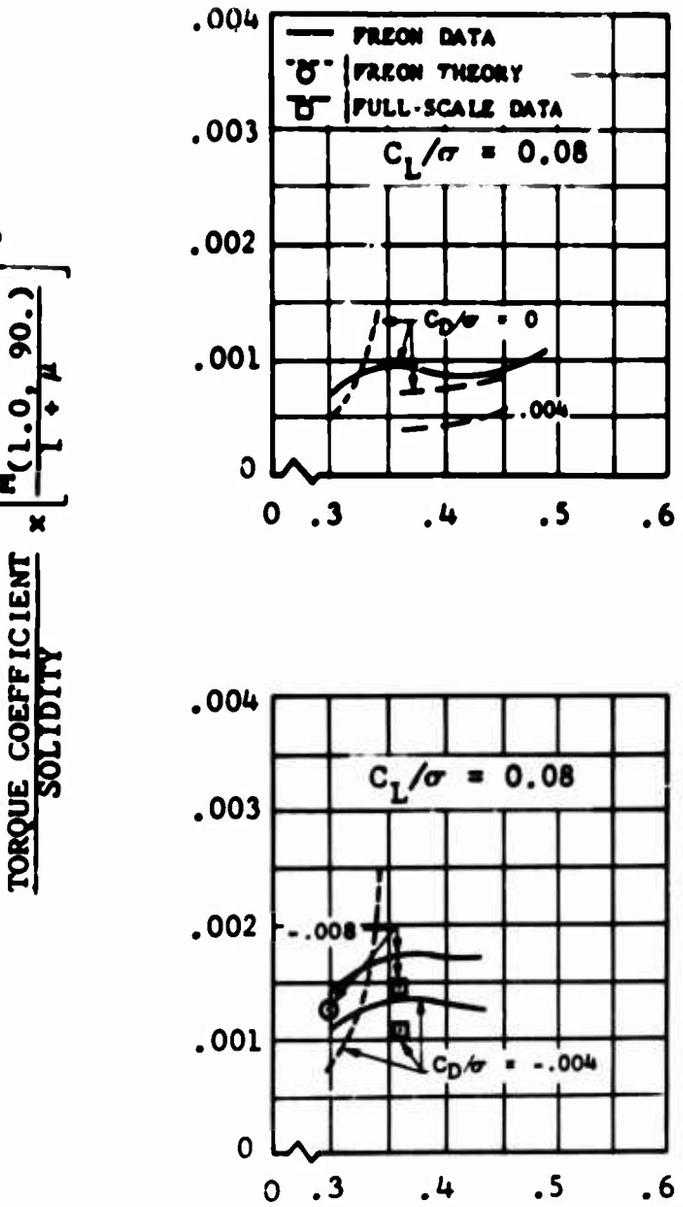

(a) Concluded.

Figure 16. Continued.

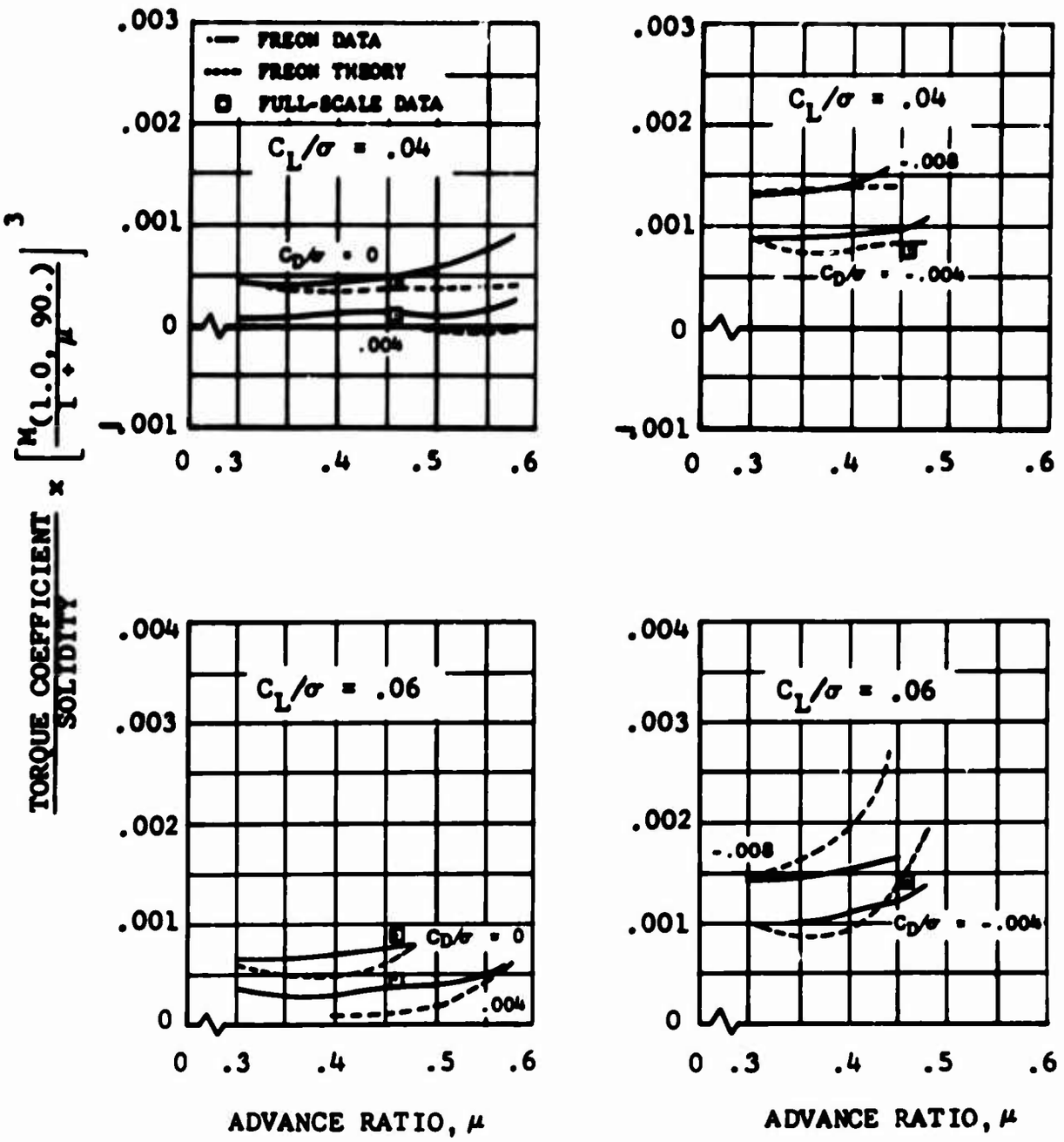

(b) $M_{(1.0,\ 90.)} = 0.85$

Figure 16. Continued.

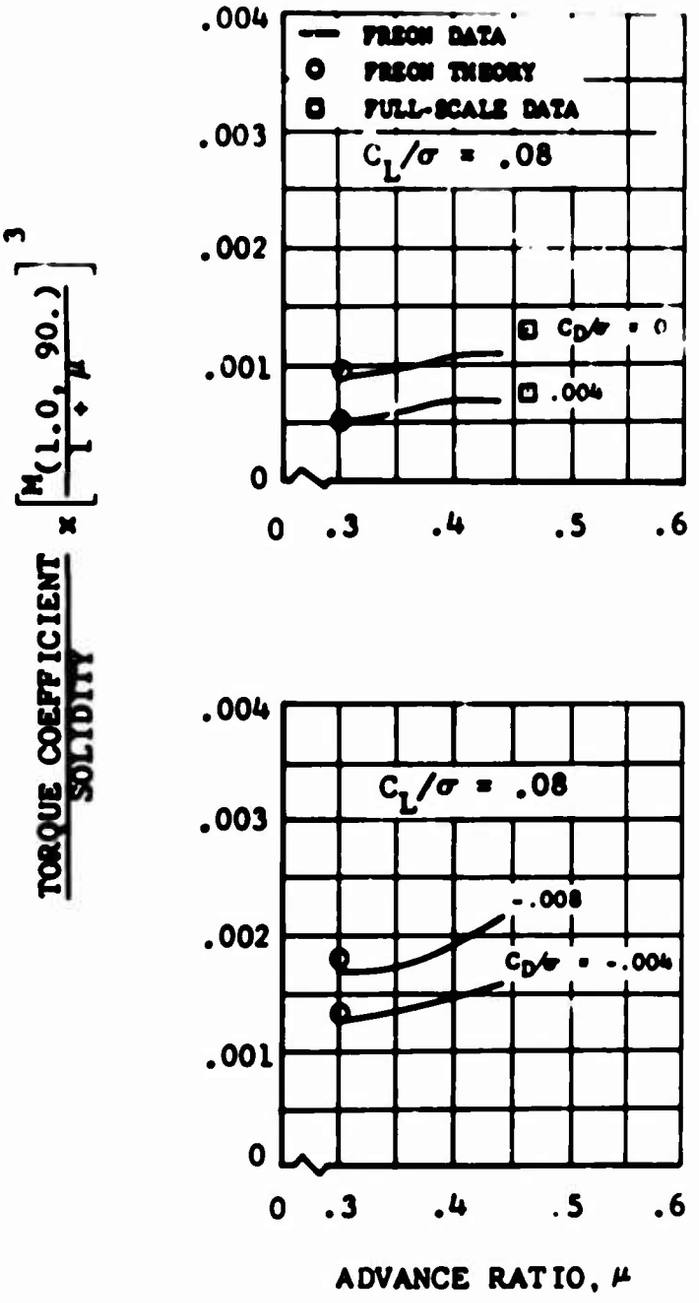

(b) Concluded.

Figure 16. Continued.

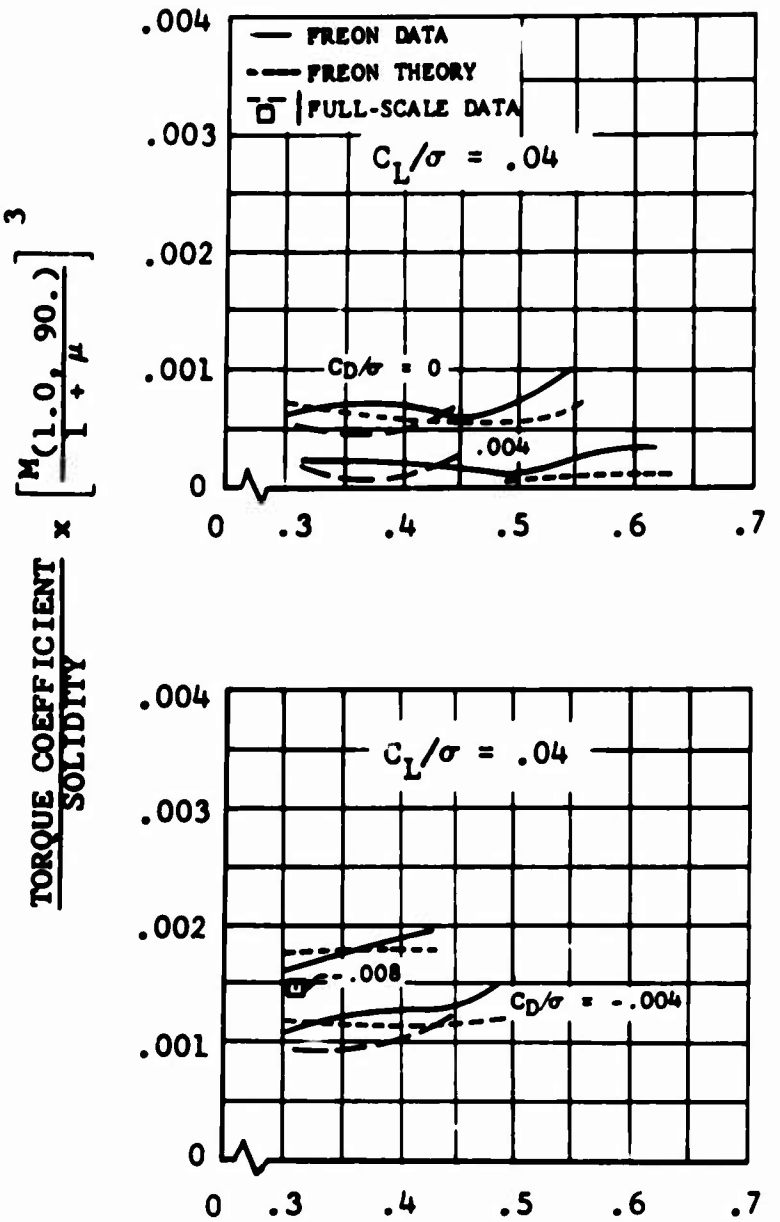

(c) $M_{(1.0,\ 90.)} = 0.90$

Figure 16. Continued.

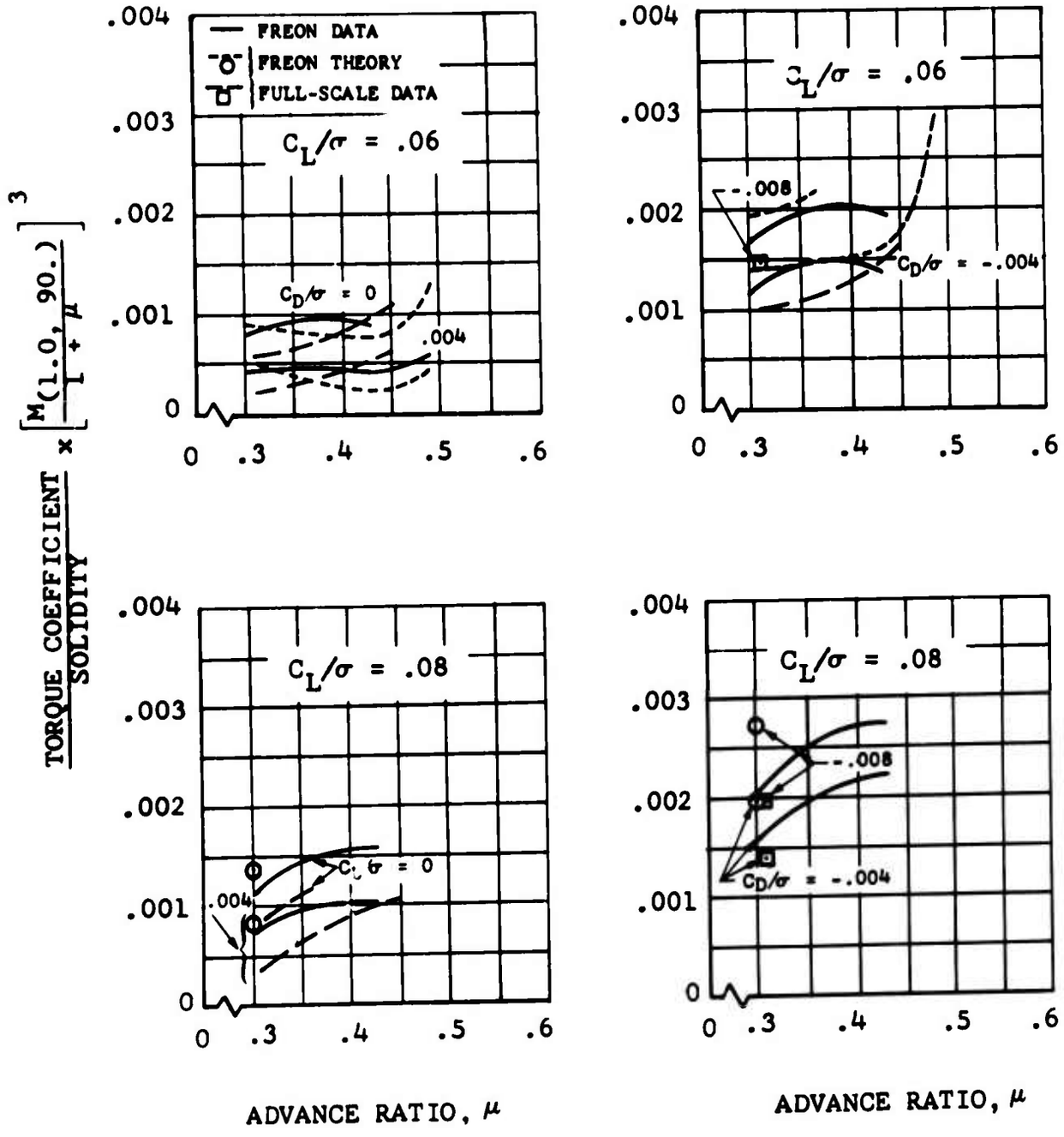

(c) Concluded.

Figure 16. Continued.

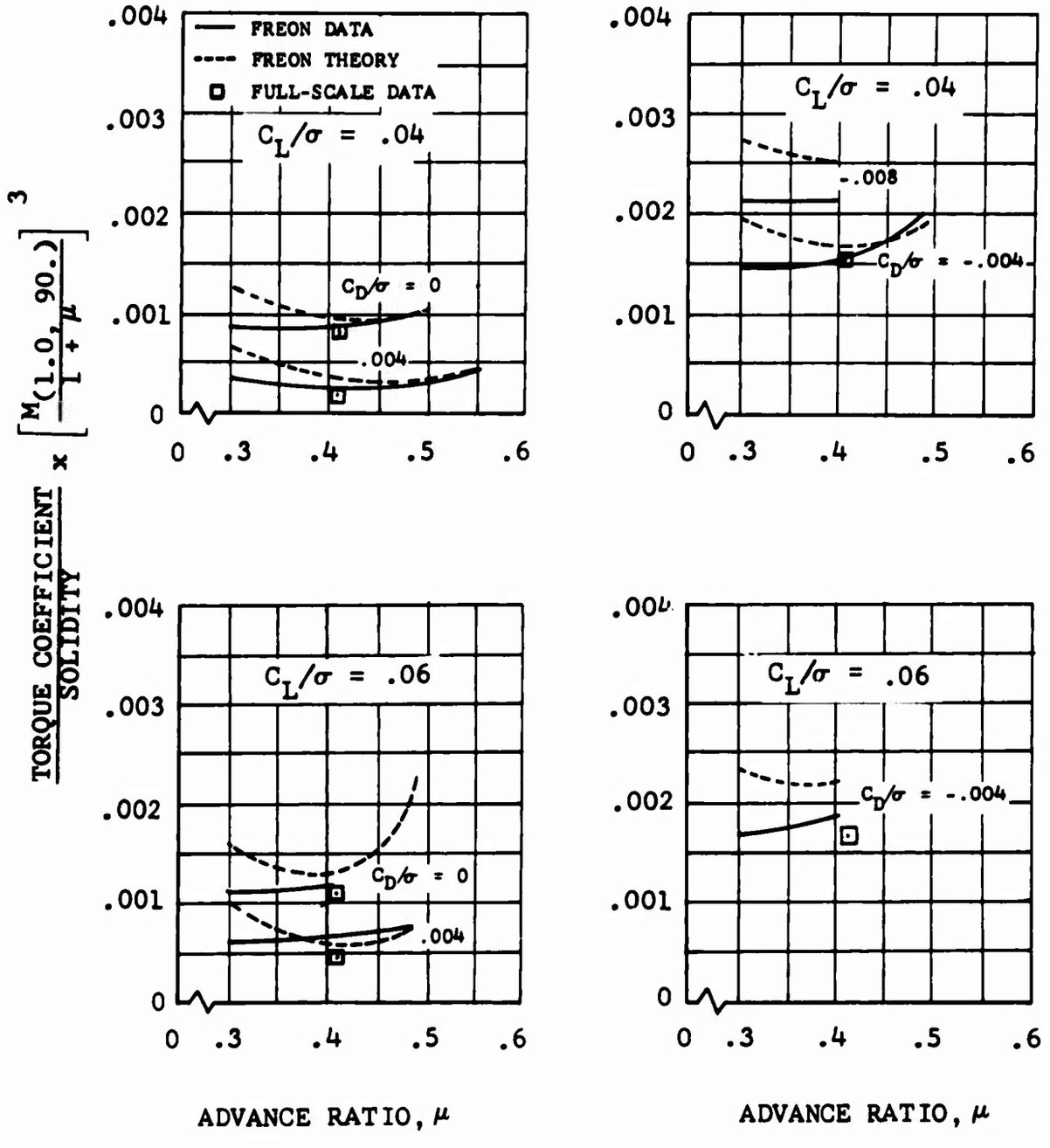

(d) $M_{(1.0,\ 90.)} = 0.95$

Figure 16. Continued.

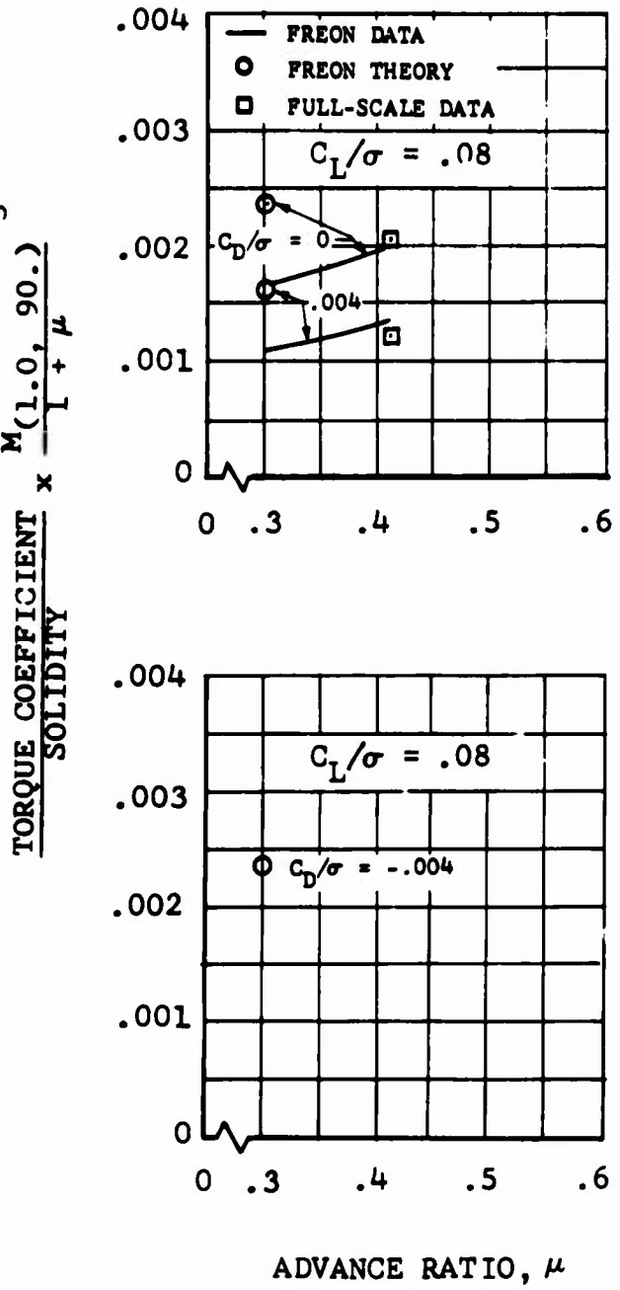

(d) Concluded.

Figure 16. Concluded.

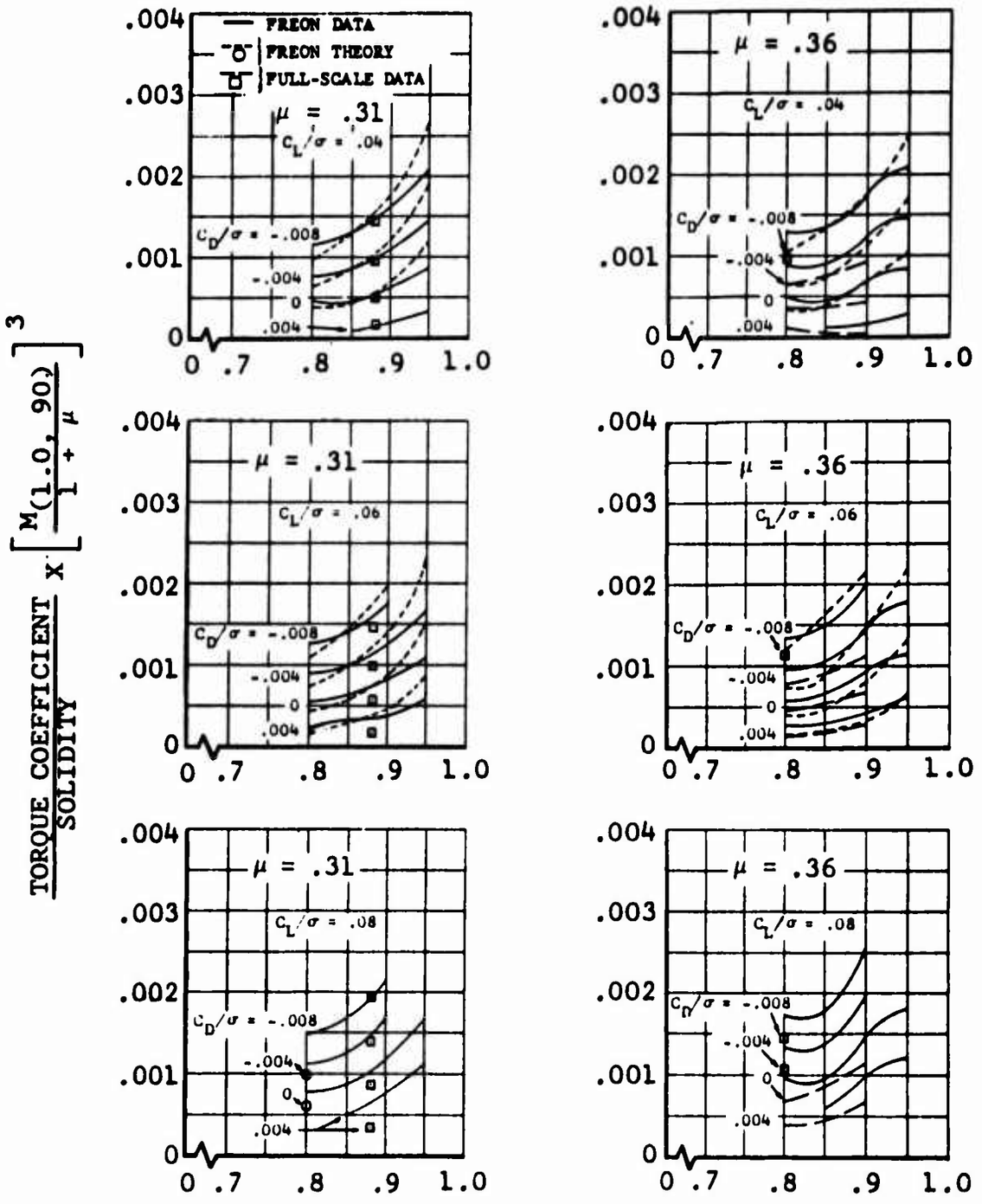

(a) μ = 0.31, 0.36

Figure 17. Nondimensional Performance of the 0-Degree-Twist Model Rotor as a Function of Advancing-Tip Mach Number at Various Advance Ratios With Full-Scale UH-1B (Modified) Rotor and Uniform-Inflow Theory Performance Comparisons.

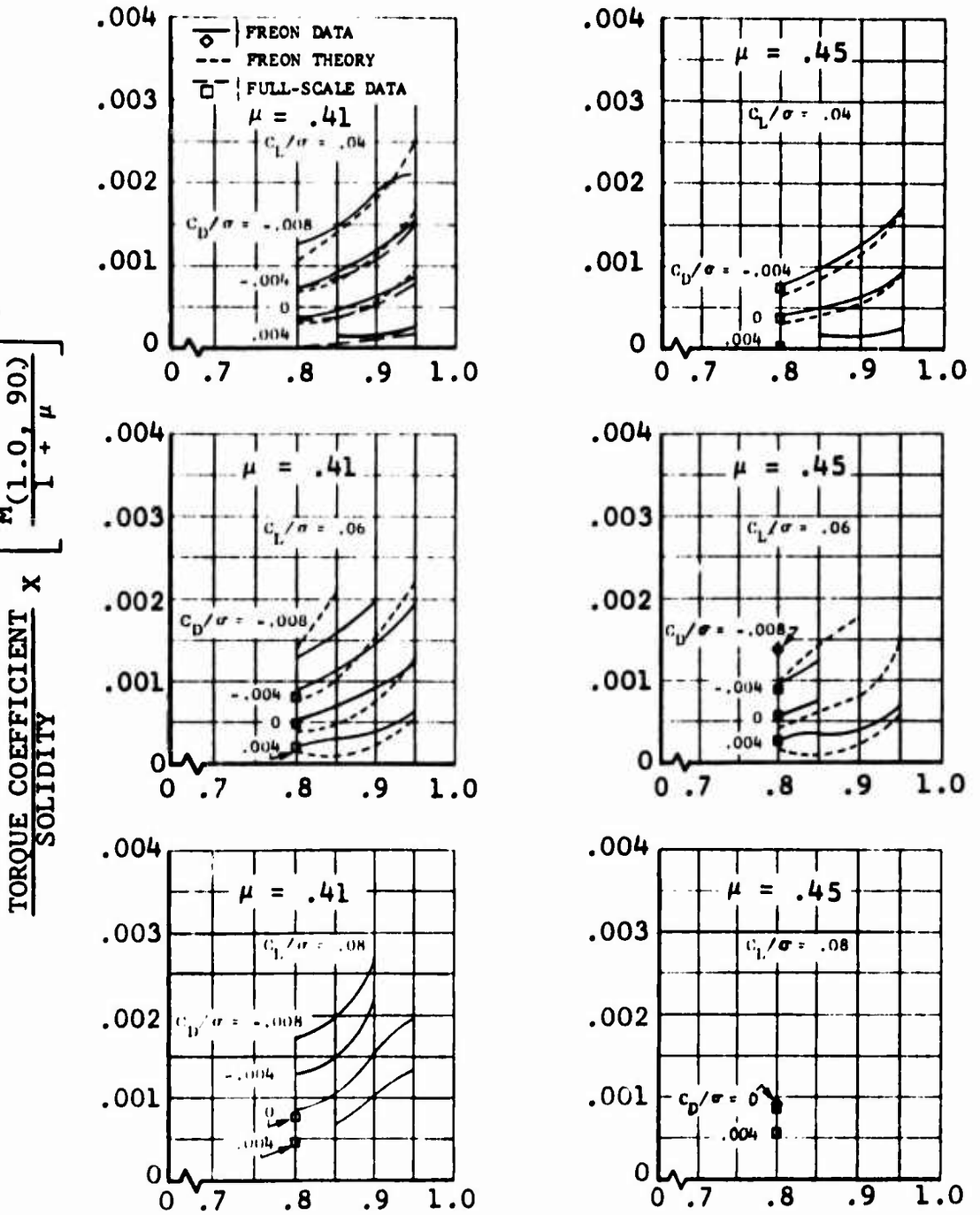

(b) μ = 0.41, 0.45

Figure 17. Concluded.

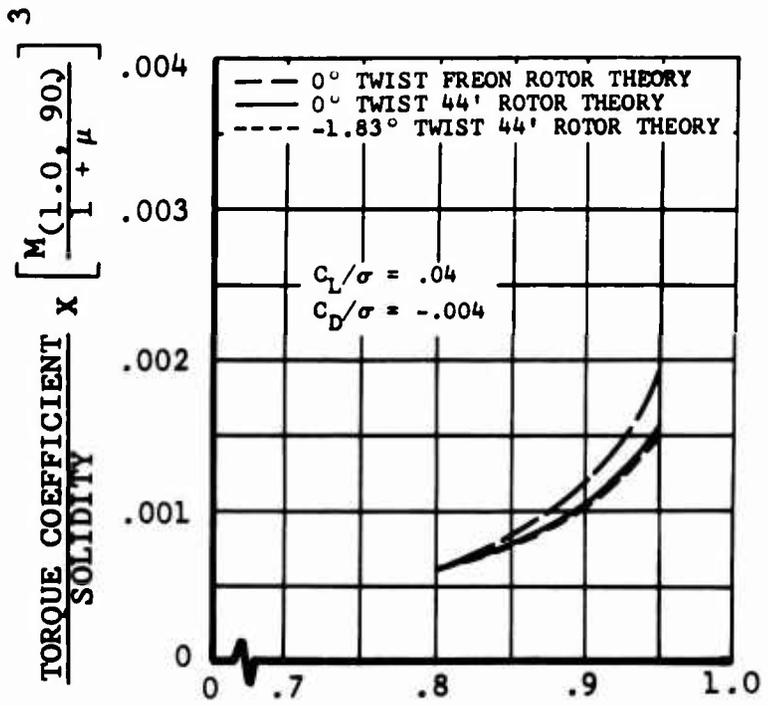

Figure 18. Nondimensional Comparison of Freon 0-Degree-Twist Model and Full-Scale UH-1B (Modified) Theoretical Rotor Performance as a Function of Advancing-Tip Mach Number at $\mu = 0.30$.

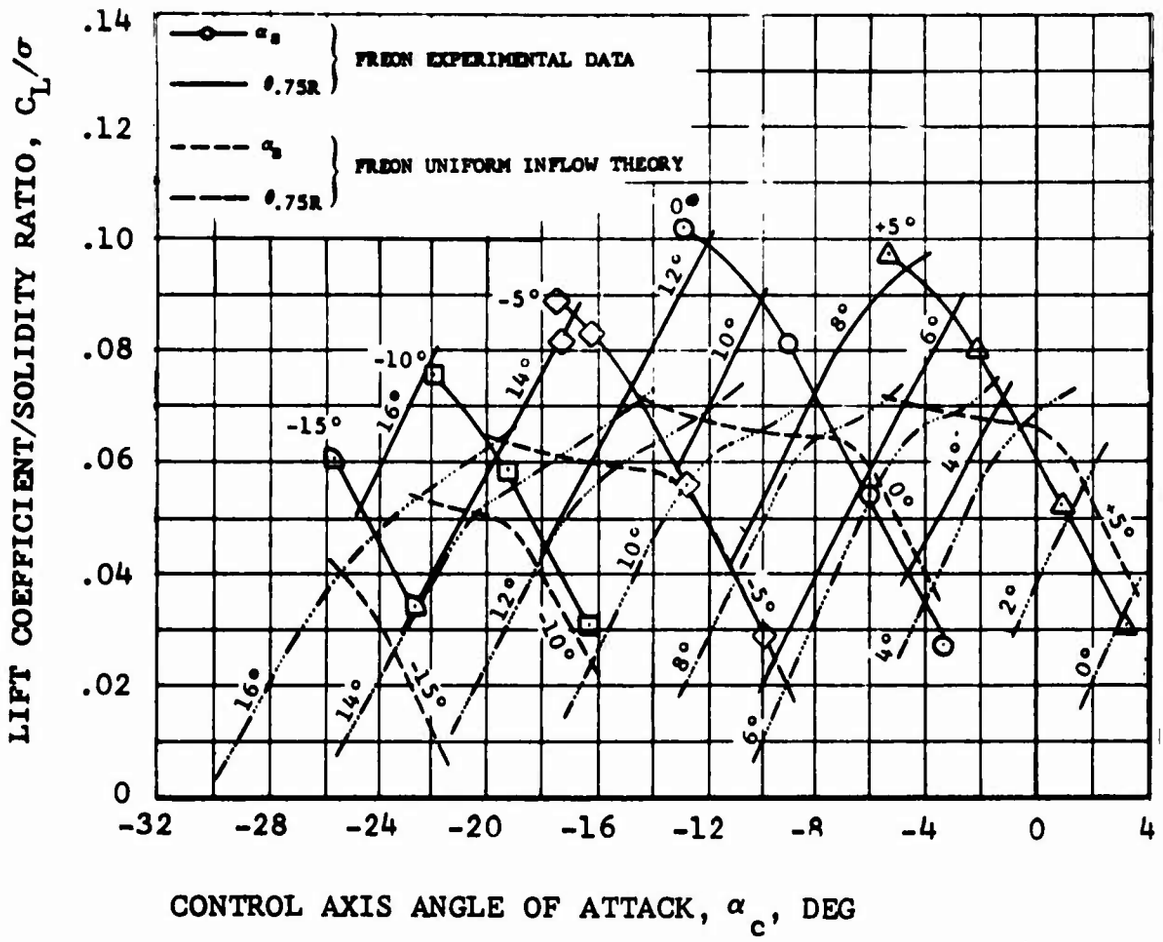

(a) C_L/σ vs α_c

Figure 19. Nondimensional Comparison of the 0-Degree-Twist Freon Experimental and Theoretical Performance, Including Various Control Positions at $\mu = 0.44$; $M_{(1.0,\ 90)} = 0.77$.

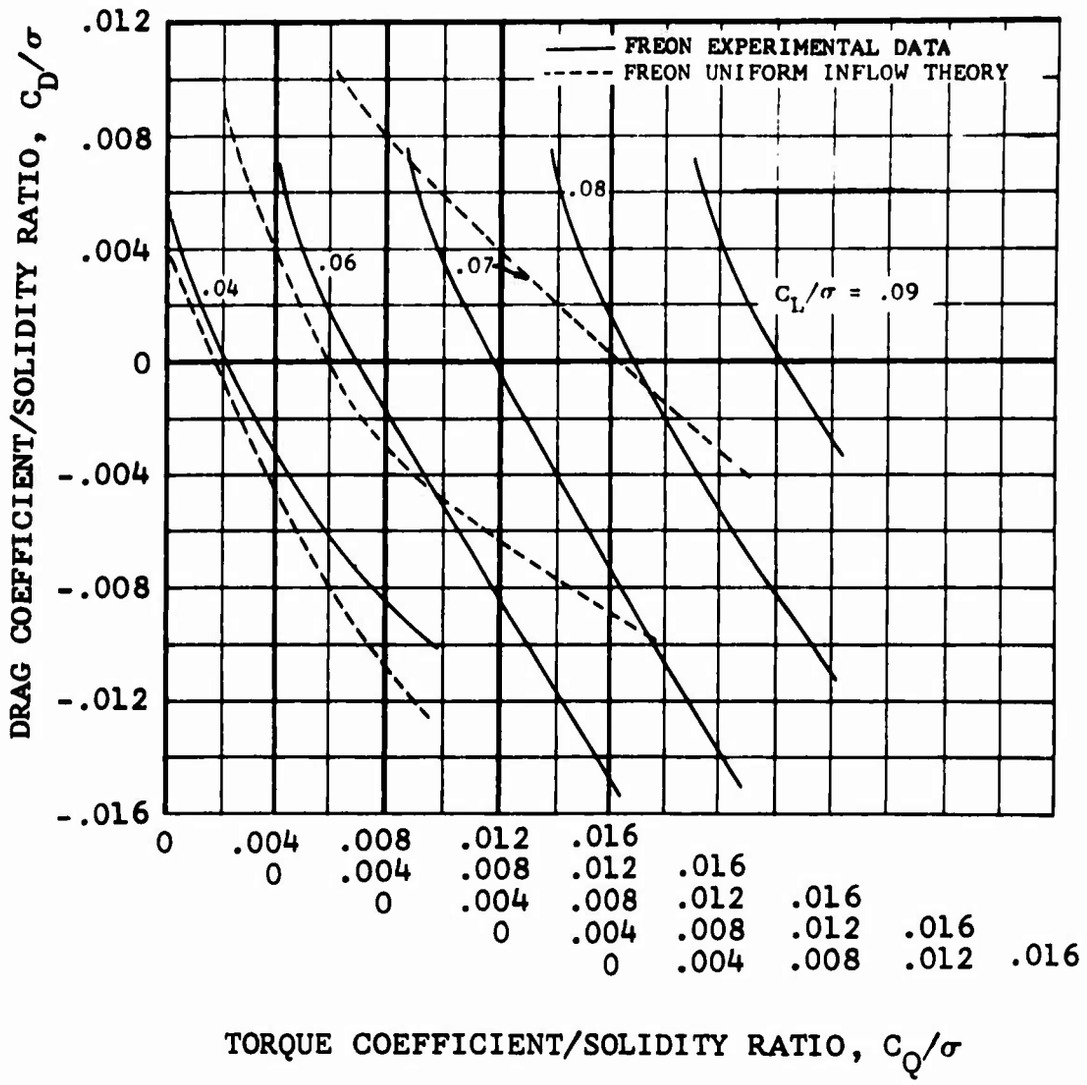

(b) C_D/σ vs C_Q/σ

Figure 19. Concluded.

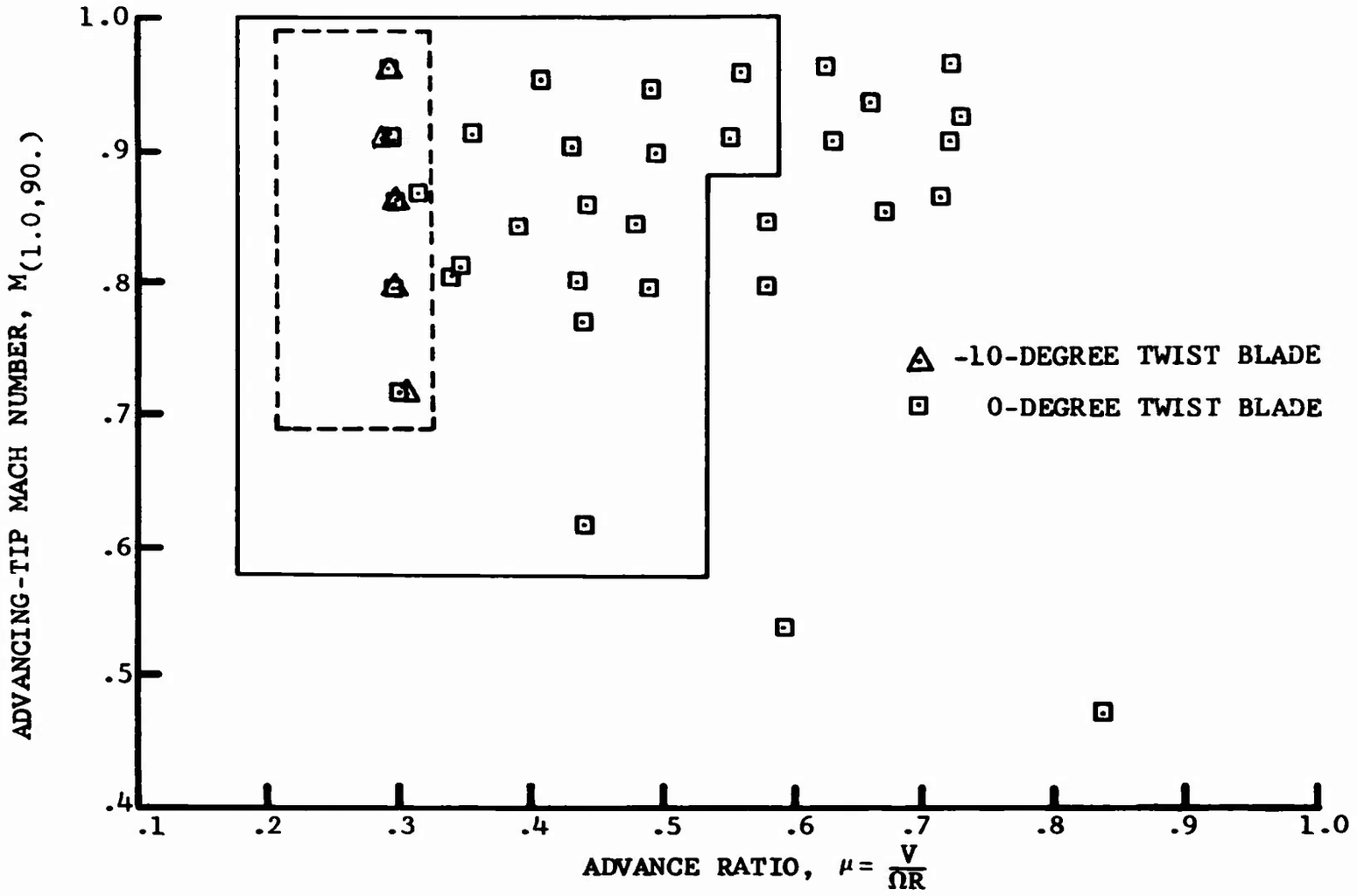

Figure 20. Model Test Conditions Emphasized in Loads Study.

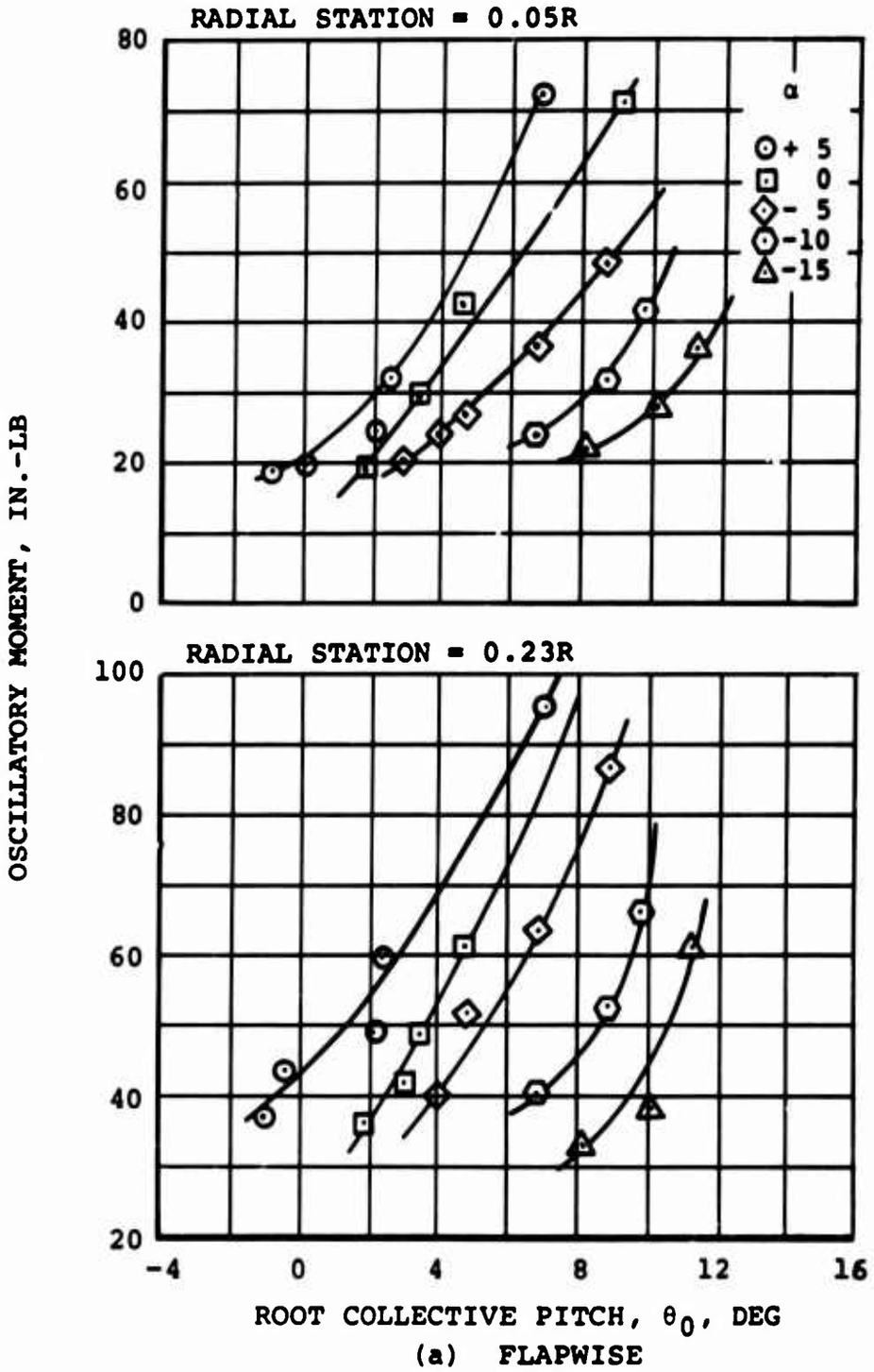

Figure 21. A Sample of Flapwise, Chordwise, and Torsional Oscillatory Bending and Twisting Moment Data at Several Radial Stations, V = 137 Knots, $\mu = 0.29$, $\theta_1 = 0^{\circ}$, $M_{(1.0,90.)} = 0.96$.

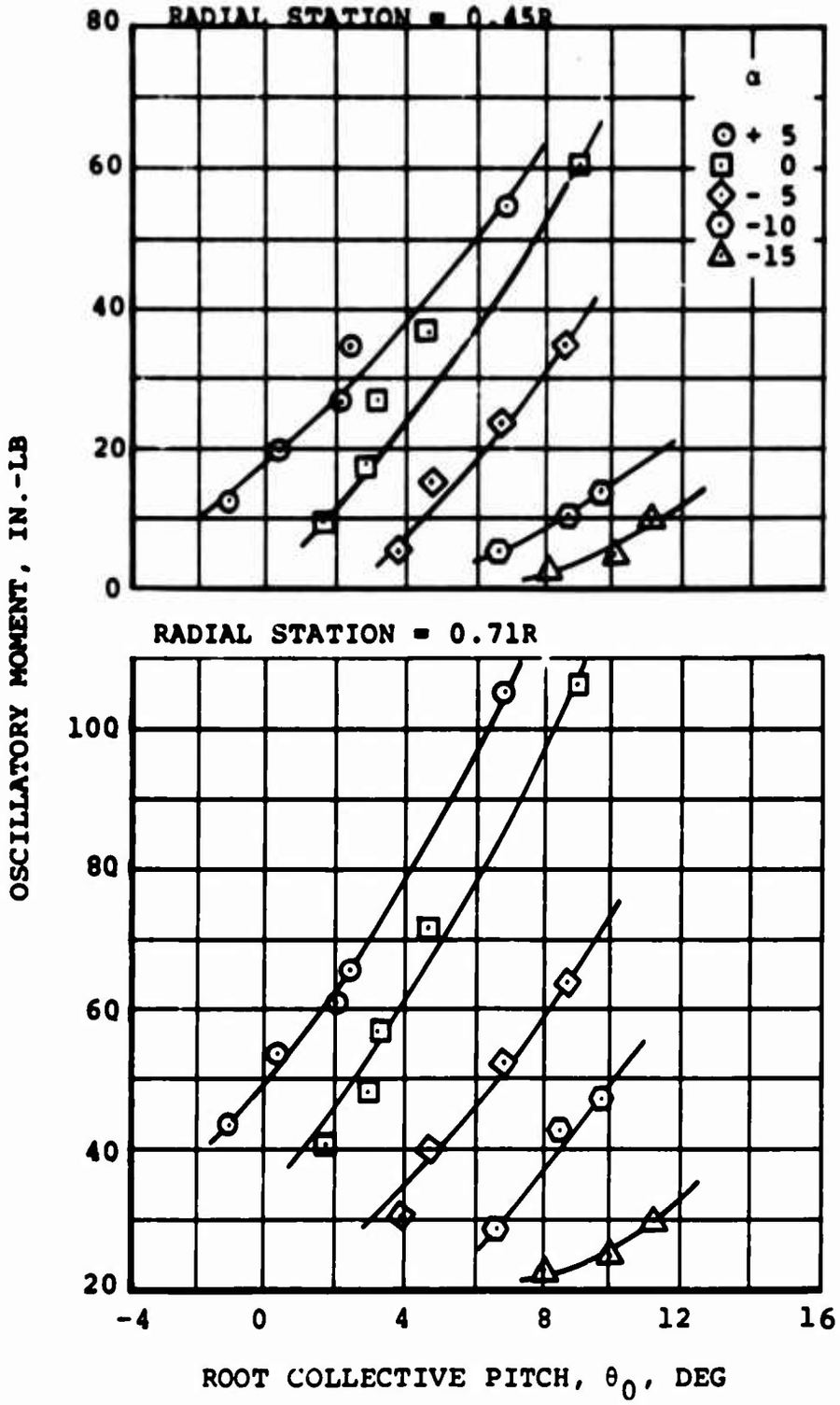

(a) FLAPWISE CONCLUDED

Figure 21. Continued.

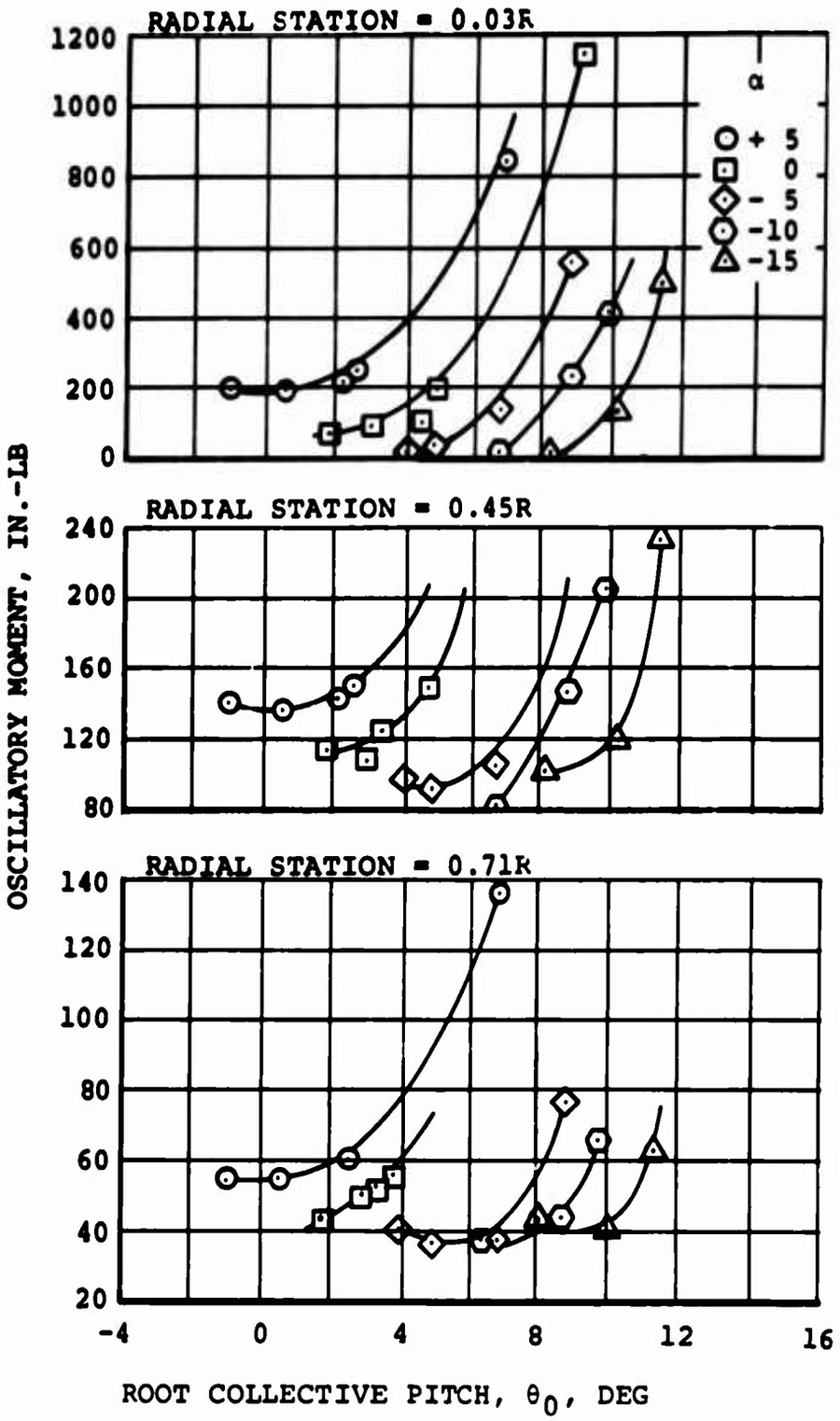

(b) CHORDWISE

Figure 21. Continued.

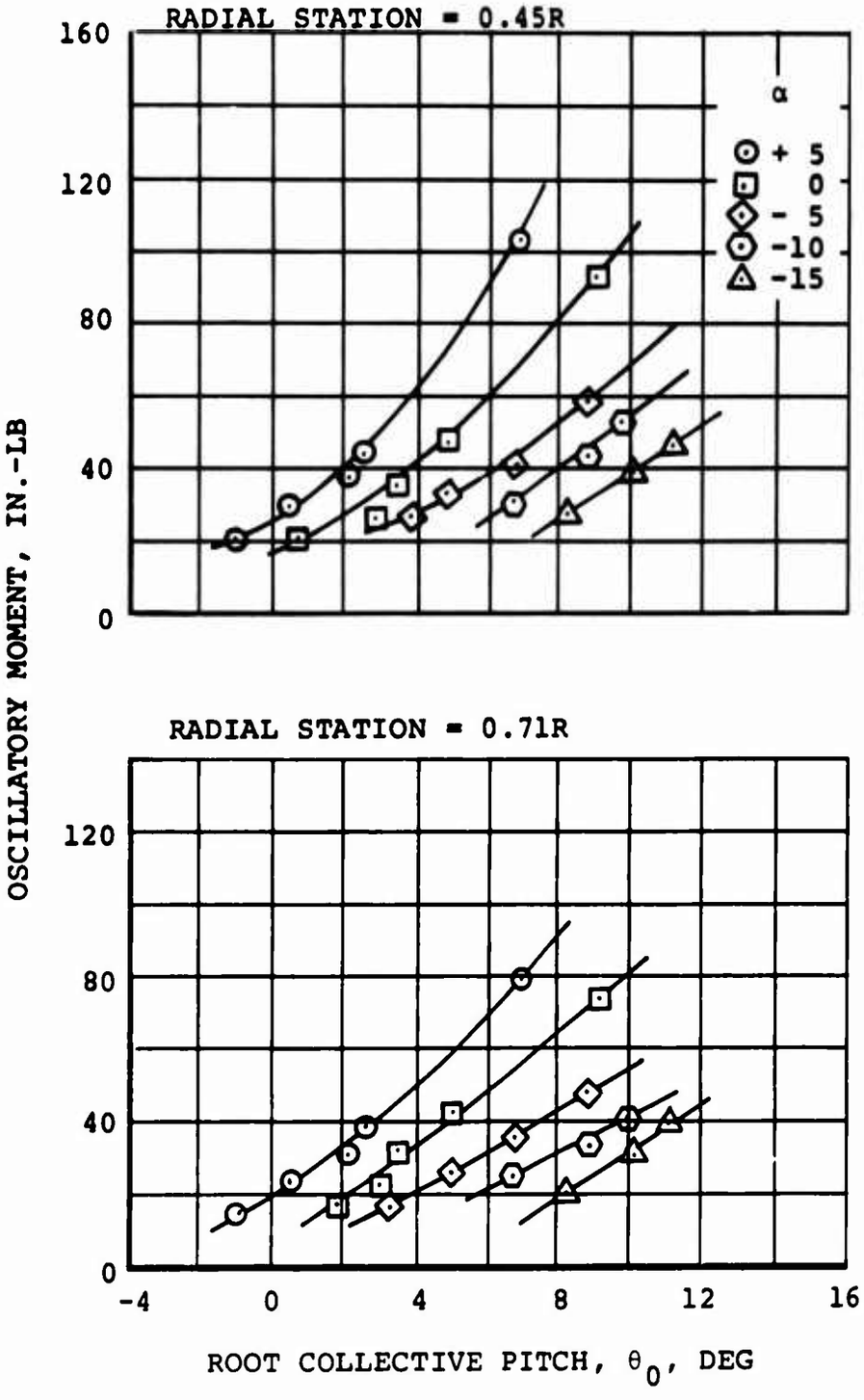

(c) TORSIONAL

Figure 21. Concluded.

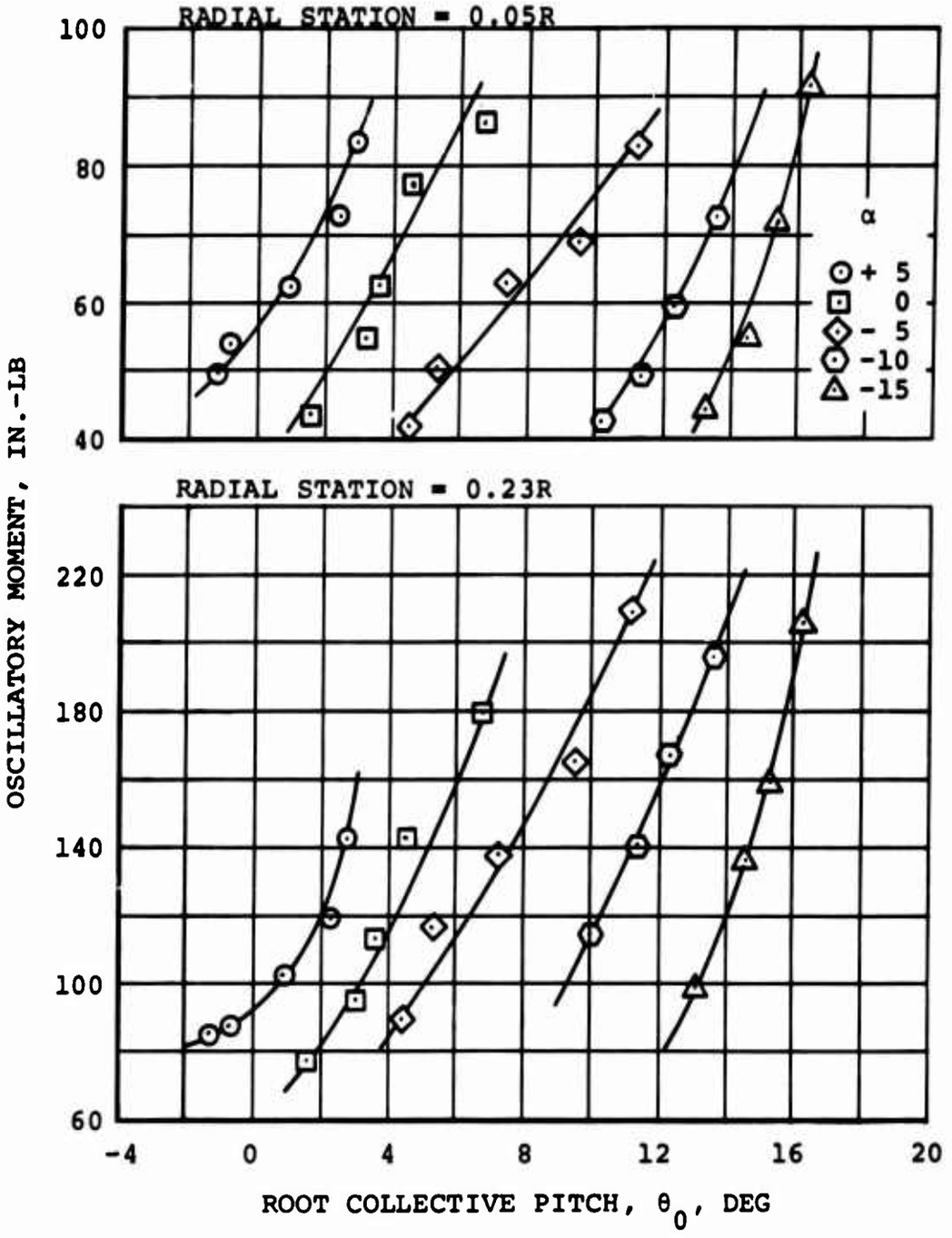

(a) FLAPWISE

Figure 22. A Sample of Flapwise, Chordwise, and Torsional Oscillatory Bending and Twisting Moment Data at Several Radial Stations, V = 201 Knots, $\mu = 0.49$, $\theta_1 = 0^\circ$, $M_{(1.0,90.)} = 0.95$.

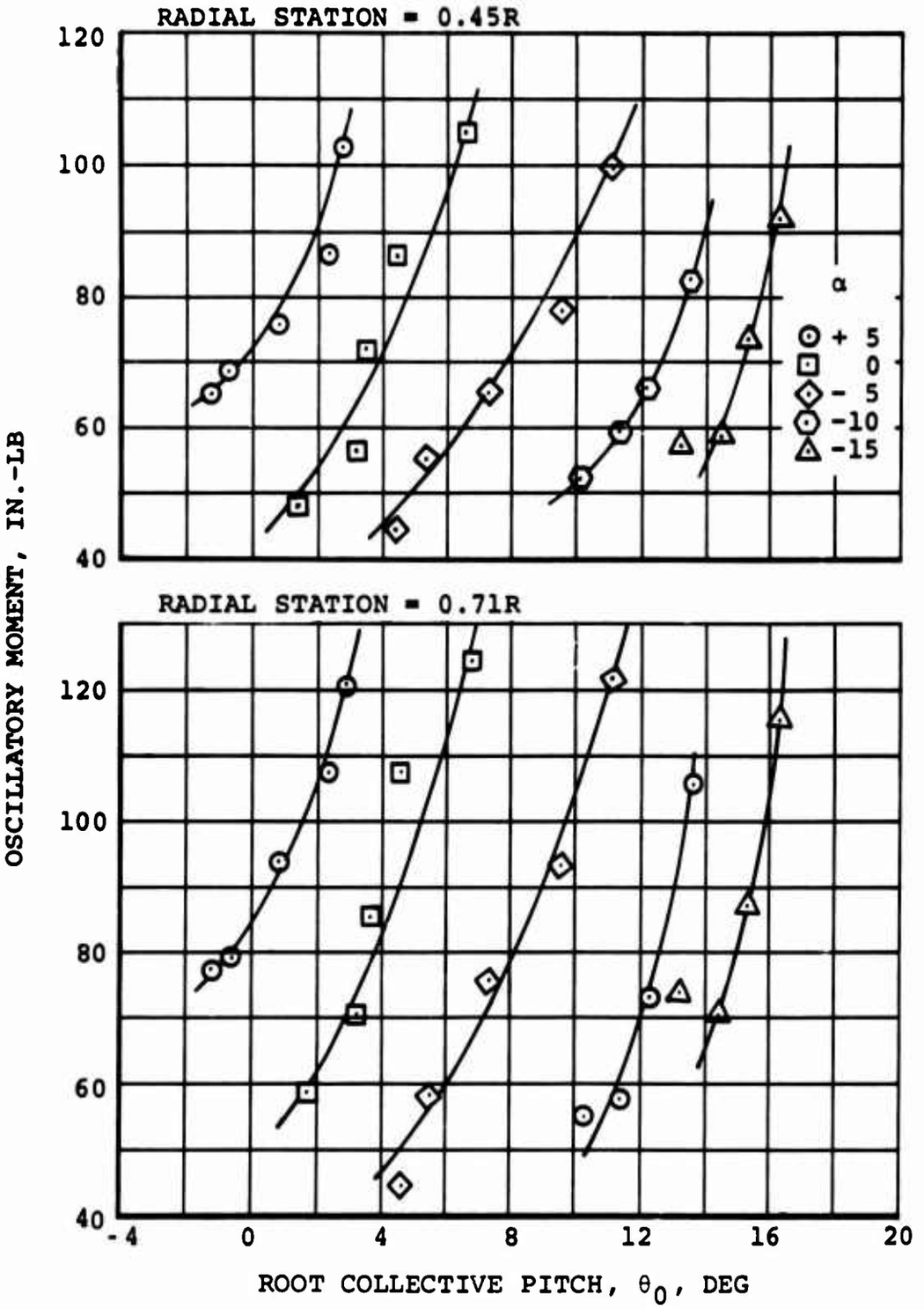

(a) FLAPWISE CONCLUDED

Figure 22. Continued.

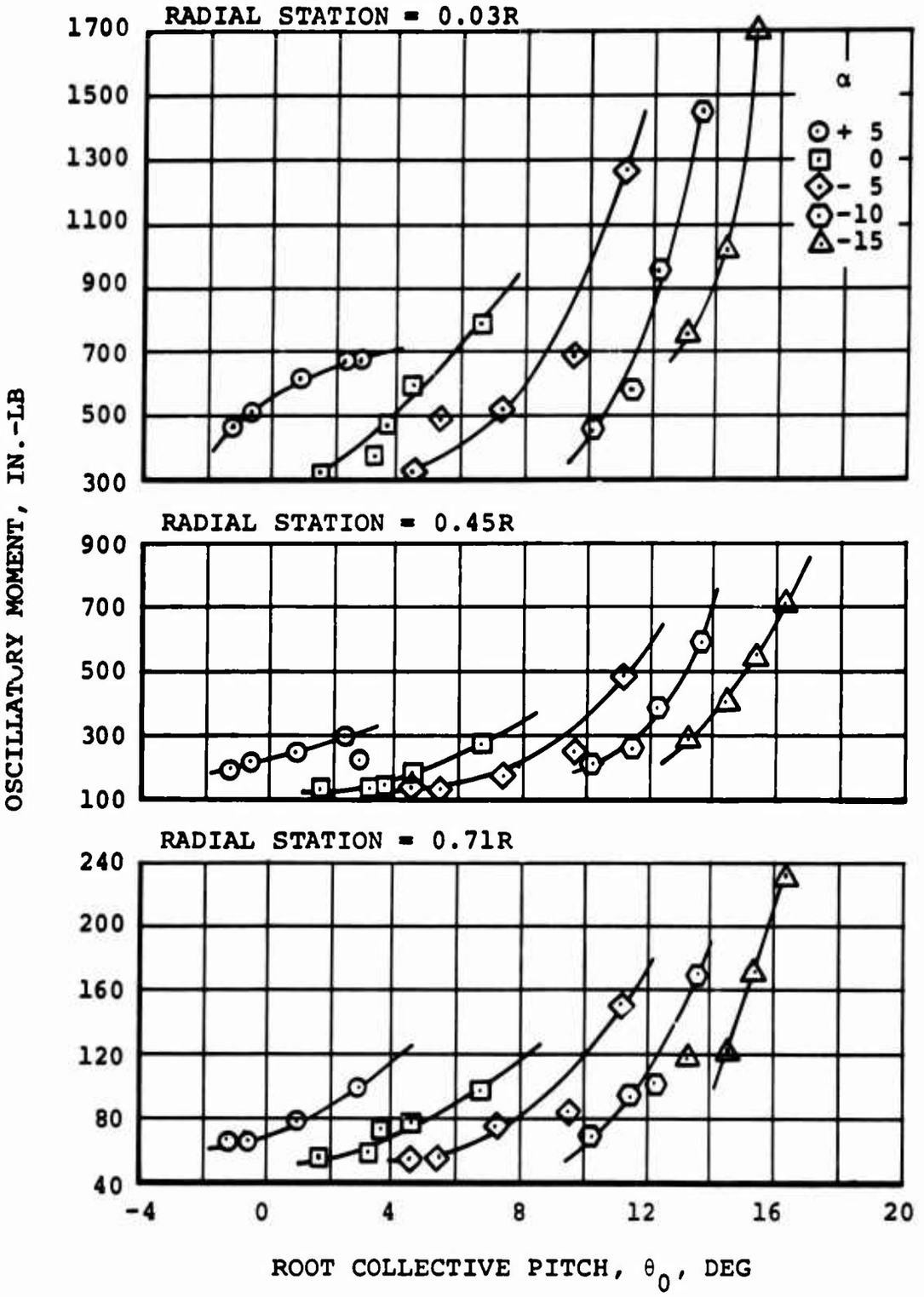

(b) CHORDWISE

Figure 22. Continued.

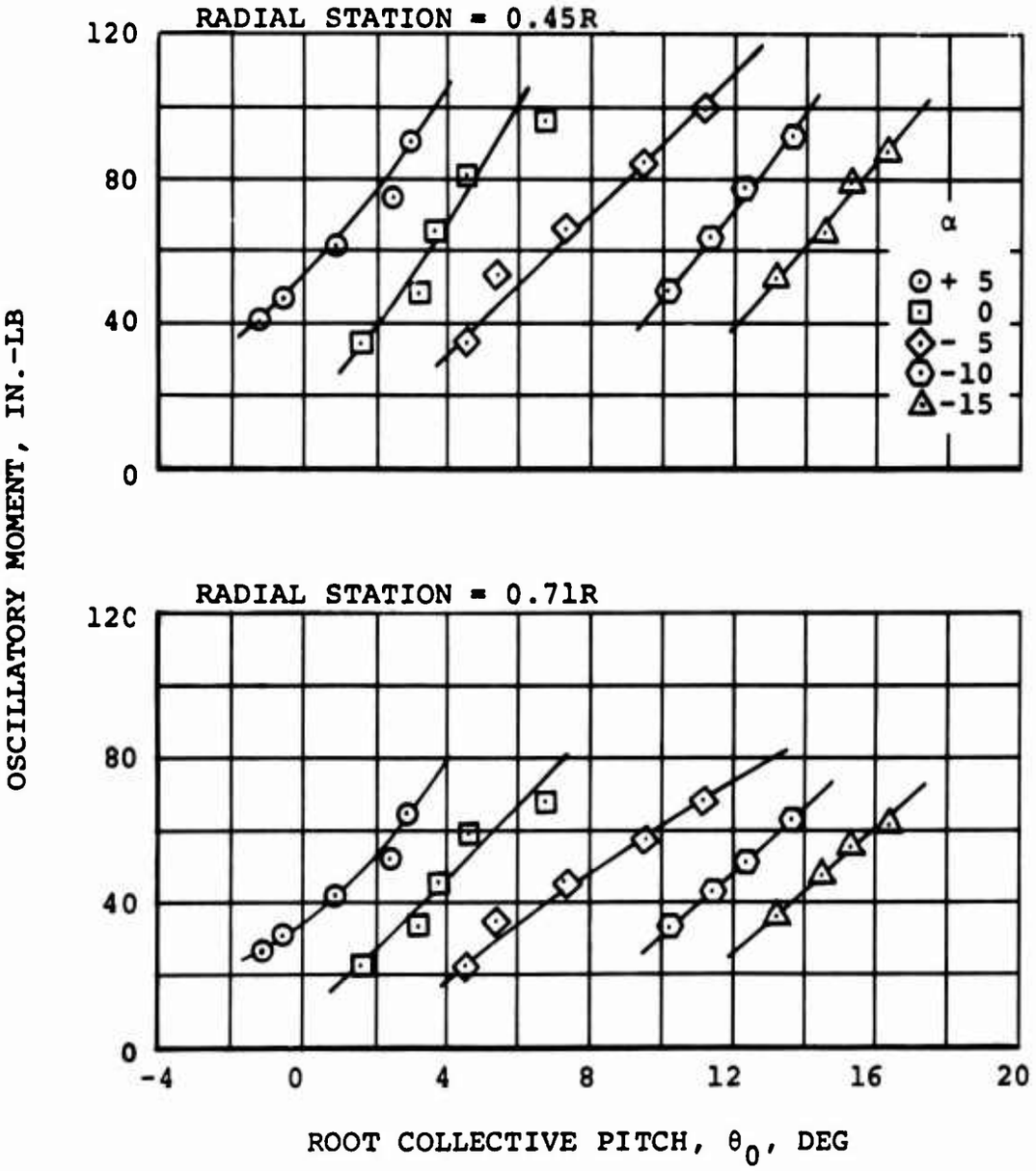

(c) TORSIONAL

Figure 22. Concluded.

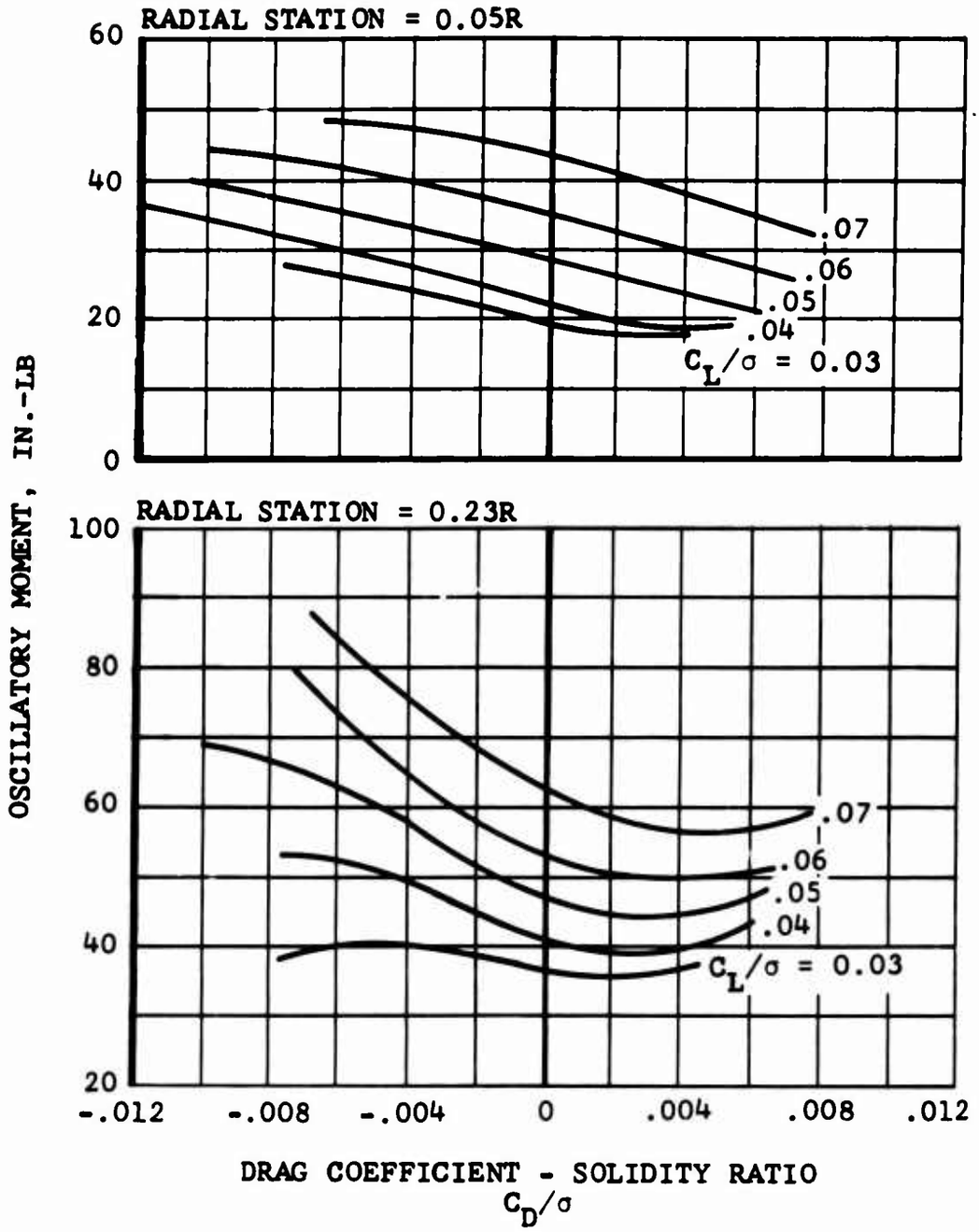

(a) FLAPWISE

Figure 23. The Effect of Drag on Flapwise, Chordwise, and Torsional Oscillatory Bending and Twisting Moment Data at Several Radial Stations for Constant Lift, V = 137 Knots, μ = 0.29, θ_1 = 0°, $M_{(1.0,90.)}$ = 0.96.

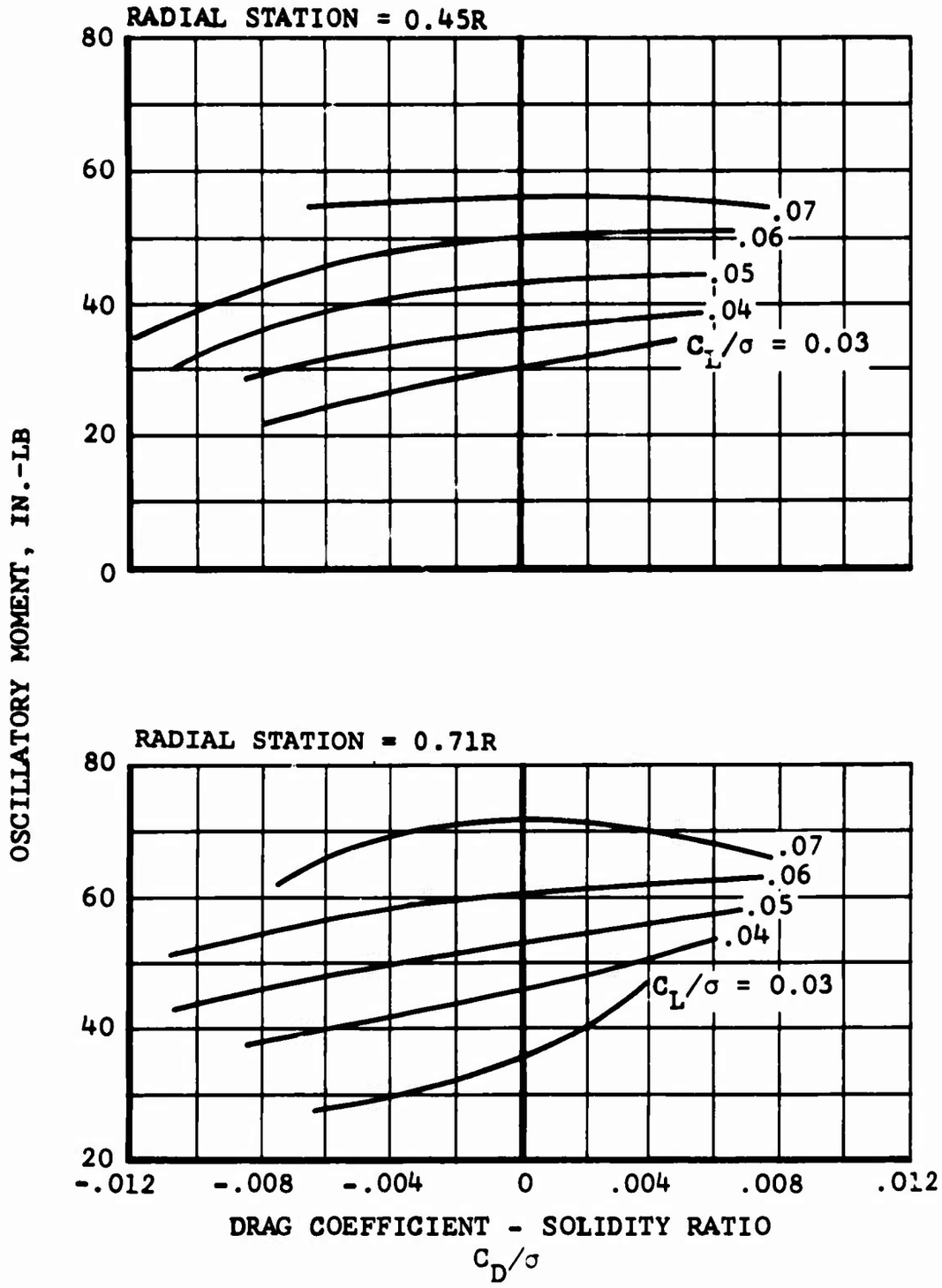

(a) FLAPWISE CONCLUDED

Figure 23. Continued.

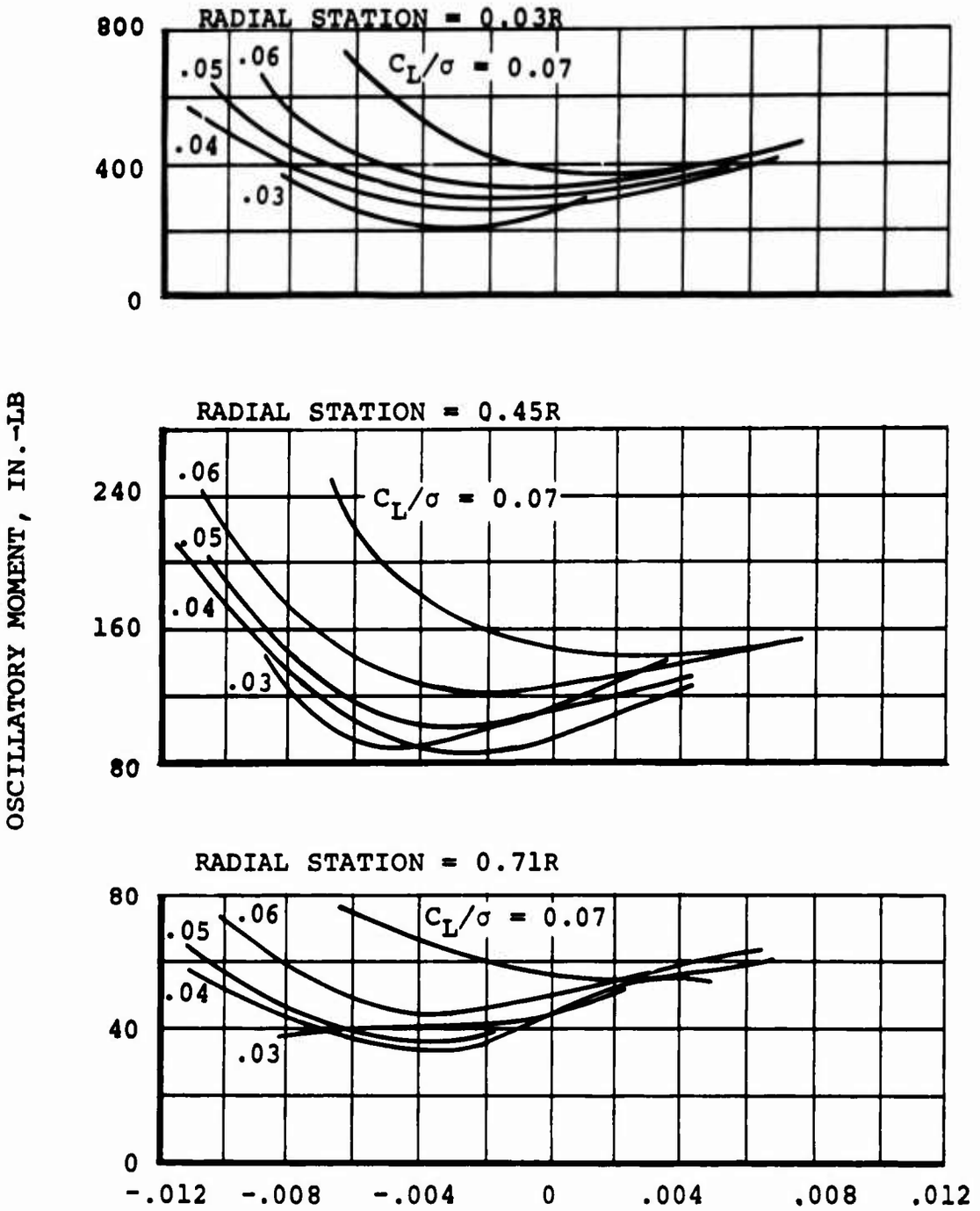

(b) CHORDWISE

Figure 23. Continued.

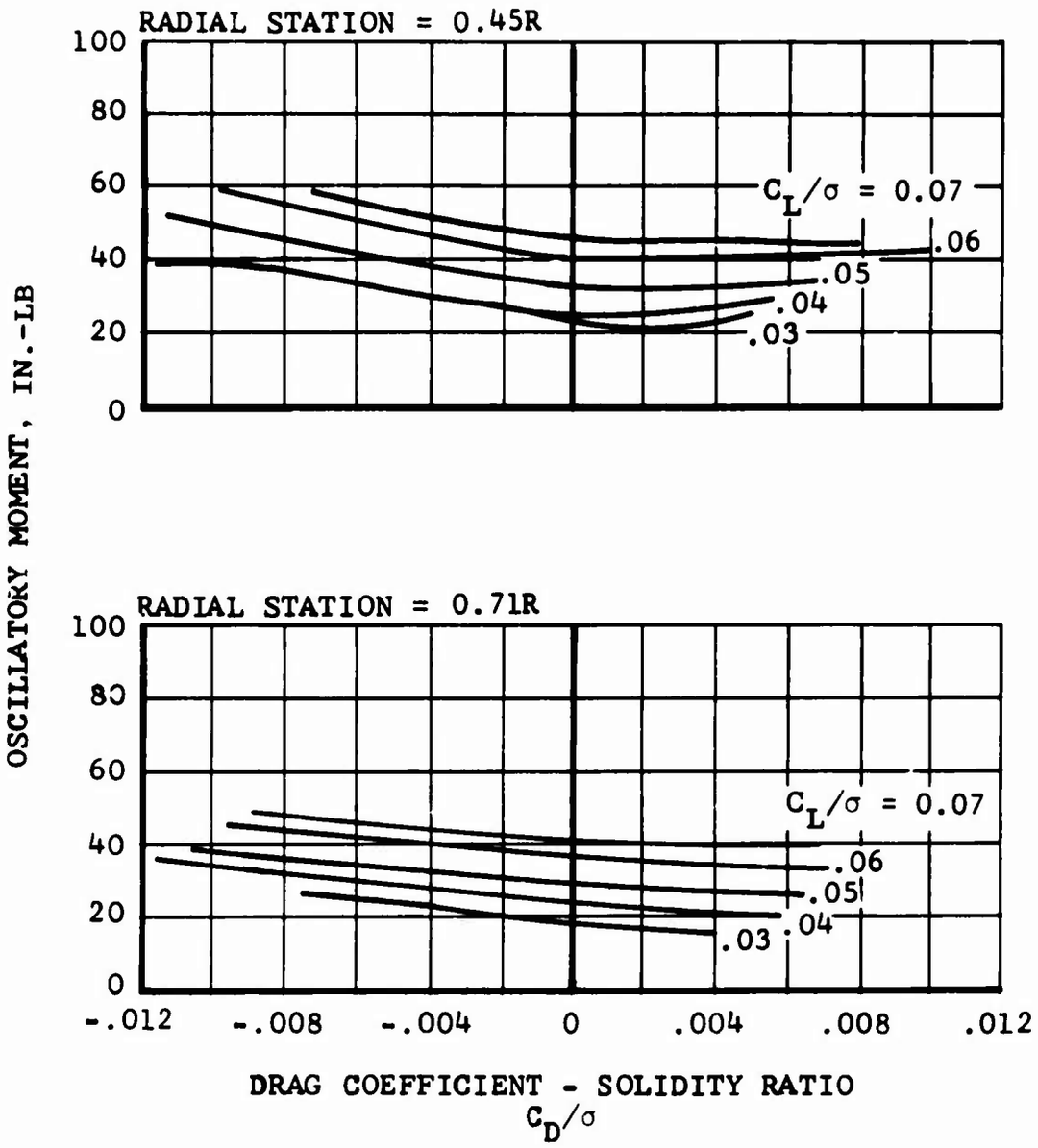

(c) TORSIONAL

Figure 23. Concluded.

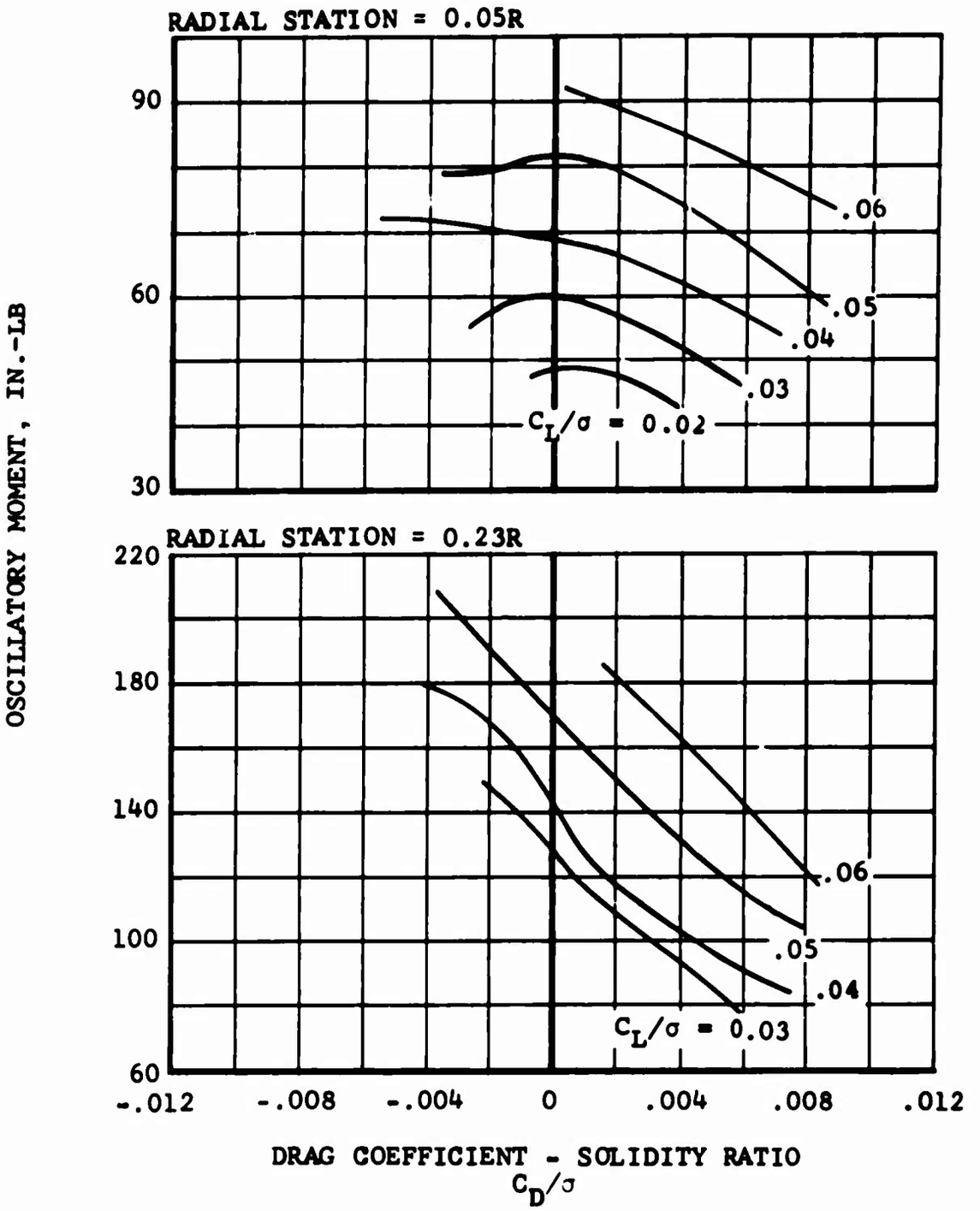

(a) FLAPWISE

Figure 24. The Effect of Drag on Flapwise, Chordwise, and Torsional Oscillatory Bending and Twisting Moment Data at Several Radial Stations for Constant Lift, V = 201 Knots, μ = 0.49, θ_1 = 0°, $M_{(1.0,90.)}$ = 0.95.

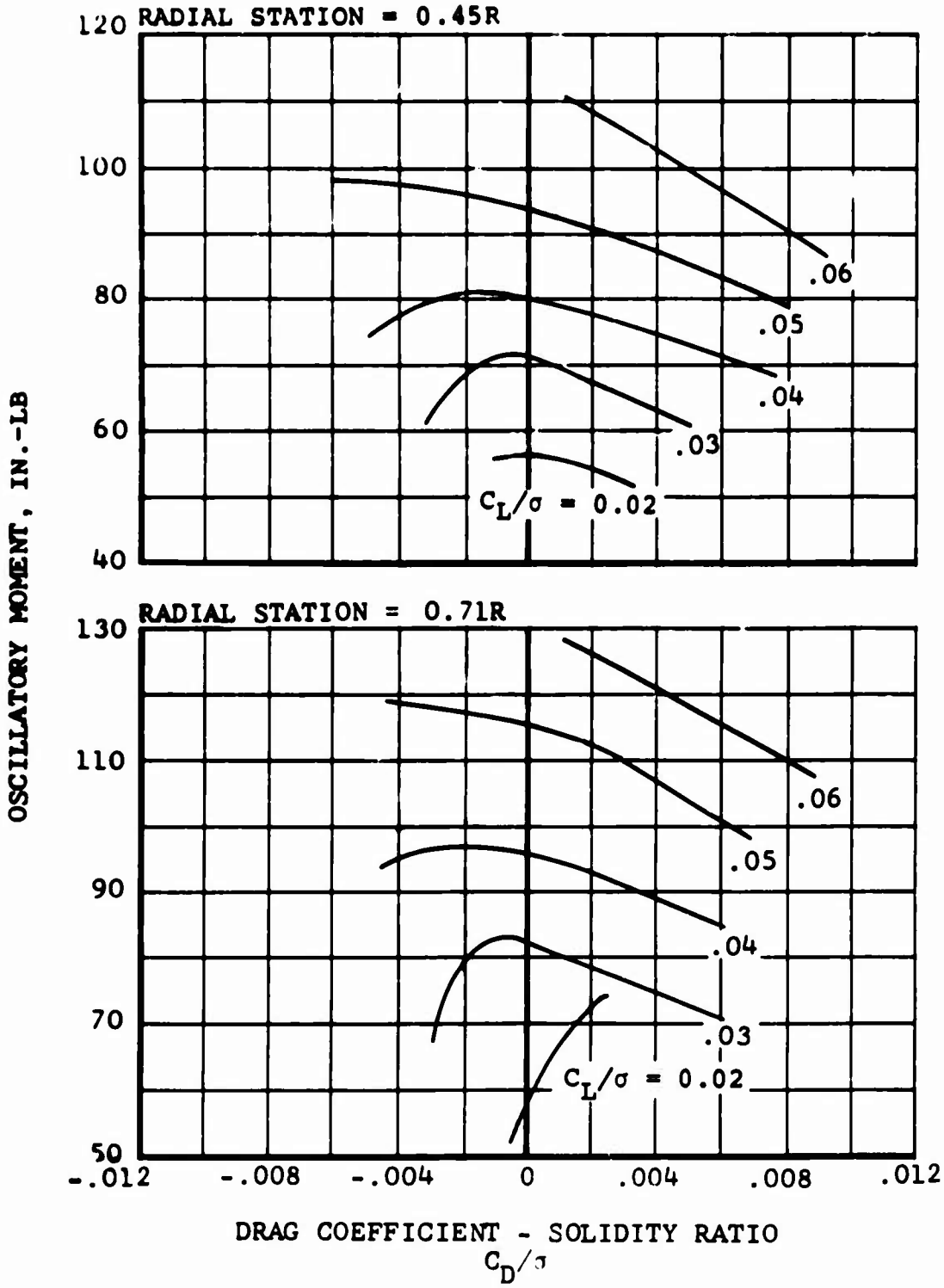

(a) FLAPWISE CONCLUDED

Figure 24. Continued.

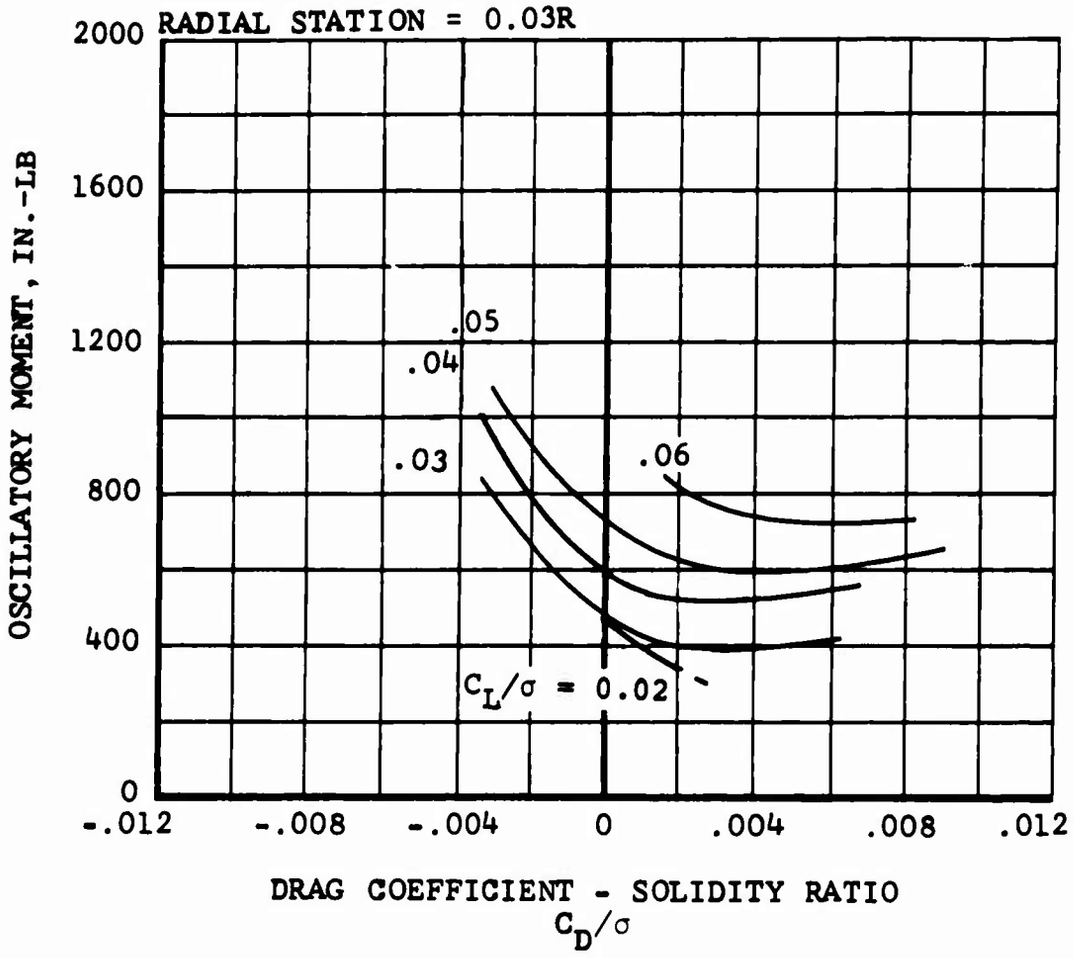

(b) CHORDWISE

Figure 24. Continued.

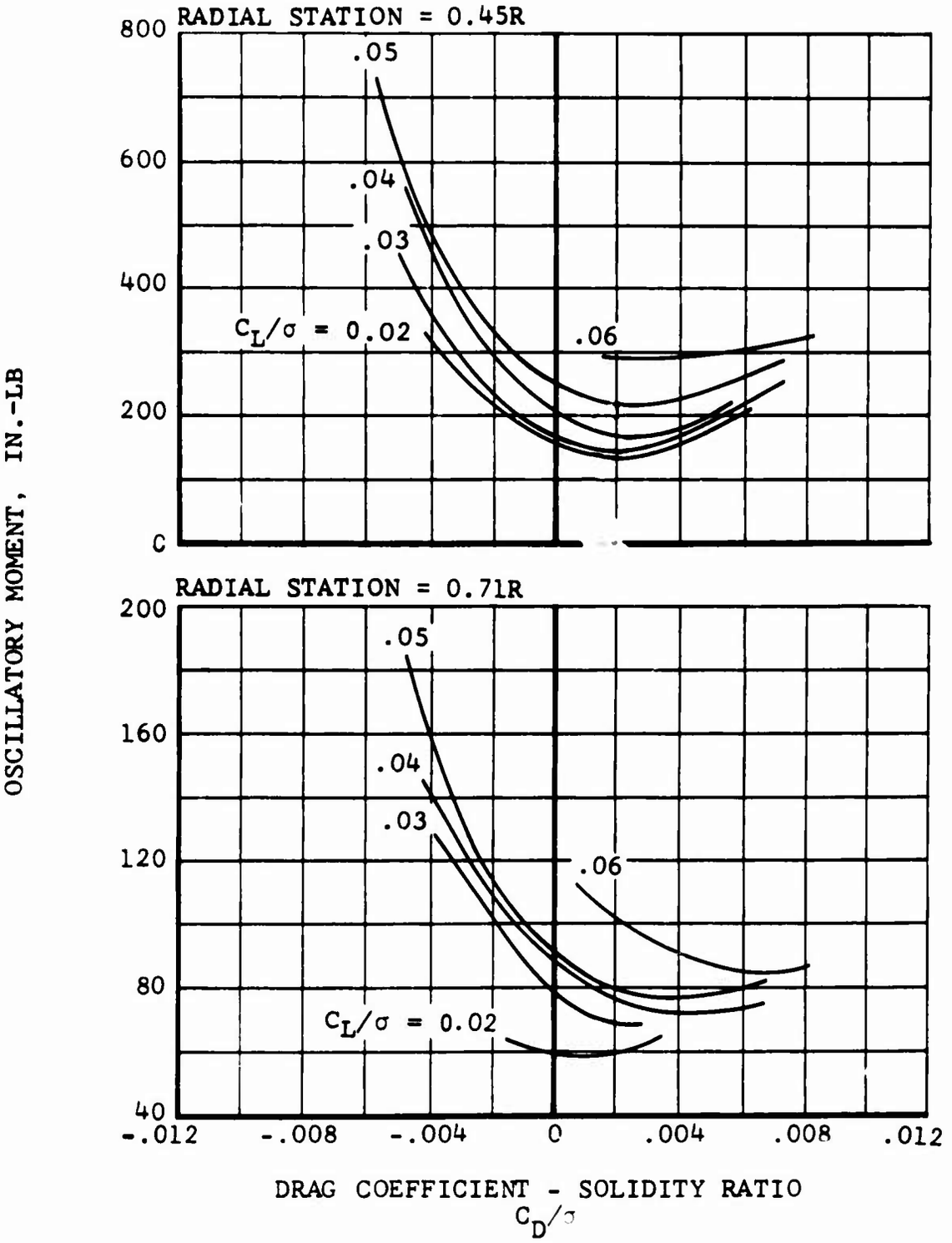

(b) CHORDWISE CONCLUDED

Figure 24. Continued.

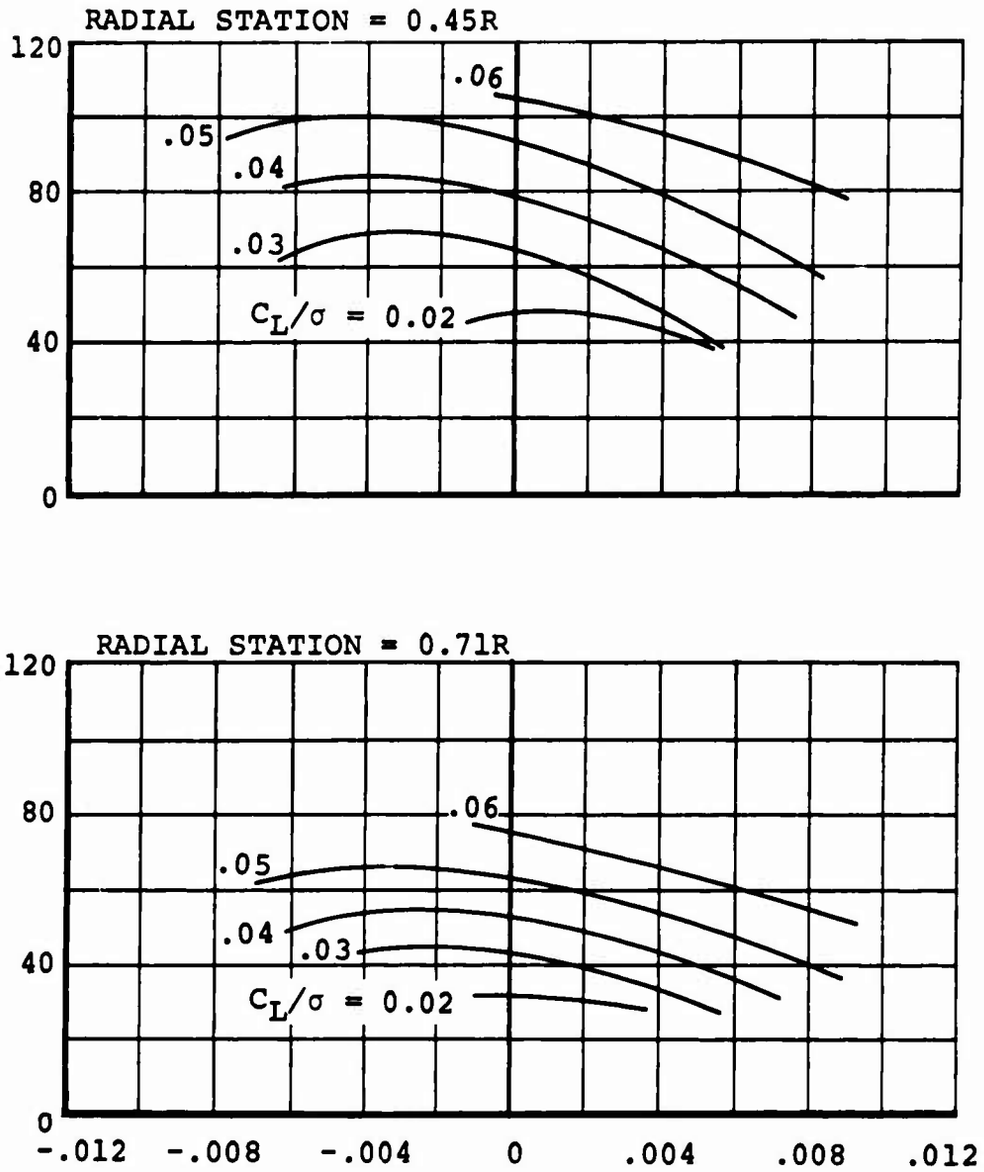

(c) TORSIONAL

Figure 24. Concluded.

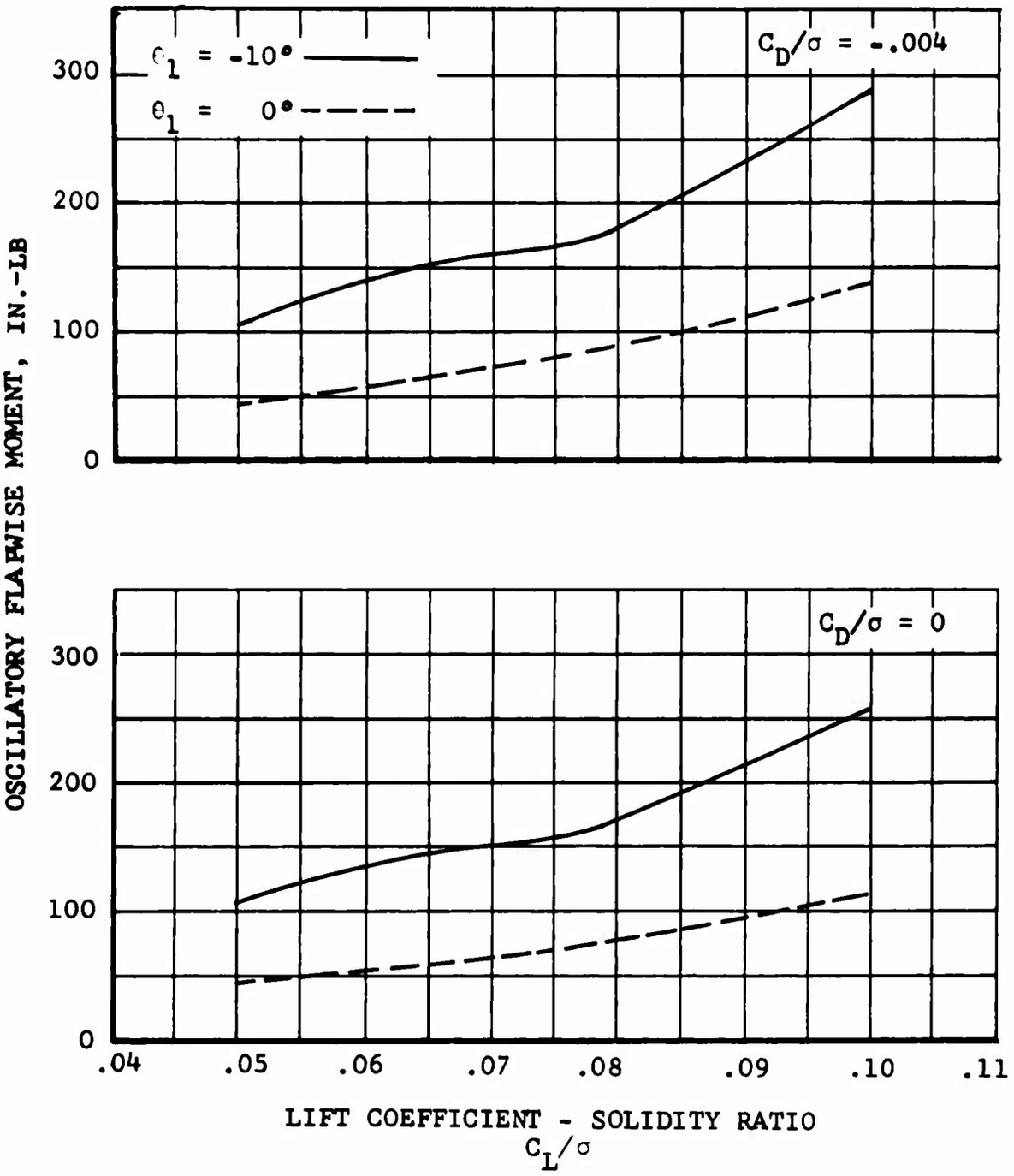

(a) RADIAL STATION = 0.23R

Figure 25. The Combined Effect of Twist and Thin Tips on Flapwise Oscillatory Bending Moments as a Function of Lift at Three Values of Drag for Three Radial Stations, V = 104 Knots, μ = 0.30, $M_{(1.0,90.)}$ = 0.72.

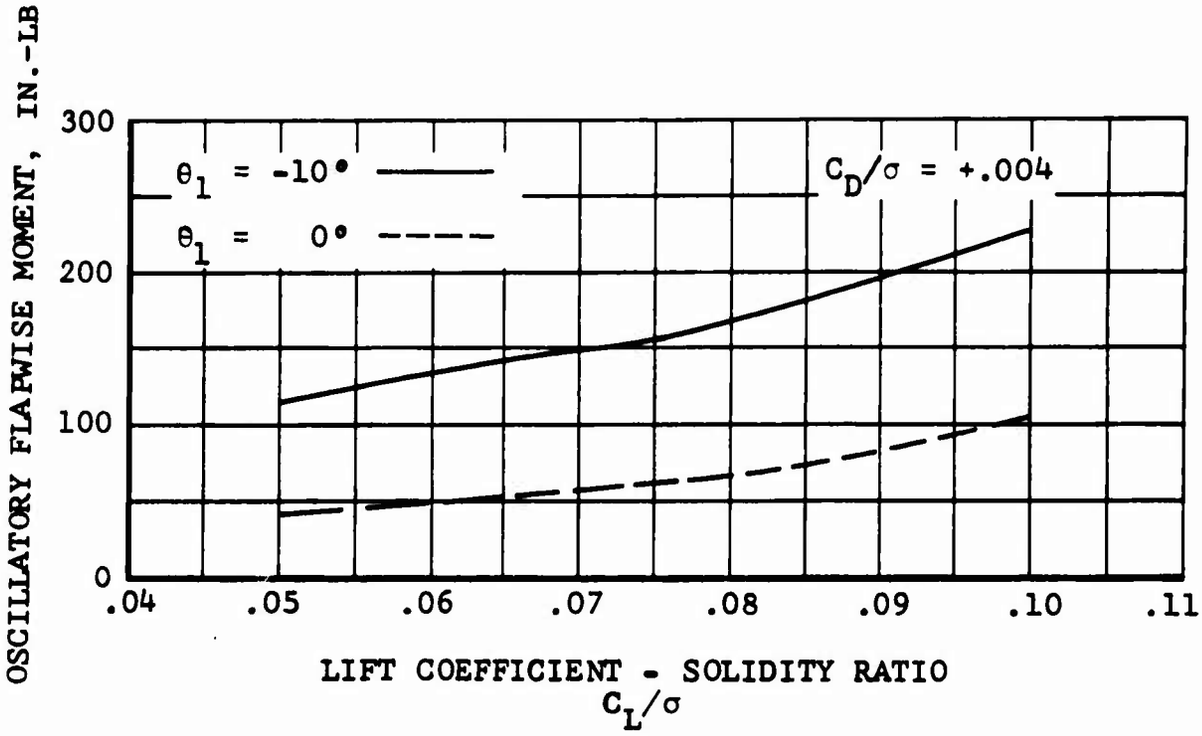

(a) RADIAL STATION = 0.23R CONCLUDED

Figure 25. Continued.

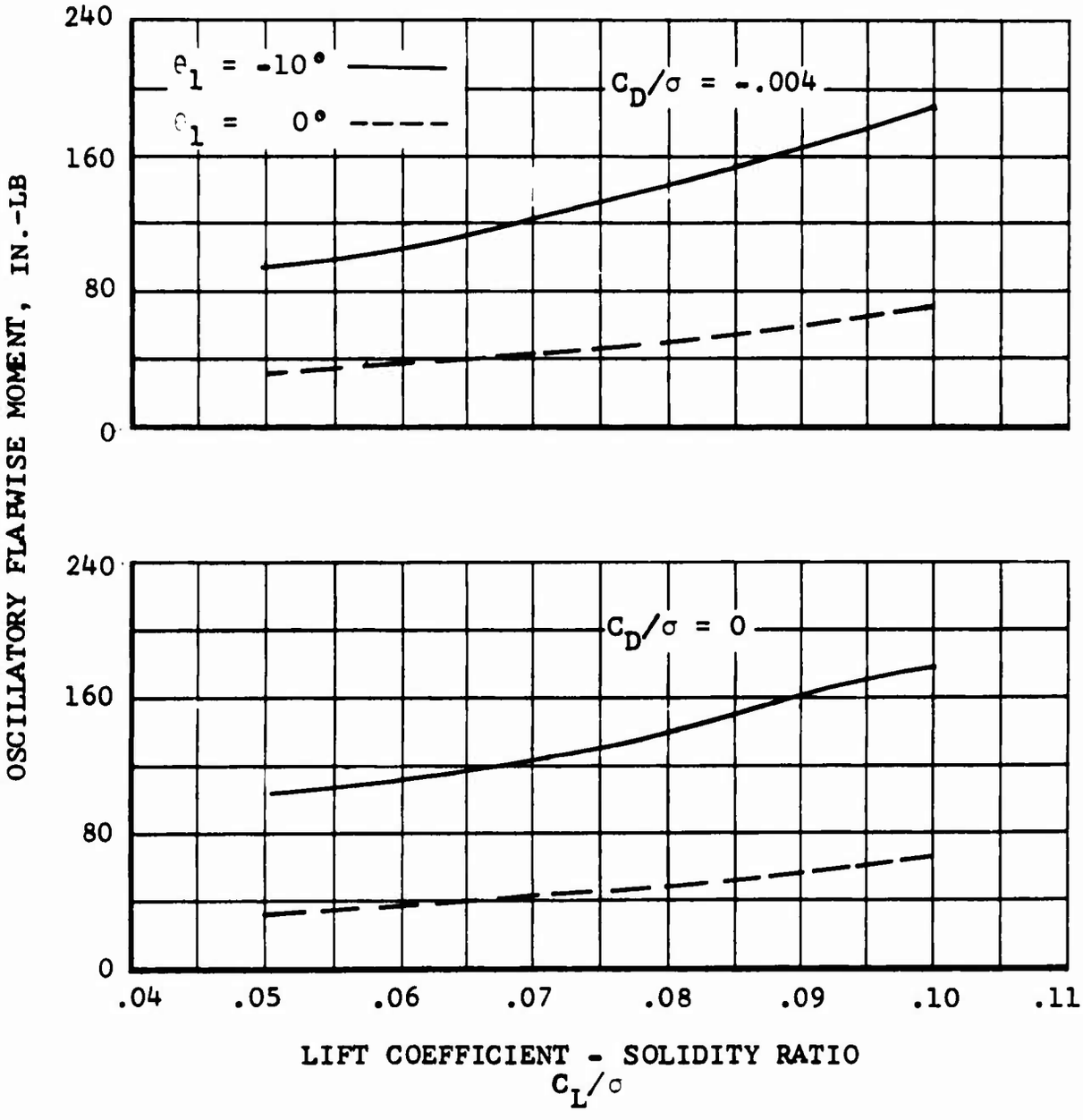

(b) RADIAL STATION = 0.45R

Figure 25. Continued.

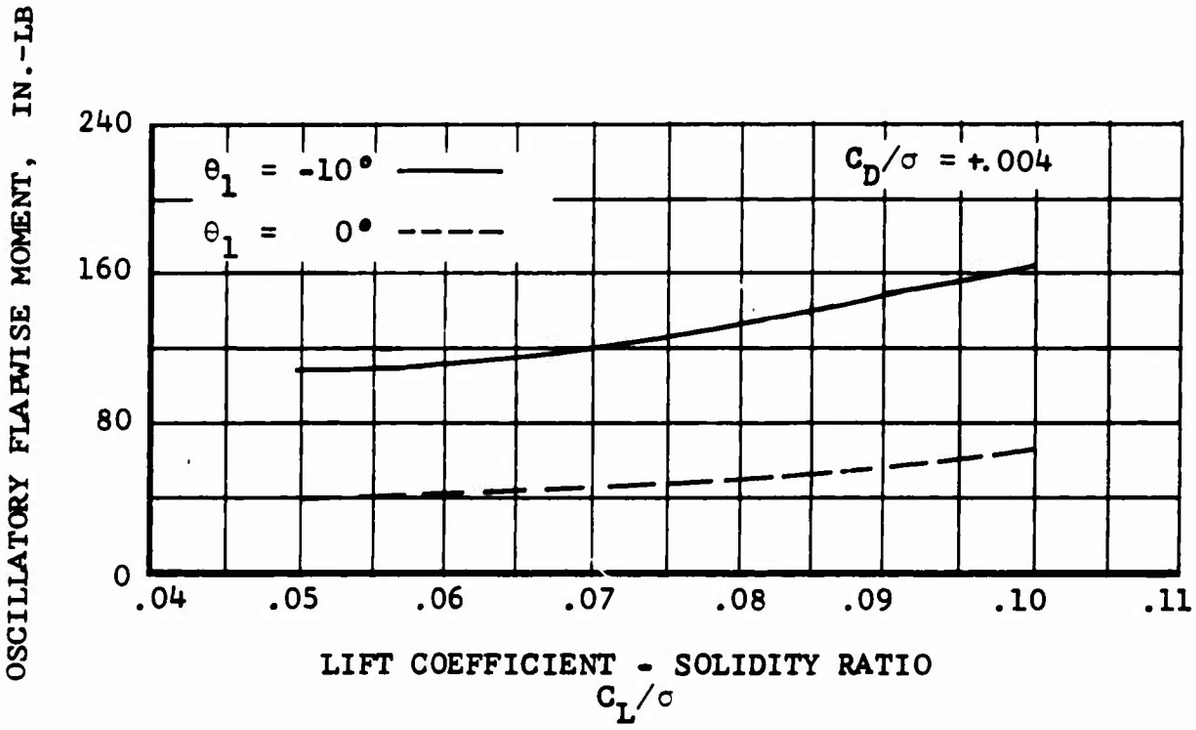

(b) RADIAL STATION = 0.45R CONCLUDED

Figure 25. Continued.

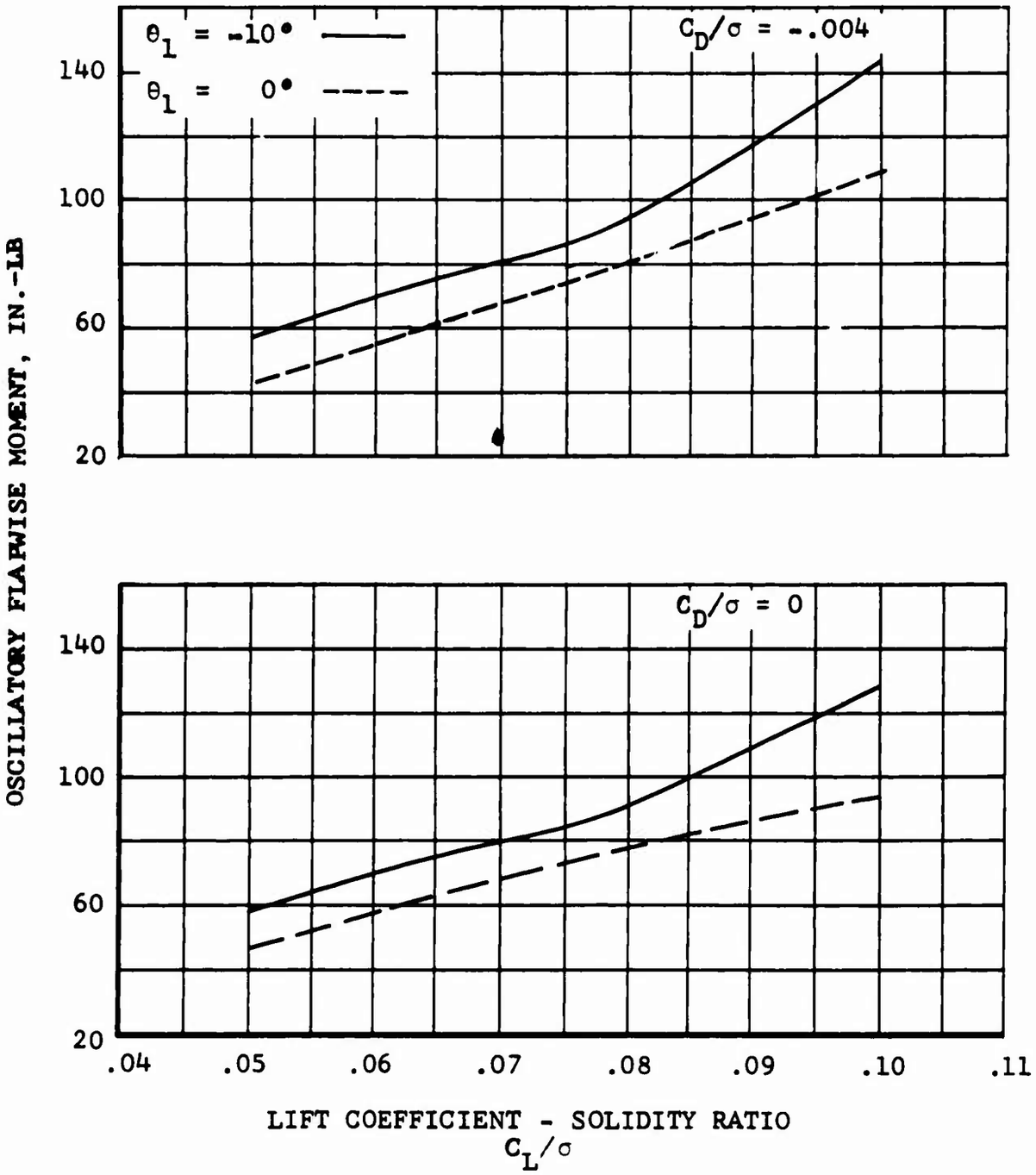

(c) RADIAL STATION = 0.71R

Figure 25. Continued.

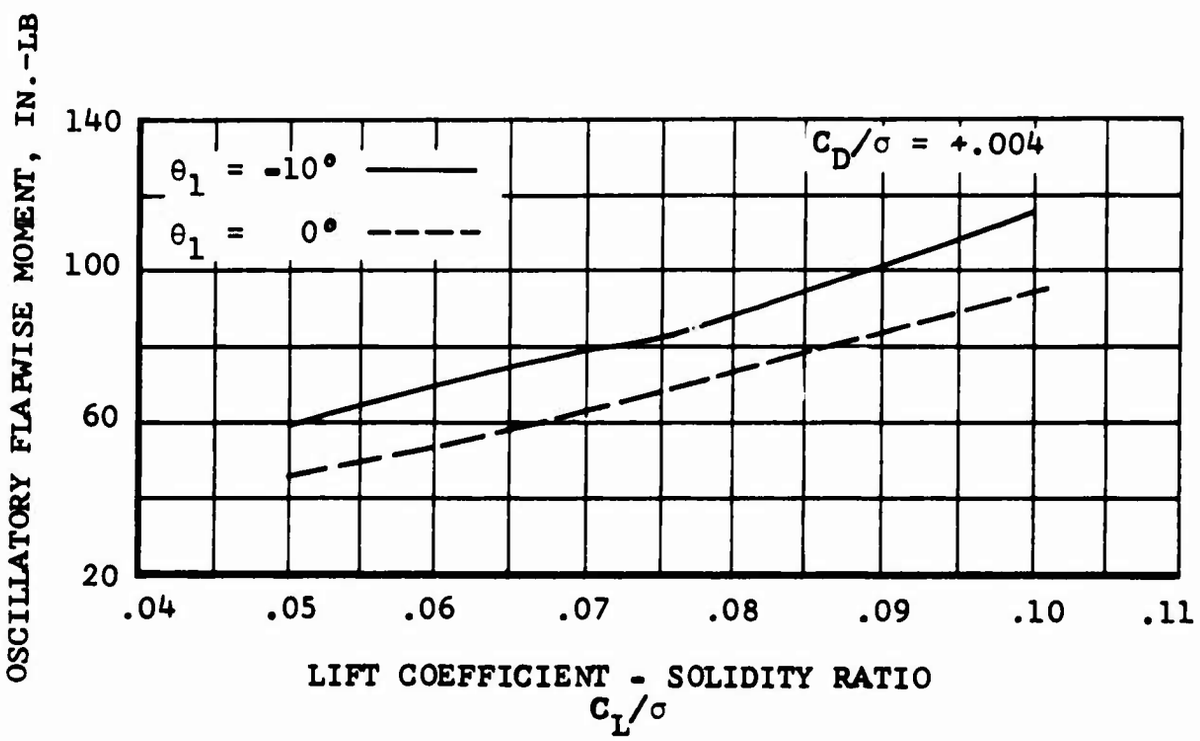

(c) RADIAL STATION = 0.71R CONCLUDED

Figure 25. Concluded.

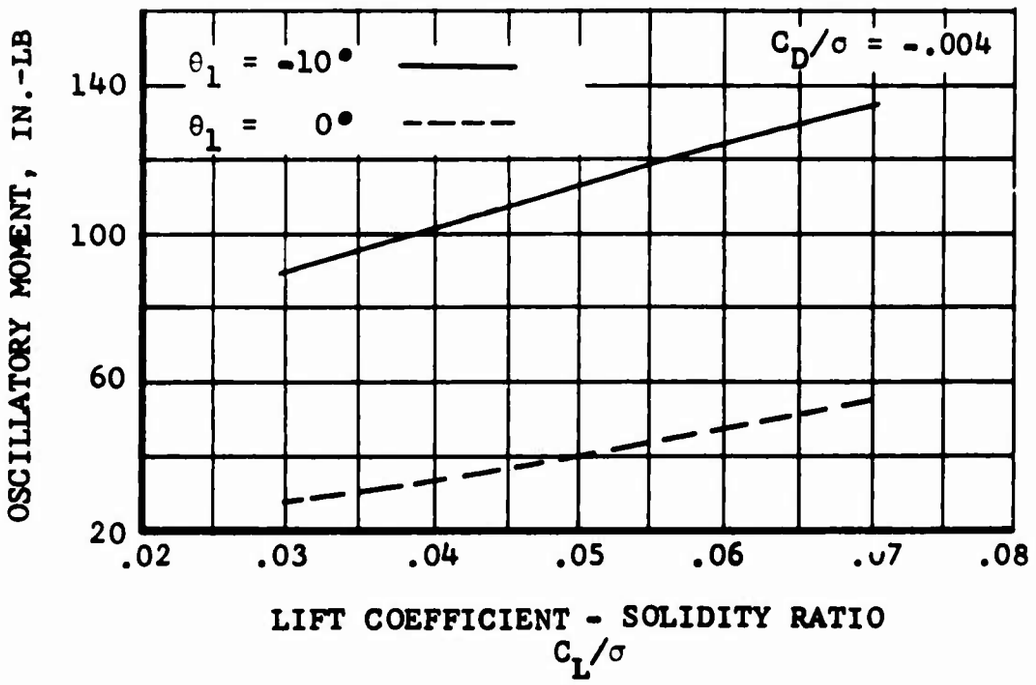

(a) FLAPWISE

Figure 26. The Combined Effect of Twist and Thin Tips on Flapwise, Chordwise, and Torsional Oscillatory Moment Data as a Function of Lift for Three Values of Drag at Radial Station 0.45R, V = 137 Knots, μ = 0.29, $M_{(1.0,90.)}$ = 0.96.

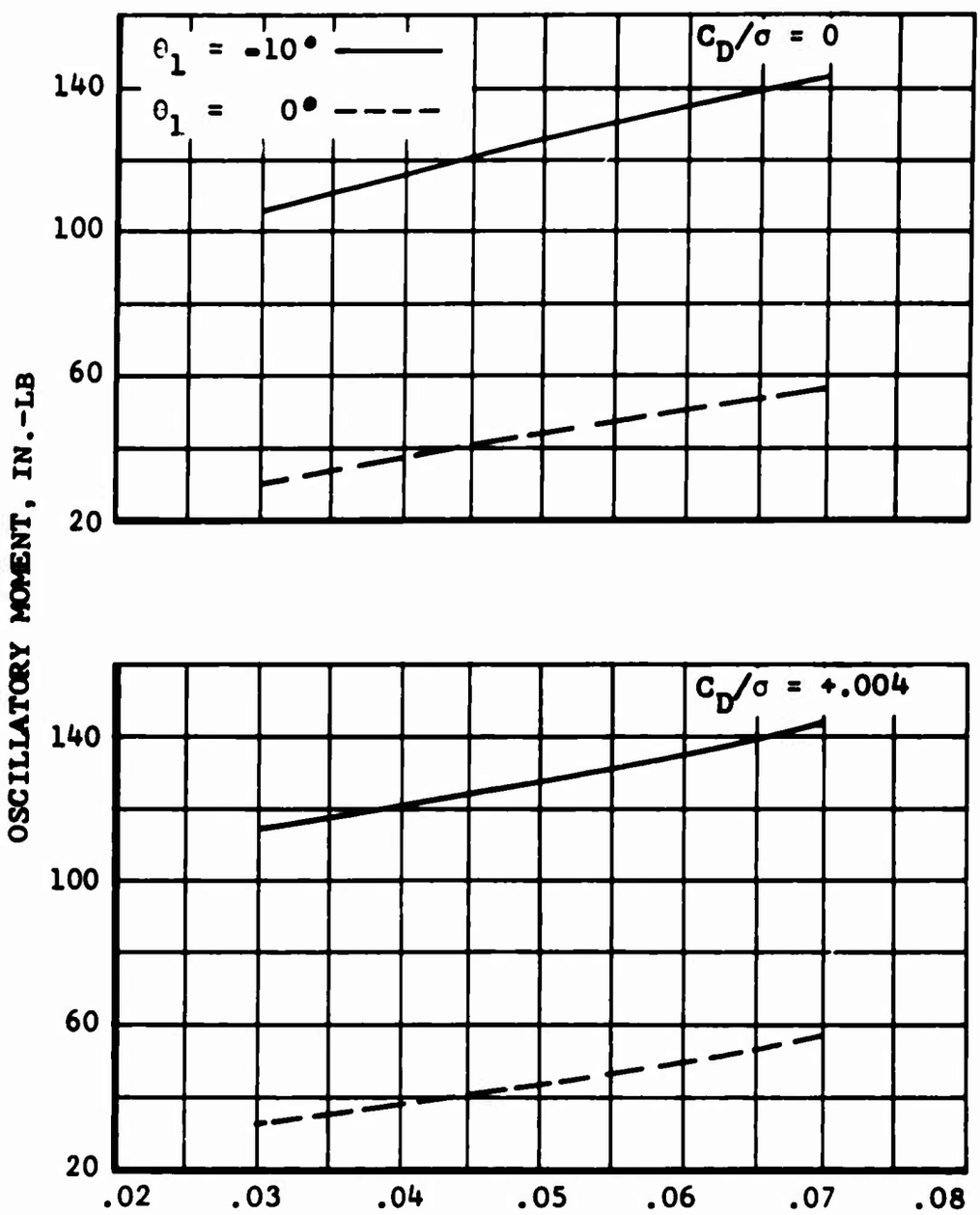

(a) FLAPWISE CONCLUDED

Figure 26. Continued.

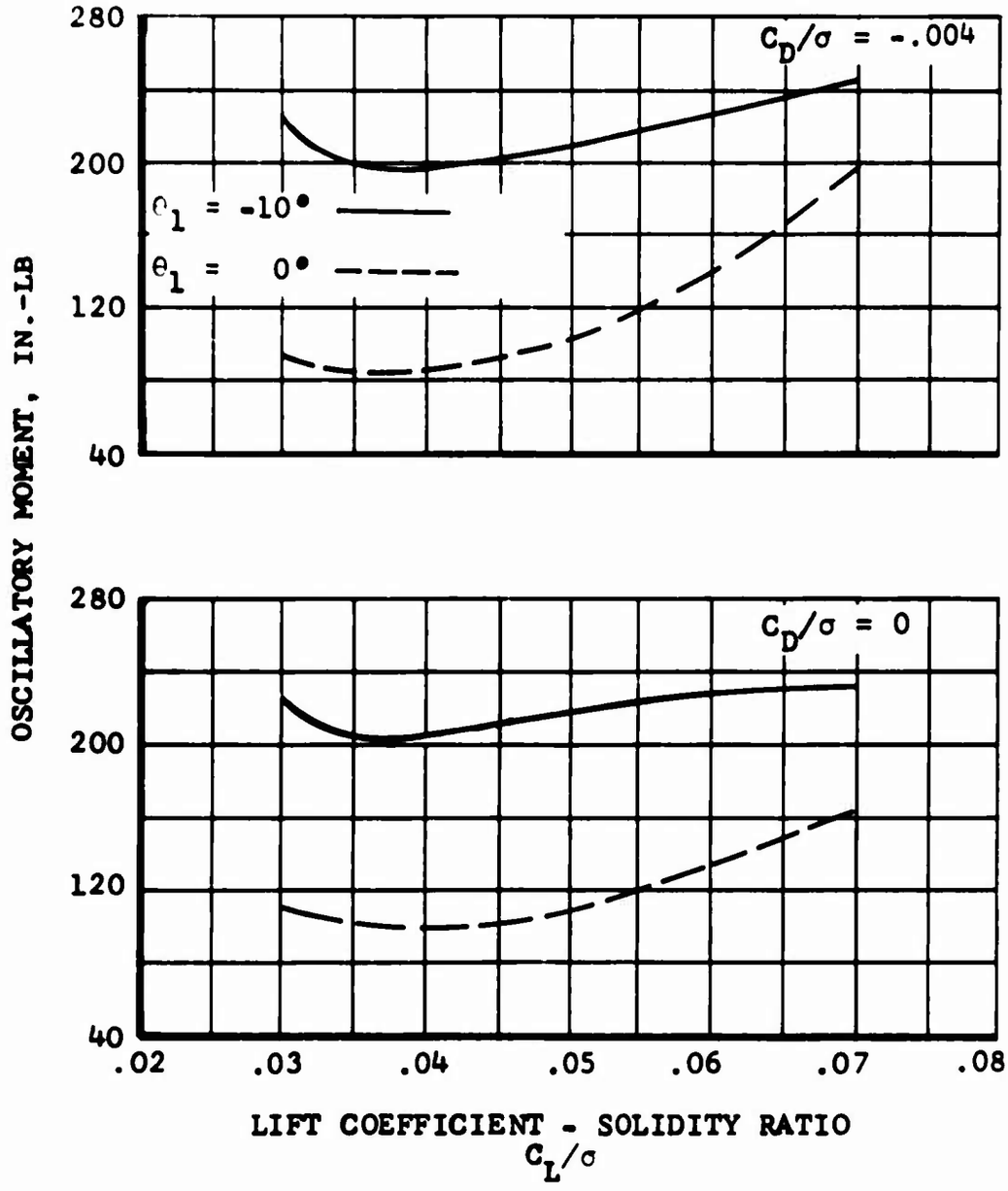

(b) CHORDWISE

Figure 26. Continued.

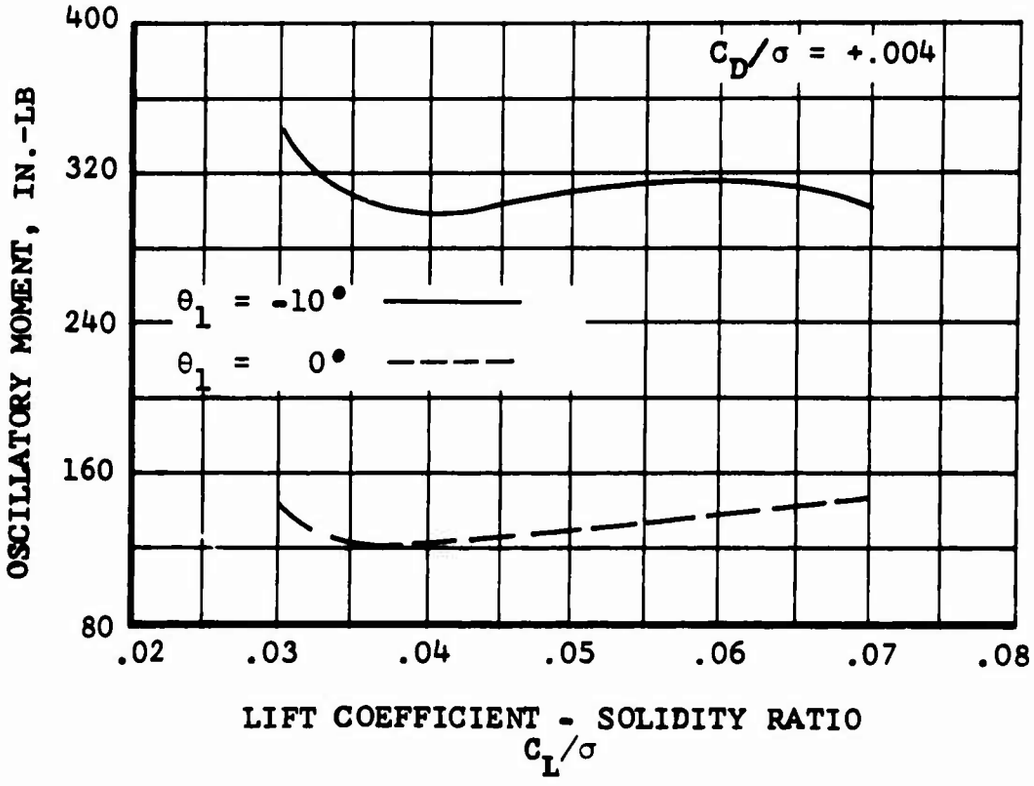

(b) CHORDWISE CONCLUDED

Figure 26. Continued.

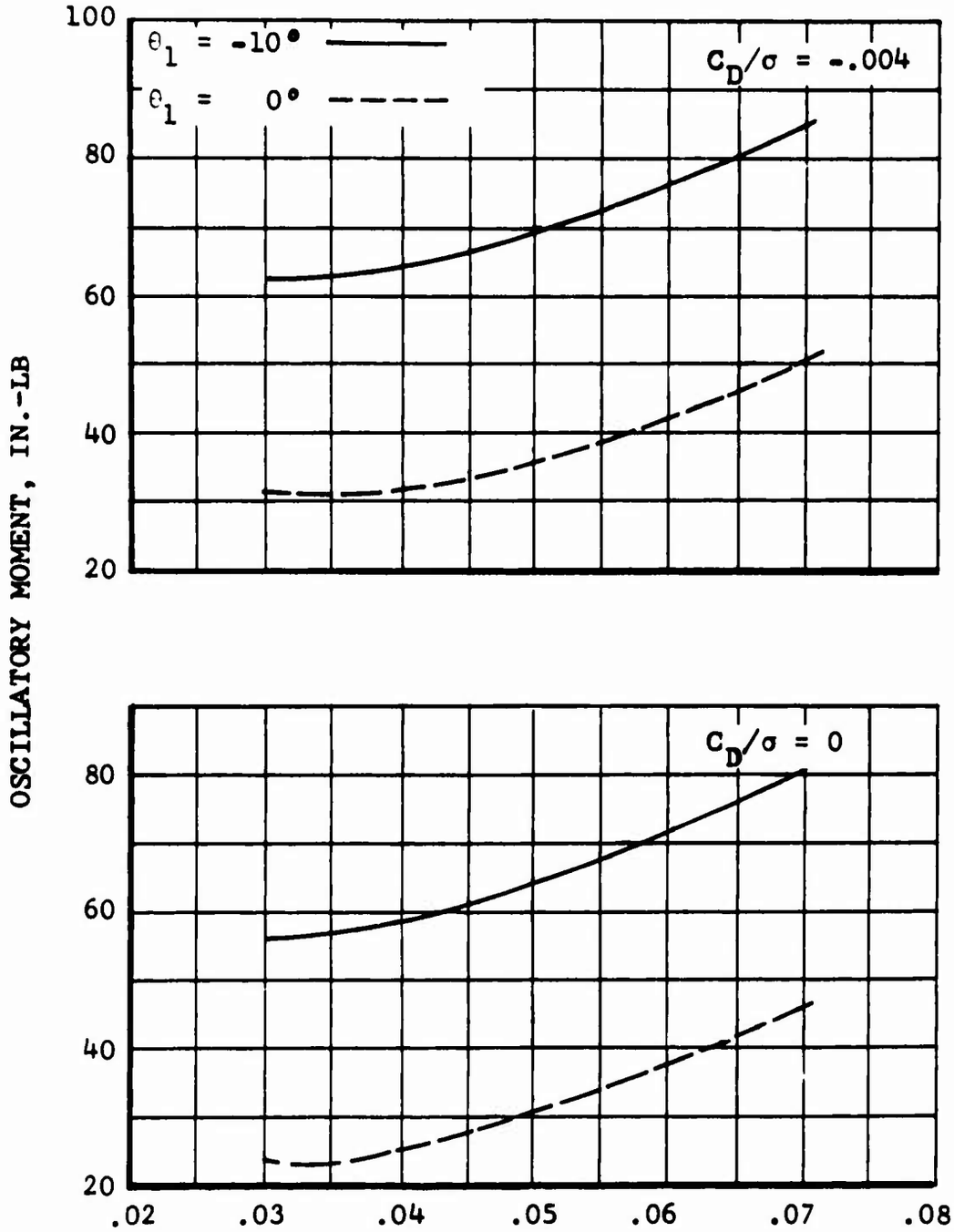

(c) TORSIONAL

Figure 26. Continued.

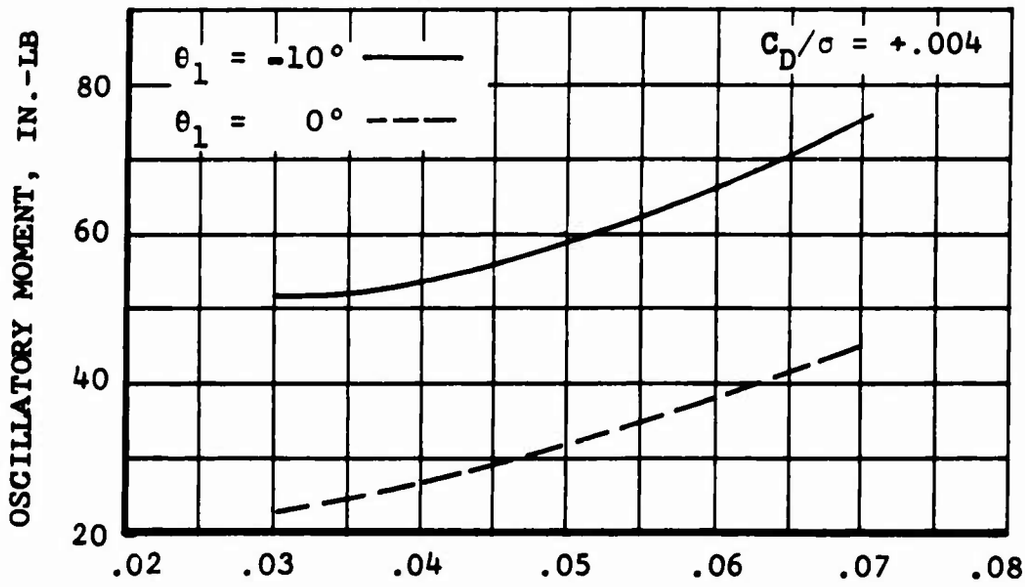

(c) TORSIONAL CONCLUDED

Figure 26. Concluded.

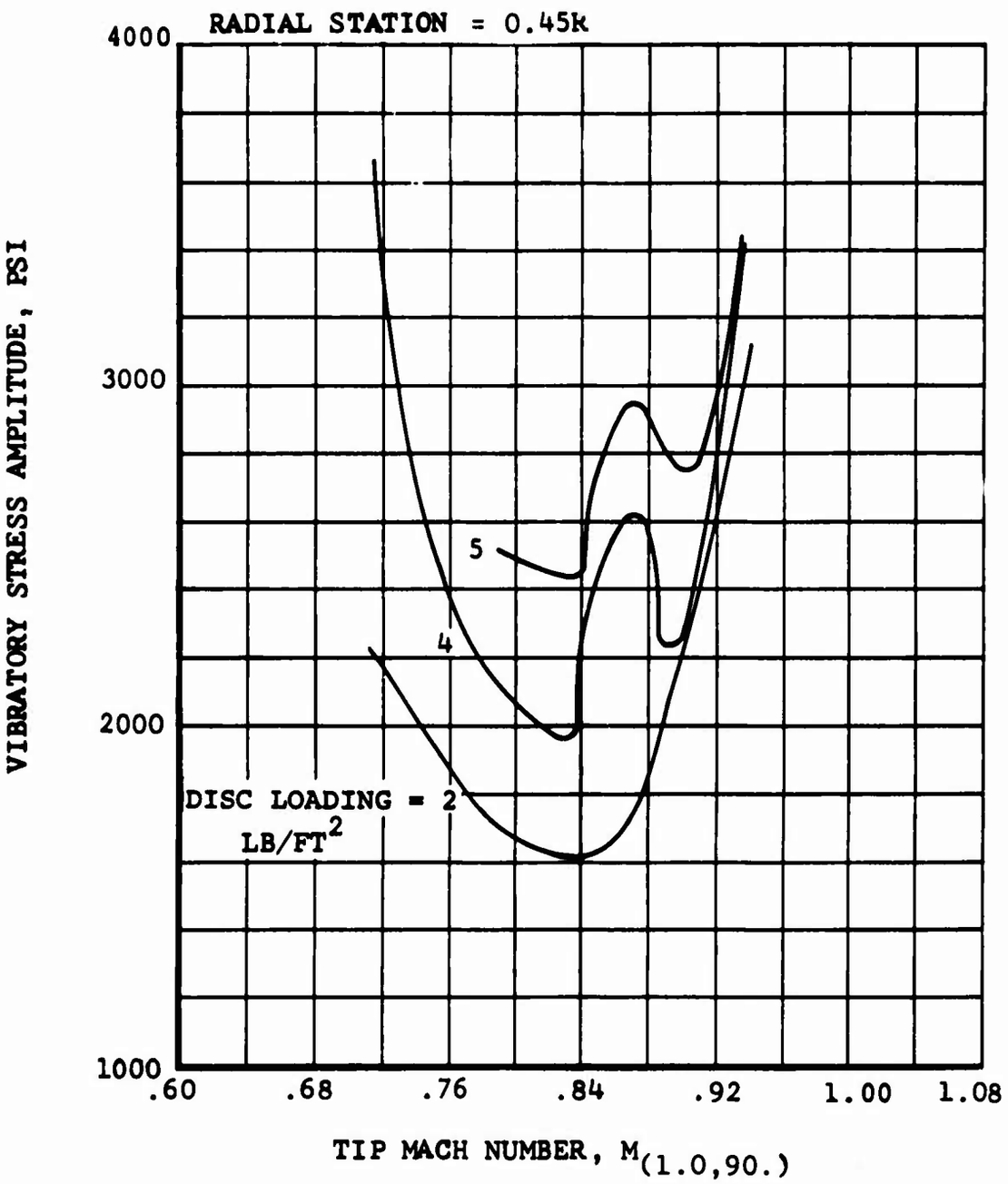

Figure 27. Example Figure Showing the Effect of Advancing-Tip Mach Number on Flapwise Rotor Loads, $C_D/\sigma = 0.004$, $\mu = 0.40$, $\theta_1 = 0°$ (From Figure 76, Reference 5).

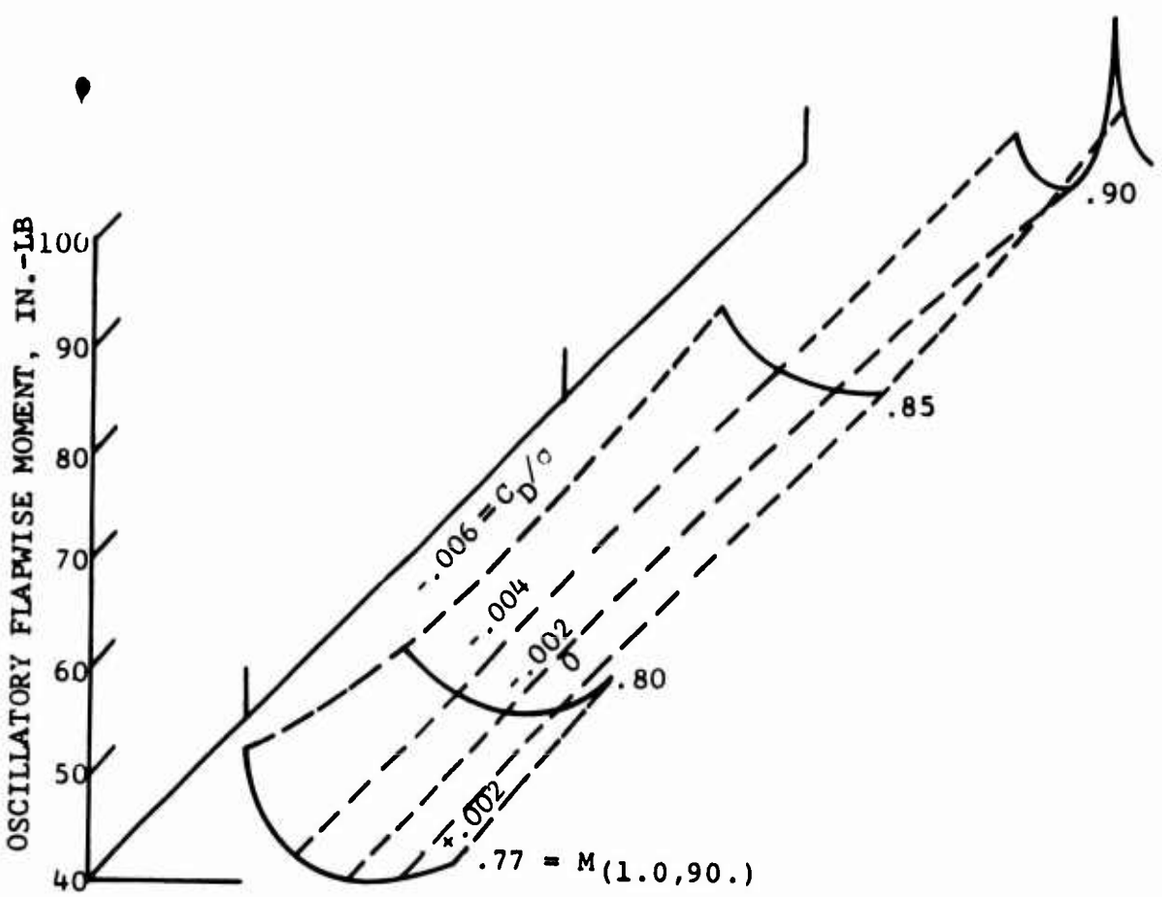

(a) DISC LOADING = 1 LB/FT^2

Figure 28. The Effect of Advancing Tip Mach Number on Flapwise Oscillatory Moments at Radial Station 0.45R for Several Values of Drag and Disc Loading at μ = 0.45.

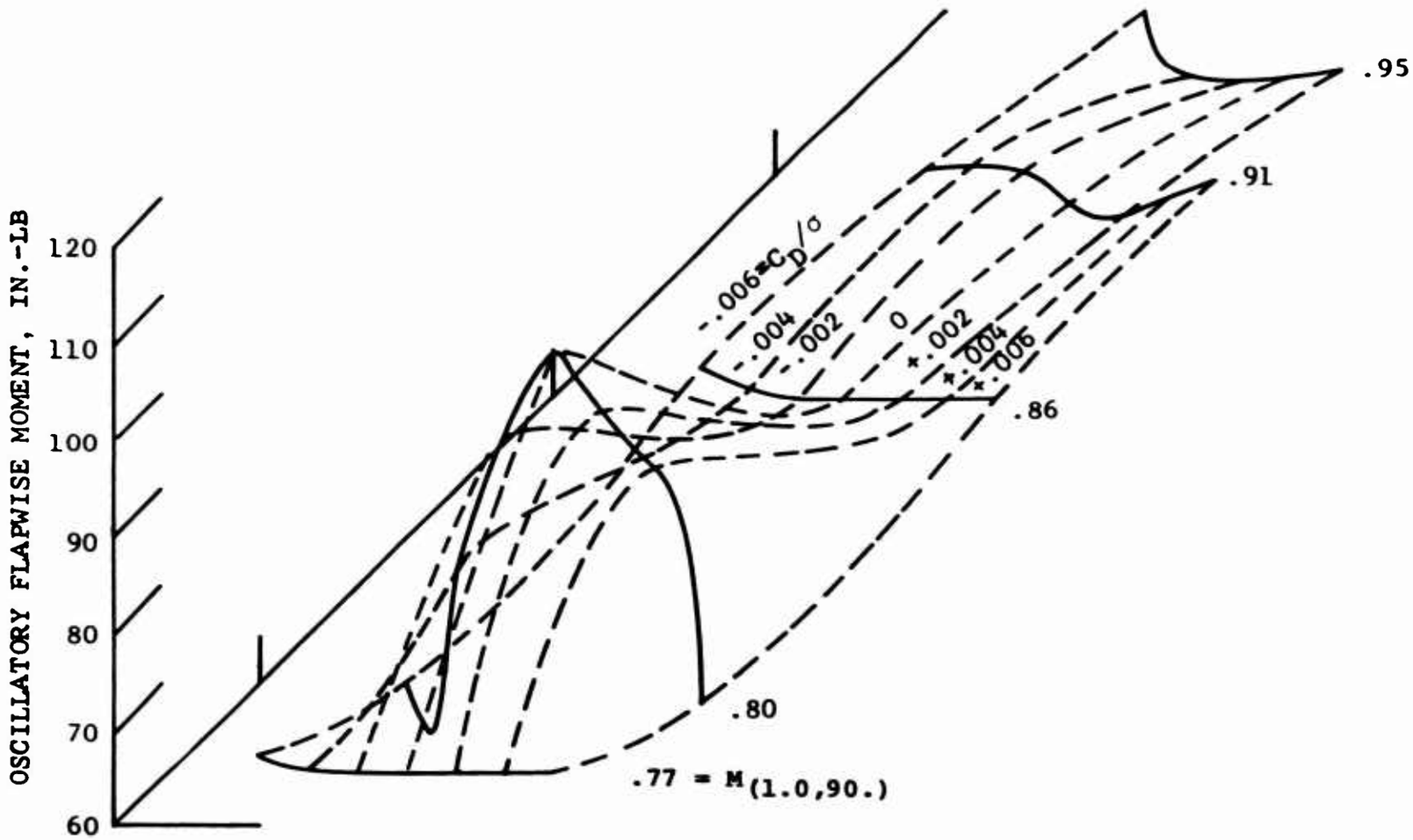

(b) DISC LOADING = 2 LB/FT^2

Figure 28. Continued.

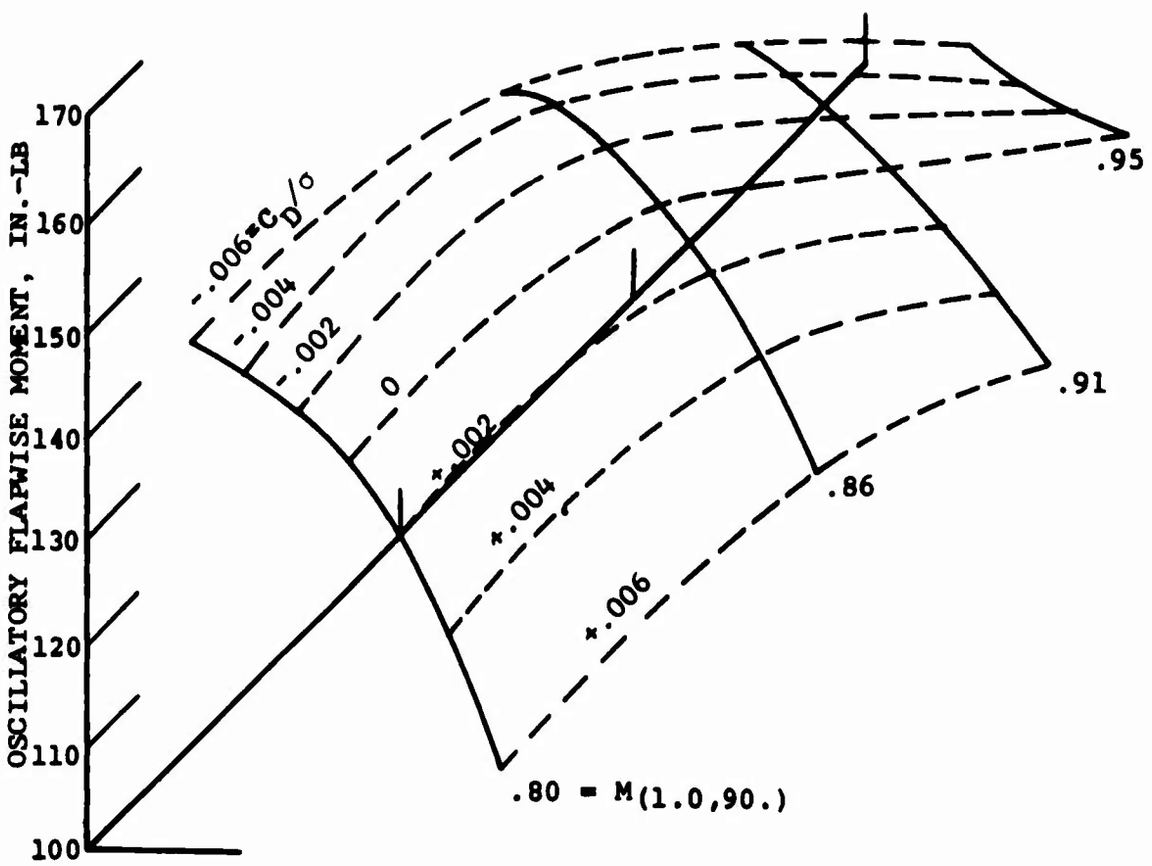

(c) DISC LOADING = 4 LB/FT^2

Figure 28. Concluded.

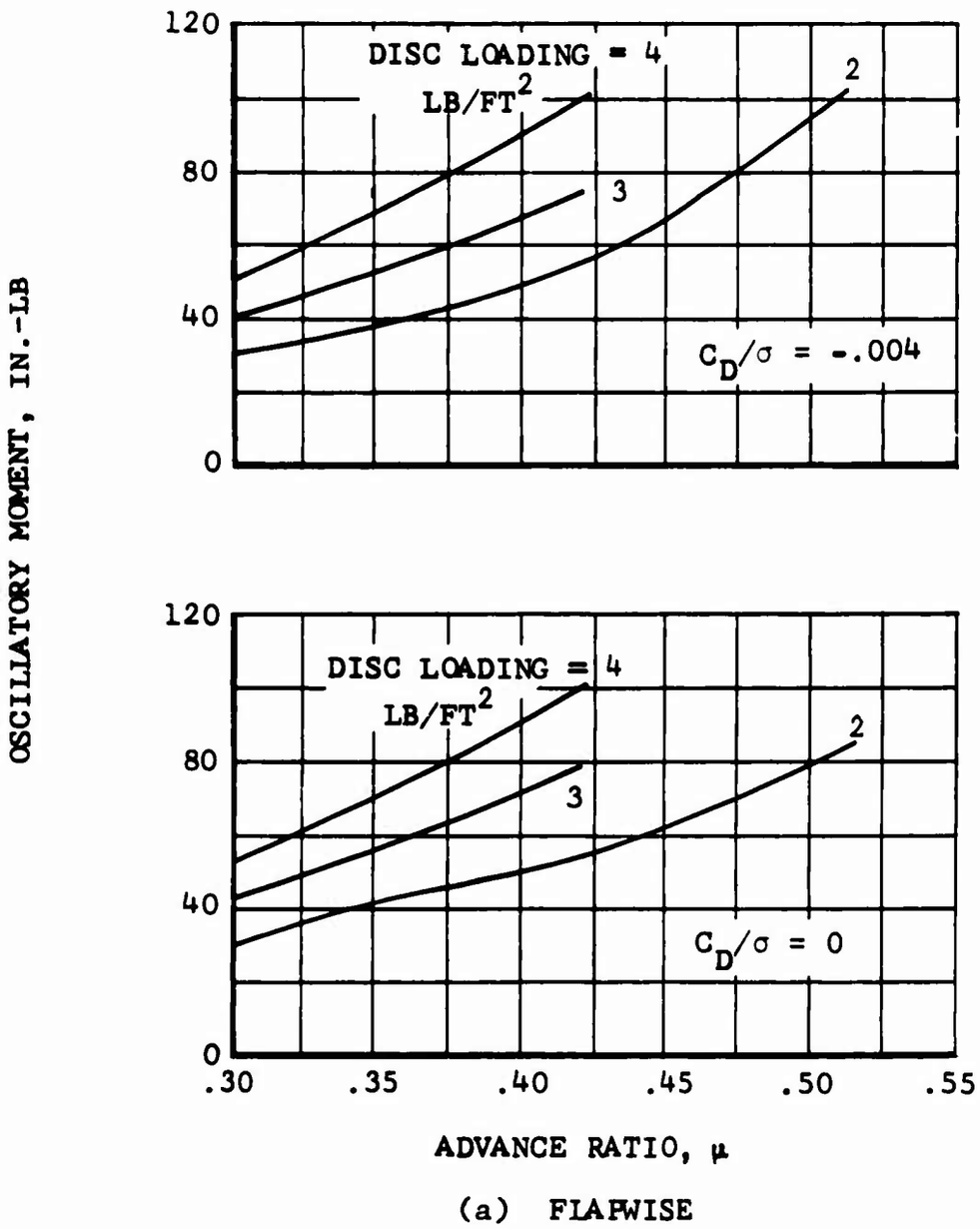

(a) FLAPWISE

Figure 29. The Effect of Advance Ratio on Flapwise, Chordwise, and Torsional Oscillatory Moments at Radial Station 0.45R at Three Values of Disc Loading, $M_{(1.0,90.)}$ = 0.90, θ_1 = 0°.

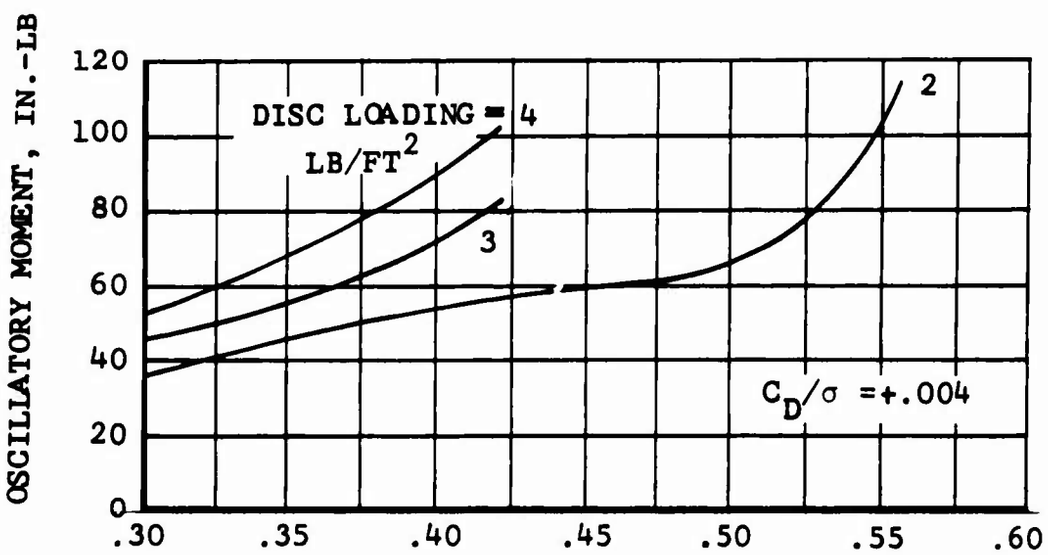

(a) FLAPWISE CONCLUDED

Figure 29. Continued.

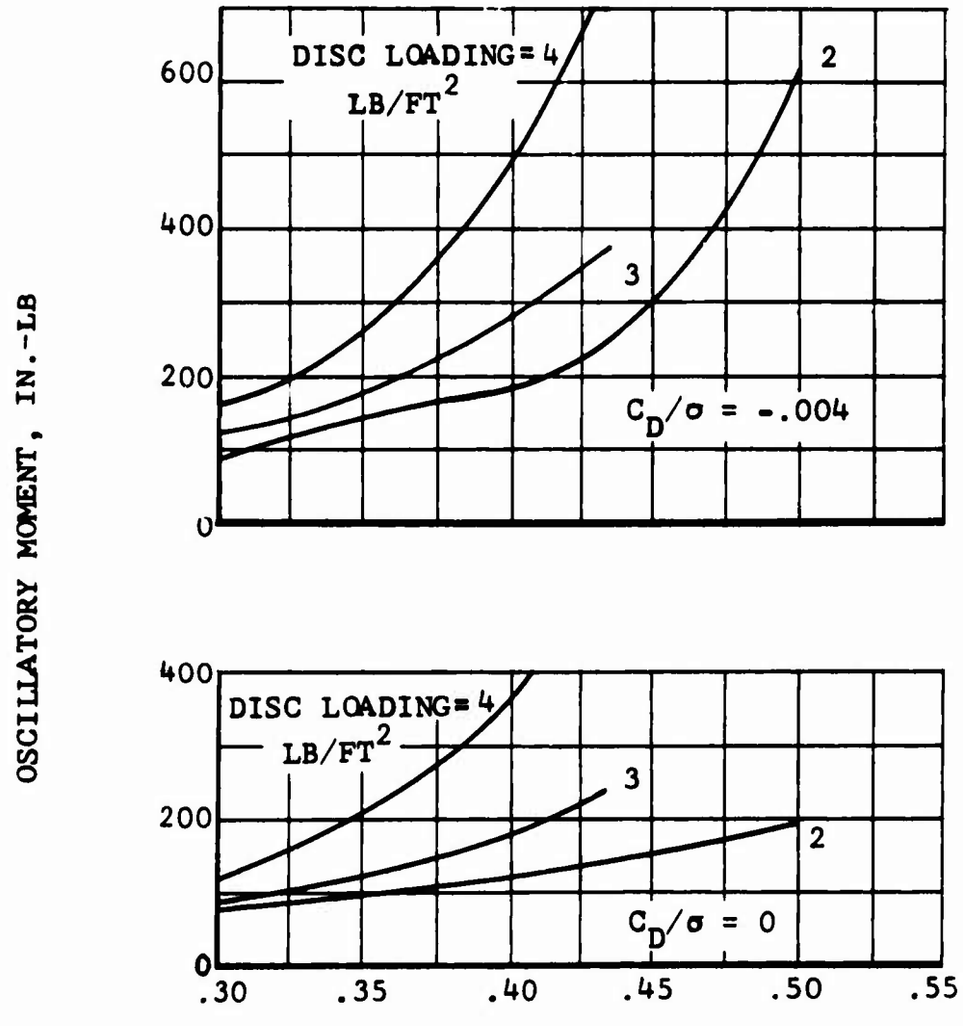

(b) CHORDWISE

Figure 29. Continued.

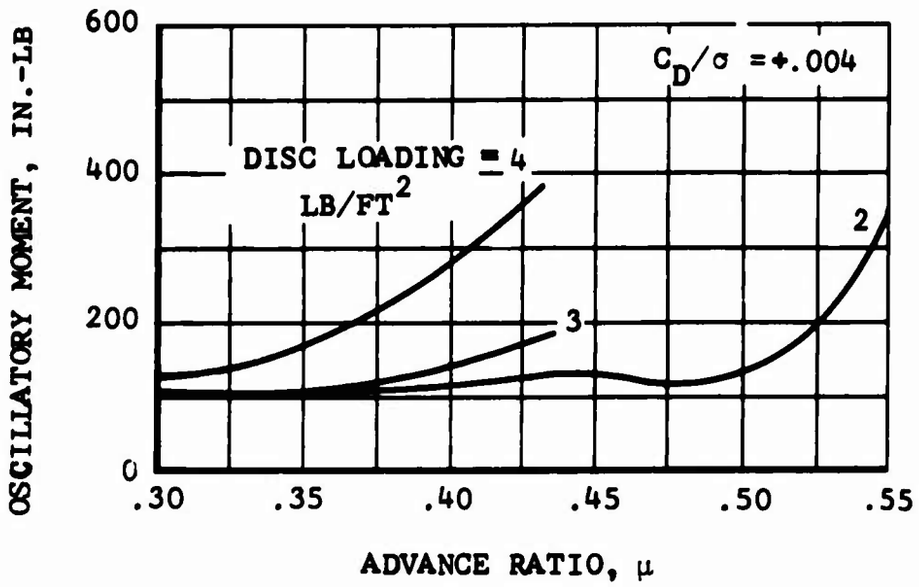

(b) CHORDWISE CONCLUDED

Figure 29. Continued.

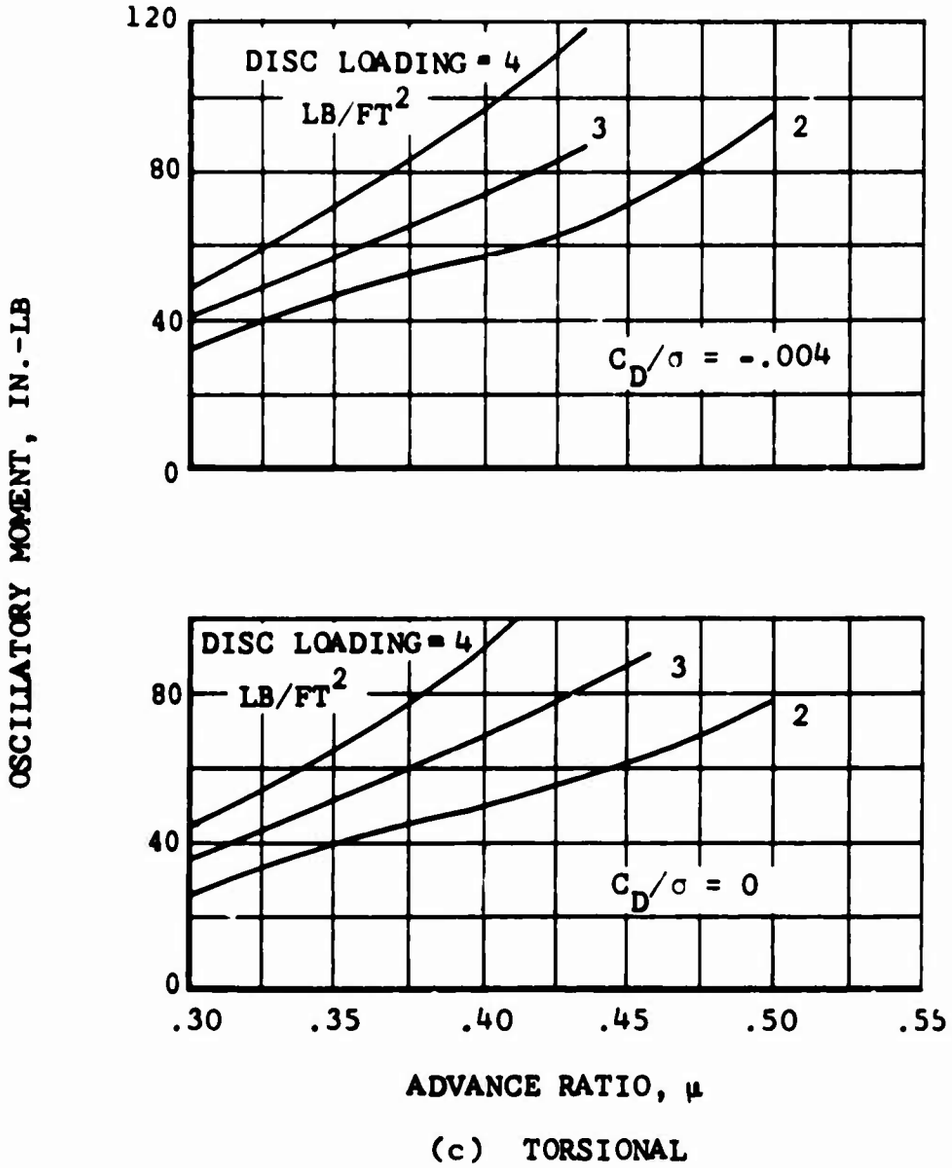

(c) TORSIONAL

Figure 29. Continued.

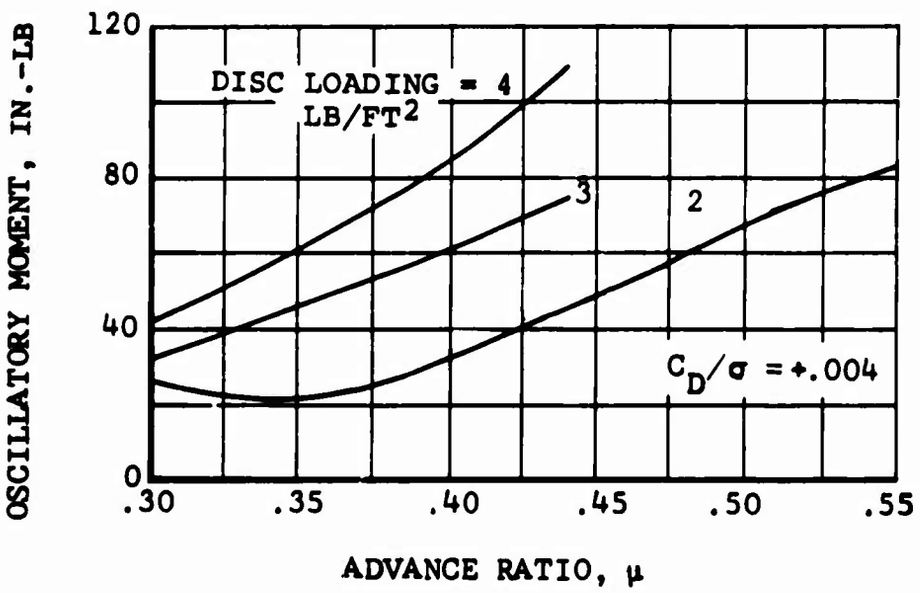

(c) TORSIONAL CONCLUDED

Figure 29. Concluded.

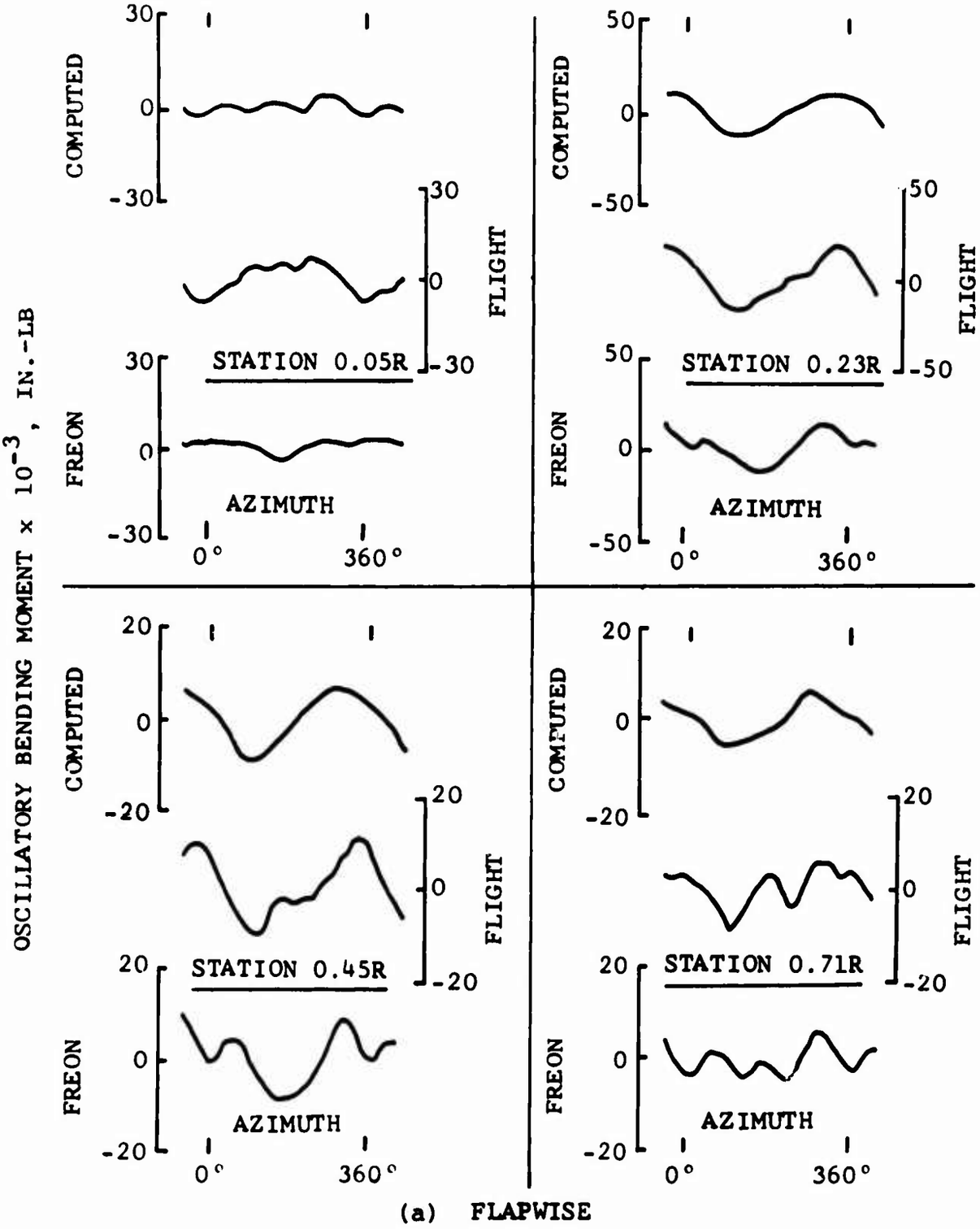

(a) FLAPWISE

Figure 30. Comparison of Computed and Measured Flapwise and Chordwise Bending Moment Waveforms at Several Radial Stations, V = 128 Knots, θ_1 = -10°, μ = 0.29, $M_{(1.0,90.)}$ = 0.89.

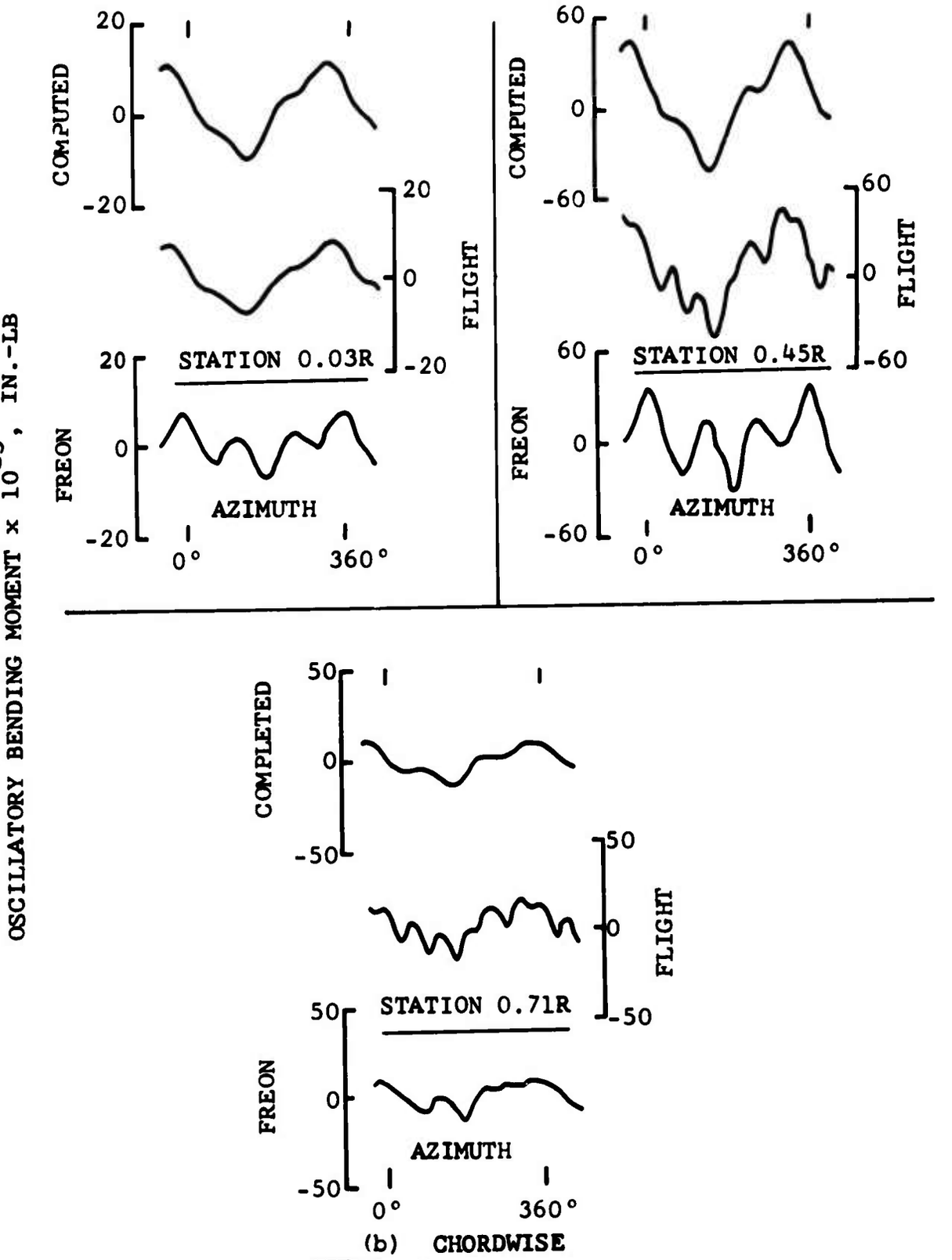

(b) CHORDWISE

Figure 30. Concluded.

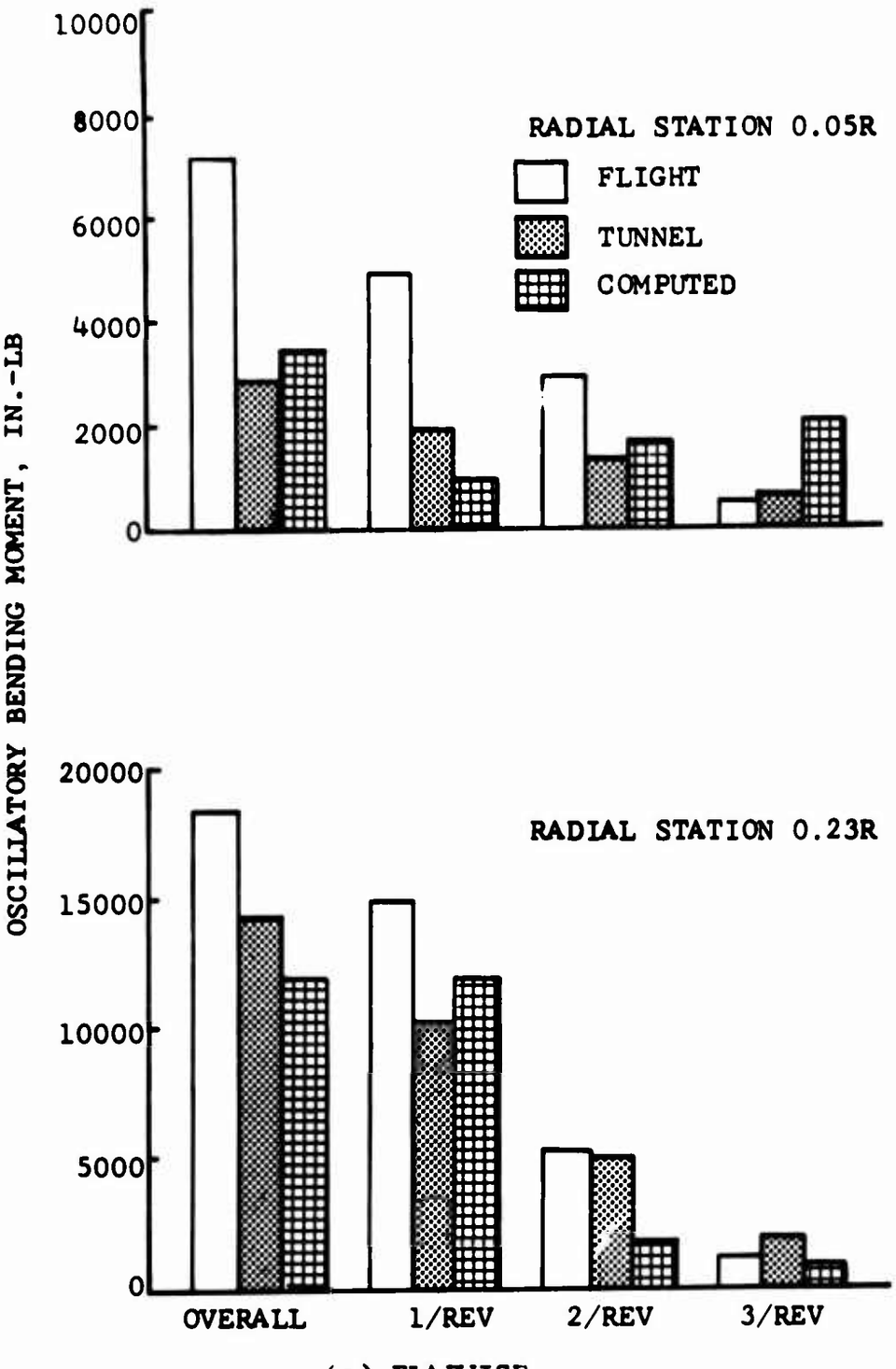

(a) FLAPWISE

Figure 31. Comparison of Computed and Measured Flapwise and Chordwise Bending Moment Harmonic Amplitudes at Several Radial Stations, V = 128 Knots, θ_1 = -10°, μ = 0.29, $M_{(1.0,90.)}$ = 0.89.

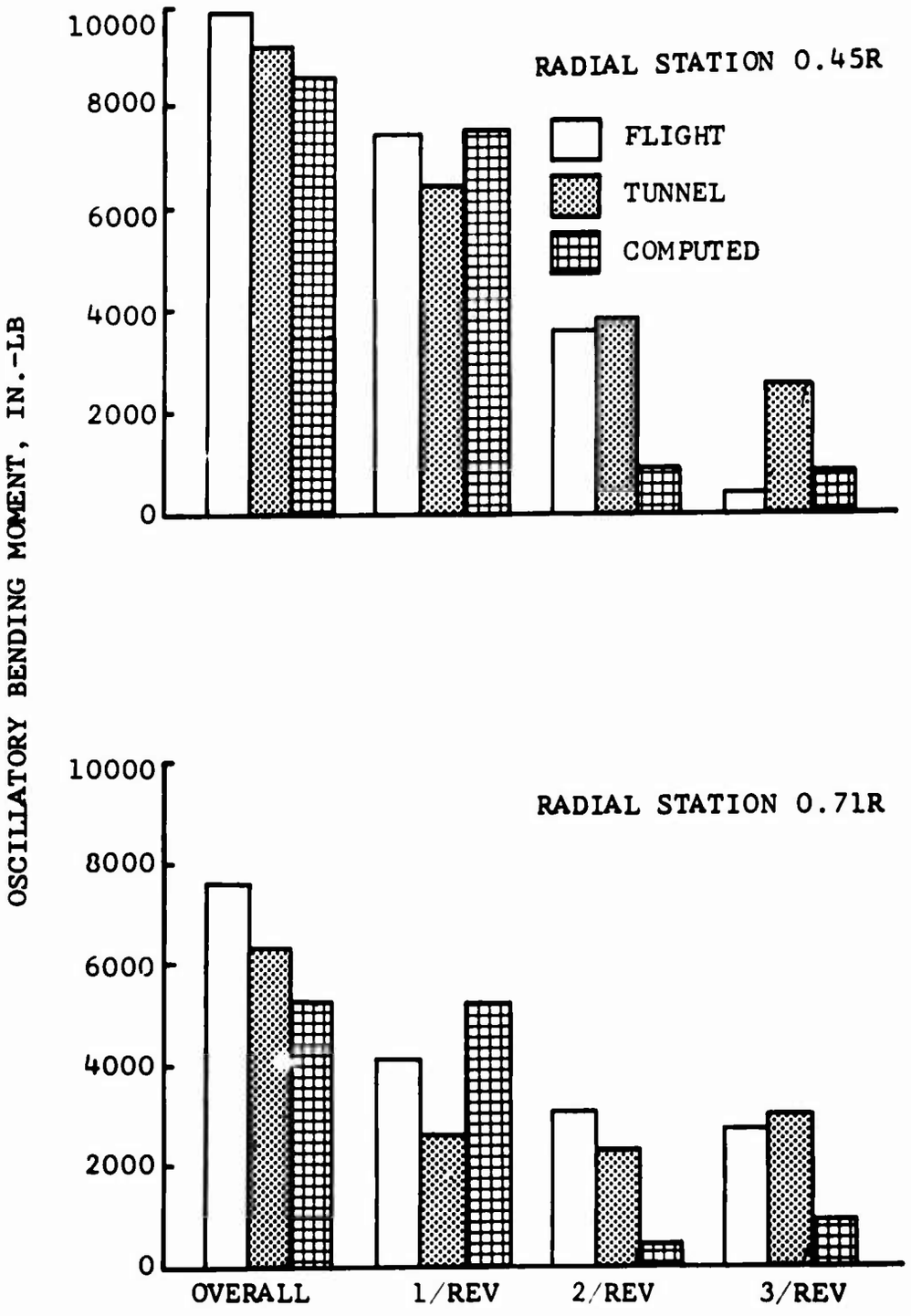

(a) FLAPWISE CONCLUDED

Figure 31. Continued.

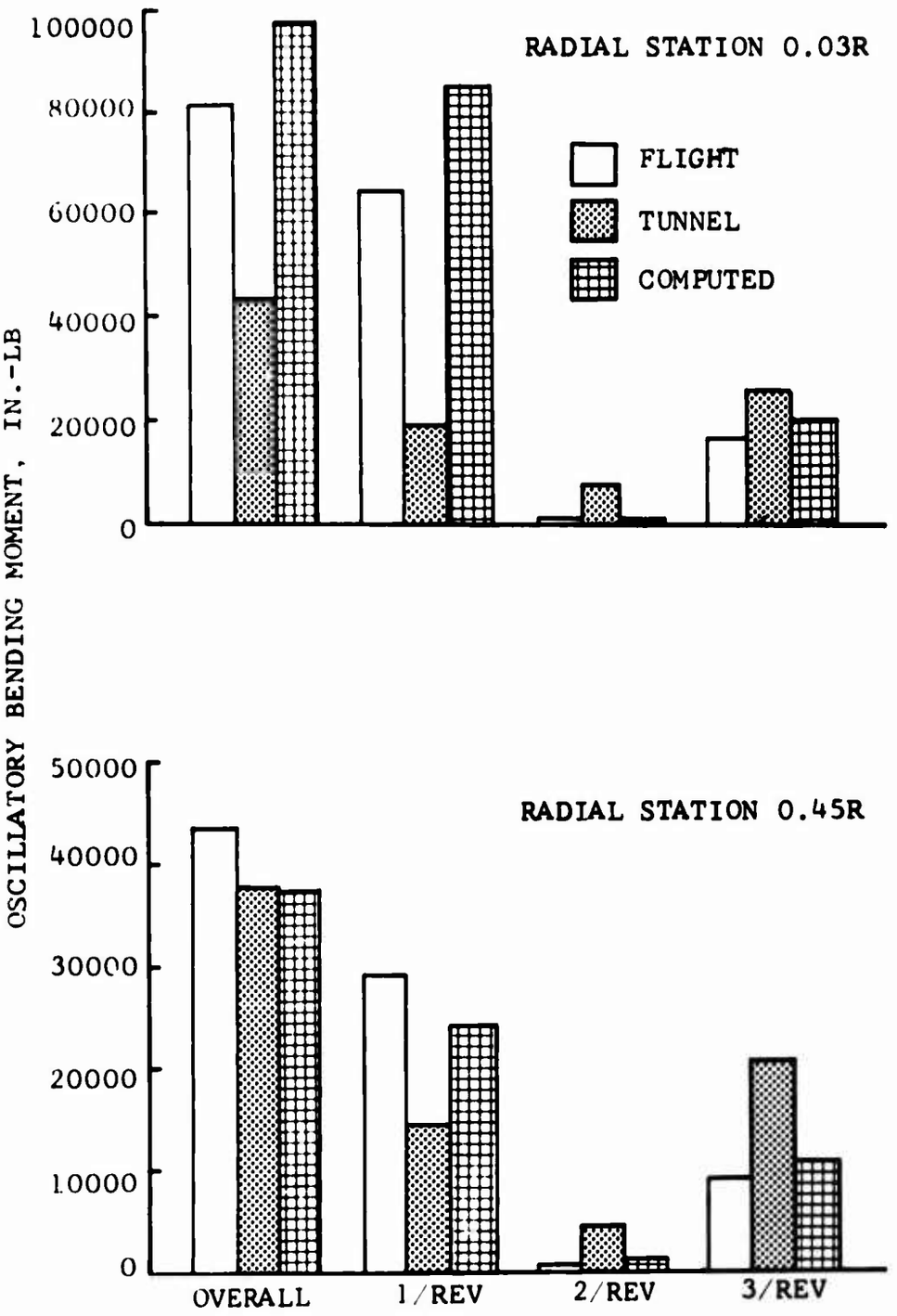

(b) CHORDWISE

Figure 31. Continued.

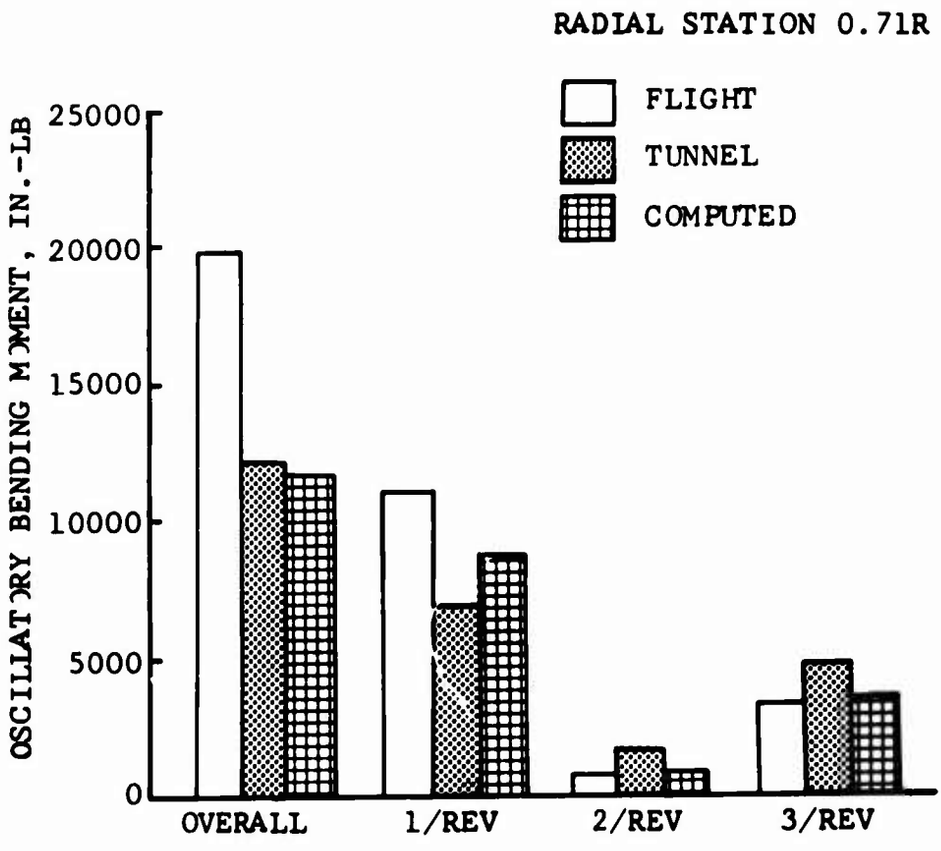

(b) CHORDWISE CONCLUDED

Figure 31. Concluded.

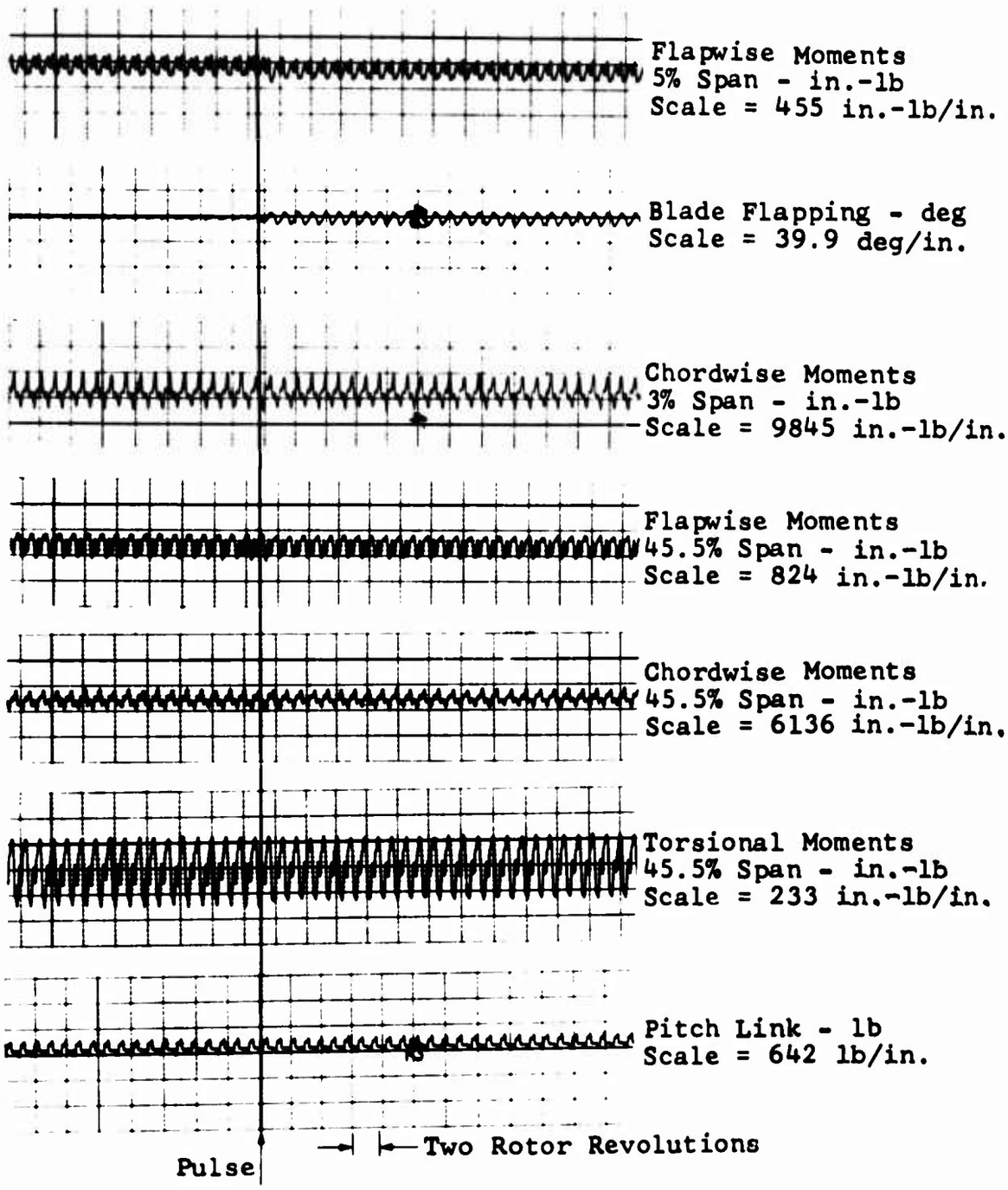

Figure 32. Transient Loads and Flapping Excited by a 1-Degree Step Input in Cyclic Pitch, V = 116 Knots, $\mu = 0.30$, $M_{(1.0,90.)} = 0.80$, $C_L/\sigma = 0.084$, $C_D/\sigma = -0.010$.

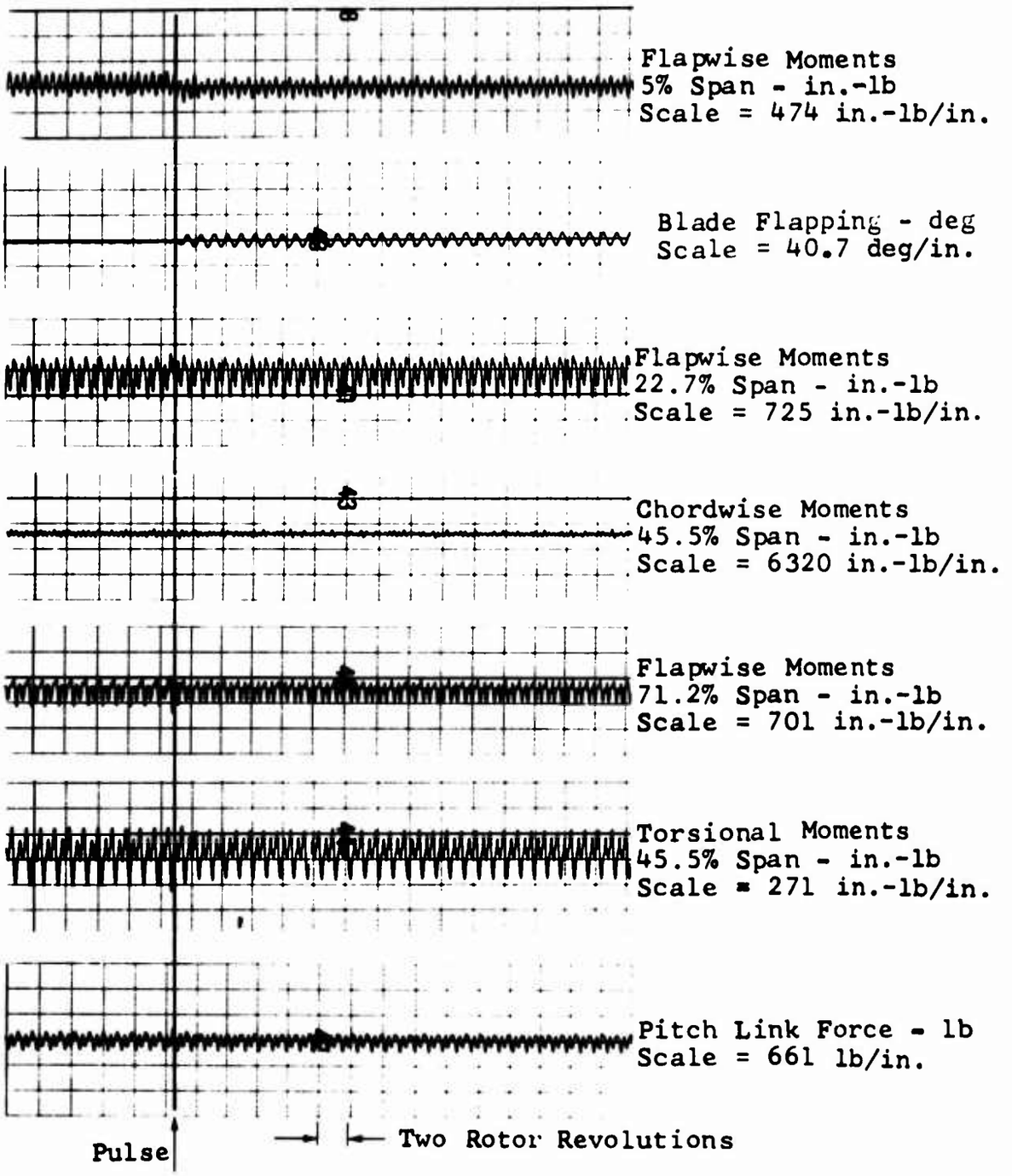

Figure 33. Transient Loads and Flapping Excited by a 1-Degree Step Input in Cyclic Pitch, V = 190 Knots, $\mu = 0.49$, $M_{(1.0,90.)} = 0.90$, $C_L/\sigma = 0.018$, $C_D/\sigma = -0.001$.

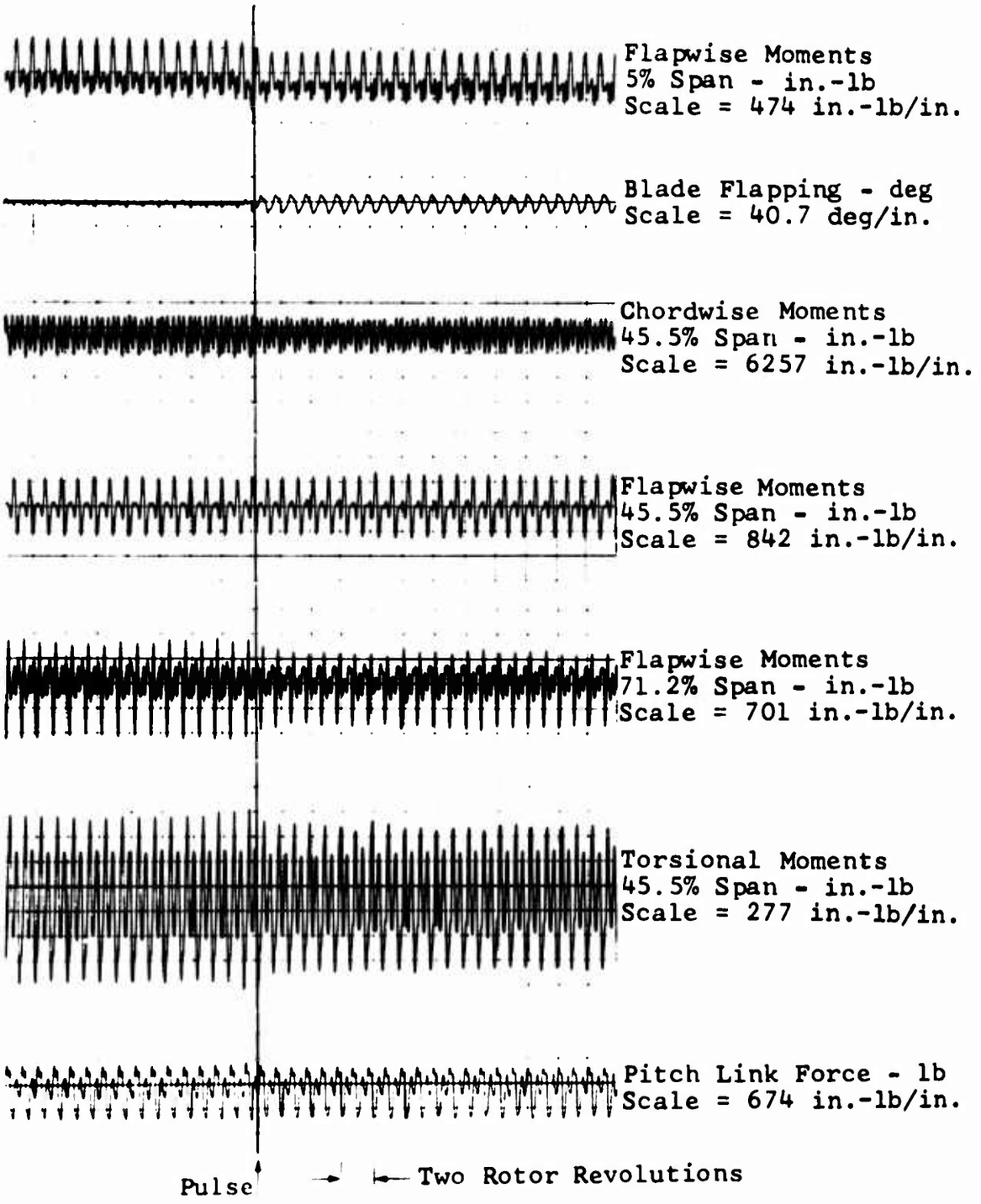

Figure 34. Transient Loads and Flapping Excited by a 1-Degree Step Input in Cyclic Pitch, V = 243 Knots, $\mu = 0.72$, $M_{(1.0,90.)} = 0.91$, $C_L/\sigma = 0.013$, $C_D/\sigma = 0.010$.

LITERATURE CITED

1. Lee, Charles D., WEIGHT CONSIDERATIONS IN DYNAMICALLY SIMILAR MODEL ROTOR DESIGN, Bell Helicopter Company, S.A.W.E. Paper 659, S.A.W.E., Inc., P. O. Box 60024, Terminal Annex, Los Angeles, California, 90054, May 1968.

2. Tanner, W. H., and Van Wyckhouse, J. F., WIND TUNNEL TESTS OF FULL-SCALE ROTORS OPERATING AT HIGH ADVANCING TIP MACH NUMBERS AND ADVANCE RATIOS, Bell Helicopter Company, Fort Worth, Texas, USAAVLABS Technical Report 68-44, U. S. Army Aviation Materiel Laboratories, Fort Eustis, Virginia, July 1968, AD674188.

3. Charles, B. D., and Tanner, W. H., WIND TUNNEL INVESTIGATION OF SEMIRIGID FULL-SCALE ROTORS OPERATING AT HIGH ADVANCE RATIOS, Bell Helicopter Company, Fort Worth, Texas, USAAVLABS Technical Report 69-2, U. S. Army Aviation Materiel Laboratories, Fort Eustis, Virginia, January 1969, AD684396.

4. Tanner, W. H., CHARTS FOR ESTIMATING ROTARY WING PERFORMANCE IN HOVER AND AT HIGH FORWARD SPEEDS, Sikorsky Aircraft, Division of United Aircraft Corporation, Stratford, Connecticut, NASA CR-114, National Aeronautics and Space Administration, Washington, D. C., November 1964.

5. Paglino, Vincent M., and Logan, Andrew H., AN EXPERIMENTAL STUDY OF THE PERFORMANCE AND STRUCTURAL LOADS OF A FULL-SCALE ROTOR AT EXTREME OPERATING CONDITIONS, Sikorsky Aircraft, Division of United Aircraft Corporation, Stratford, Connecticut, USAAVLABS Technical Report 68-3, U. S. Army Aviation Materiel Laboratories, Fort Eustis, Virginia, July 1968, AD674187.

6. Drees, J. M., HIGH SPEED HELICOPTER ROTOR DESIGN, Journal of the American Helicopter Society, Vol. 8, No. 3, July 1963, pp. 21-29.

7. Van Wyckhouse, J. F., and Cresap, W. L., HIGH-PERFORMANCE HELICOPTER PROGRAM - SUMMARY REPORT, PHASE II, Bell Helicopter Company, TRECOM Technical Report 64-61, U. S. Army Transportation Research Command, Fort Eustis, Virginia, October 1964.

8. Fradenburg, E. A., and Segel, R. M., MODEL AND FULL-SCALE COMPOUND HELICOPTER RESEARCH, Proceedings of the 21st Annual American Helicopter Society Forum, May 12-14, 1965, pp. 38-64.

9. Norman, O. L., LOAD LEVEL SURVEY WITH THE 540 ROTOR SYSTEM ON THE UH-1B HELICOPTER, Bell Report 204-100-103, Bell Helicopter Company, Fort Worth, Texas, August 4, 1965.

10. Rabbott, J. P., Lizak, A. A., and Paglino, V. M., A PRESENTATION OF MEASURED AND CALCULATED FULL-SCALE ROTOR BLADE AERODYNAMIC AND STRUCTURAL LOADS, USAAVLABS Technical Report 66-31, U. S. Army Aviation Materiel Laboratories, Fort Eustis, Virginia, July 1966, AD639981.

APPENDIX
TABULATED AERODYNAMIC DATA

The data presented in this appendix were recorded by the Transonic Dynamics Tunnel at the NASA-Langley Research Center. These data include the test conditions, rotor configuration, root collective pitch, blade flapping angle, and lift, drag, and torque coefficients divided by the rotor solidity.

Six-component forces and moments were measured by an internal balance. The tare corrections are shown on Figure 35, and were applied to the balance data to account for the forces and moments produced by the basic model, fairings, and rotating hub. The rotating hub tares included all hardware inboard of the blade attachment point (Blade Station 11.4). The tares were applied based on tunnel dynamic pressure and shaft angle. Rotor downwash effects on the tares were neglected, and no data adjustments were made for wall effects.

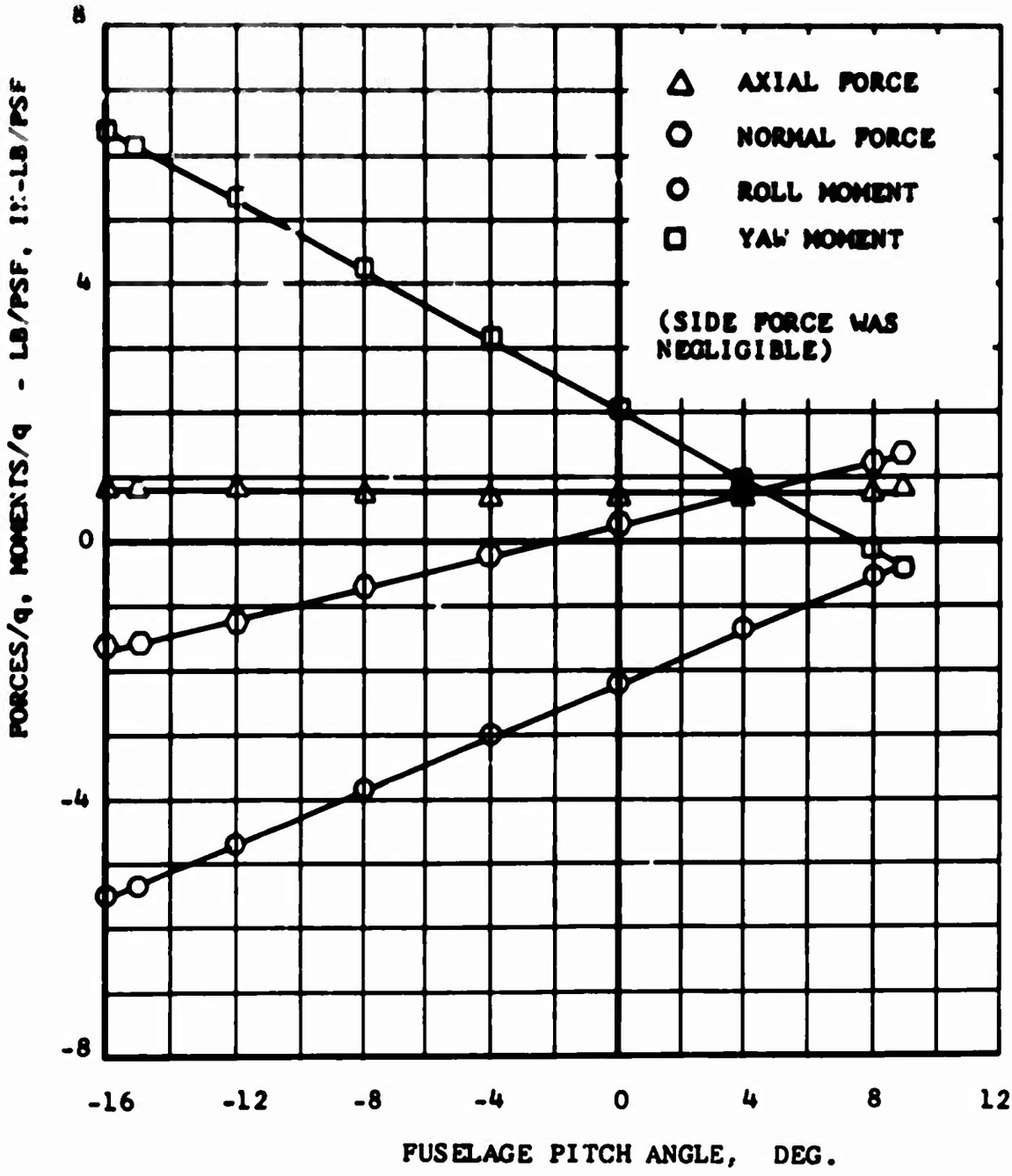

(a) DYNAMIC TARES

Figure 35. Model Tare Corrections.

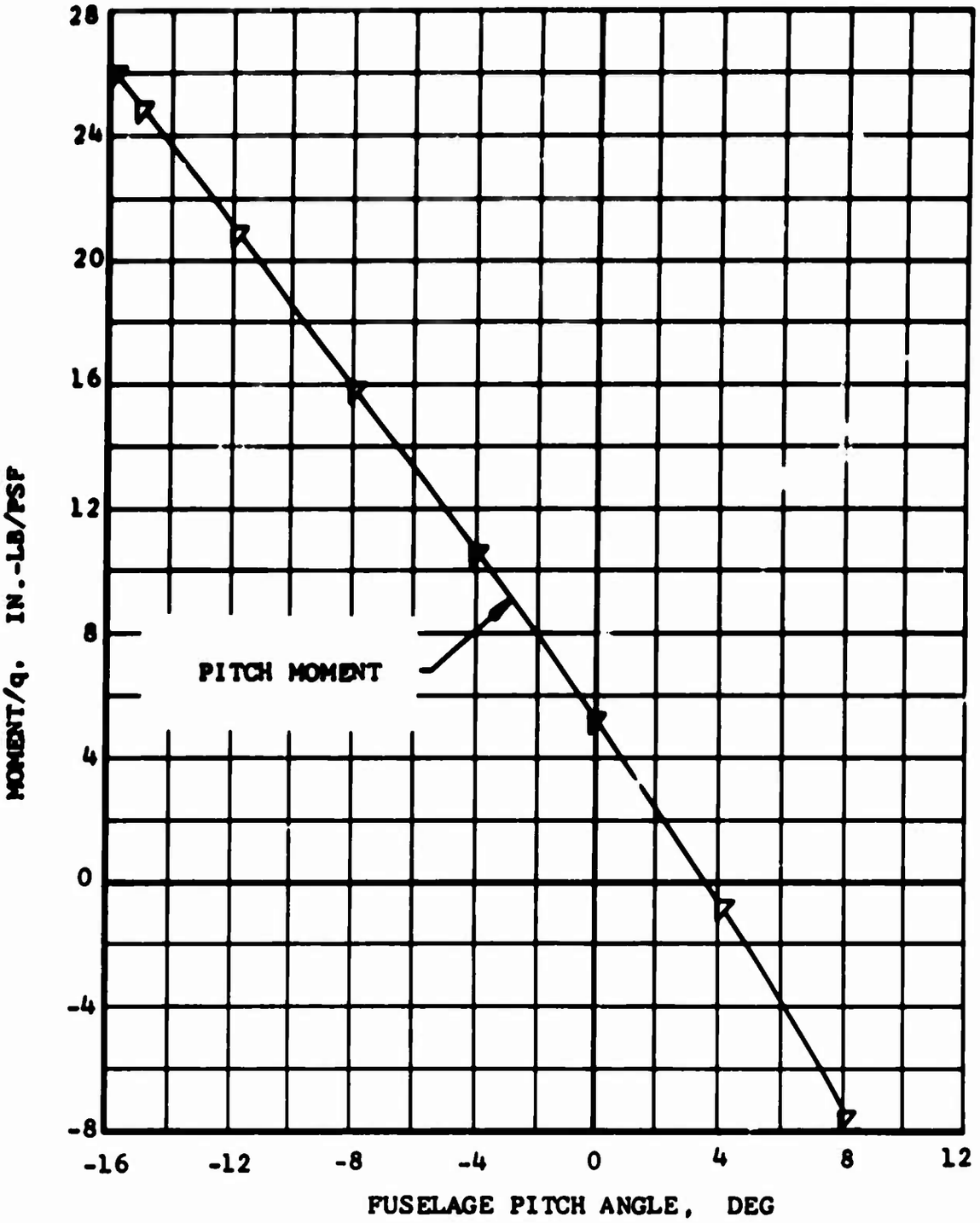

(b) DYNAMIC TARES CONCLUDED

Figure 35. Continued.

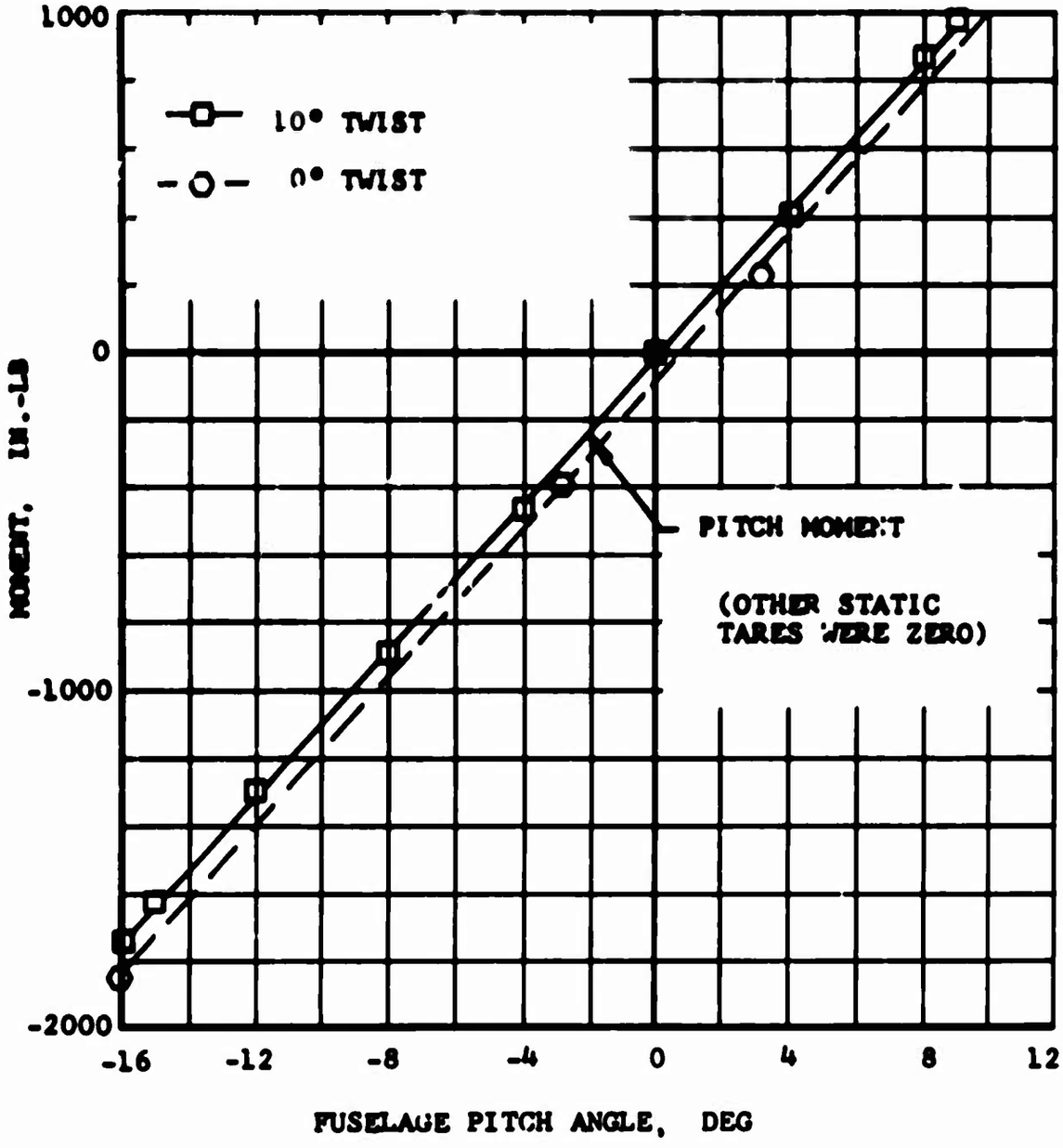

(c) STATIC TARES

Figure 35. Concluded.

TEST 151 11-FOOT ROTOR

RUN 5 μ = .30 $M_{(1.0,\ 90)}$ = .73 RPM = 491 θ_1 = -10°

PT	ALPHA	THETA0	CQ/SIG	CLP/SIG	CDP/SIG	VFS	V/VMAX	R TIP	B1
122	.14	10.93	.601e98	.J18661	.J00034	6.98	.025	.582	-.14
123	.15	10.80	.001511	.047059	.001876	83.99	.297	.735	2.83
124	.16	16.14	.004963	.C99132	-.000407	85.17	.301	.734	3.15
125	.21	17.92	.008708	.112106	-.003585	85.28	.302	.734	9.57
126	.20	13.28	.002534	.078855	.001187	84.84	.300	.733	5.41
127	5.13	9.11	.000464	.050376	.J05920	85.35	.302	.734	3.11
128	5.14	13.28	.002030	.C96545	.007993	84.61	.299	.732	3.21
129	5.14	16.43	.006783	.117018	.J05469	84.46	.299	.732	3.21
130	5.14	10.65	.000408	.071730	.007660	84.88	.300	.733	4.12
131	-5.51	14.07	.003649	.053460	-.004677	85.15	.301	.733	2.00
132	-5.51	16.95	.005732	.078744	-.006490	85.14	.301	.733	7.10
133	-5.53	18.68	.008907	.099675	-.013046	85.06	.301	.732	8.96
134	-5.53	19.82	.010660	.099844	-.014232	85.74	.303	.734	5.22
135	-9.68	17.13	.005722	.059679	-.010790	85.45	.302	.733	7.51
136	-9.58	19.31	.008679	.082416	-.016855	85.44	.302	.733	8.56
137	-9.62	22.63	.014992	.132139	-.024623	85.79	.303	.733	8.22
139	-15.39	21.74	.010968	.065413	-.023135	84.34	.298	.730	.79
140	-15.39	22.79	.012741	.074310	-.025719	85.02	.301	.732	9.25
141	-5.17	13.87	.003589	.J54284	-.004186	84.85	.300	.731	6.06
142	-5.16	19.92	.011112	.132575	-.014257	85.05	.301	.731	9.97
143	-5.16	19.82	.011287	.105692	-.013923	85.20	.301	.731	9.97

TEST 151 11-FOOT ROTOR

RUN 501 μ = .31 $M_{(1.0, 90)}$ = .71 RPM = 478 θ_1 = -10°

PT	ALPHA	THETA	CD/SIG	CLP/SIG	CMP/SIG	VFS	[illegible]	[illegible] TIP	a1
249	.02	10.33	.001689	.052382	.000532	85.19	.309	.714	5.46
250	.04	12.38	.002695	.078443	-.000111	85.19	.309	.714	7.33
251	.04	15.33	.006064	.104829	-.002372	85.19	.309	.714	9.78
252	.09	19.51	.016498	.135578	-.011513	85.02	.311	.715	12.54
253	-4.92	12.82	.003639	.051679	-.004827	85.34	.310	.714	4.80
254	-4.92	12.86	.003588	.051385	-.004795	85.36	.309	.714	4.87
255	-4.92	15.01	.005422	.077744	-.008092	85.19	.309	.711	7.50
256	-4.93	18.24	.010531	.103603	-.014219	84.79	.306	.713	9.94
257	-4.94	19.94	.014892	.112830	-.016489	84.93	.304	.714	11.16
258	-4.94	18.20	.010627	.104215	-.013363	85.07	.309	.714	10.25
259	-9.92	15.50	.005627	.053288	-.010556	85.21	.310	.714	5.34
260	-9.92	17.91	.008507	.081106	-.016454	85.22	.310	.714	7.61
261	-9.90	21.76	.016219	.106509	-.020803	85.50	.311	.715	11.06
262	-14.70	18.04	.007521	.056022	-.015371	85.64	.311	.715	5.47
263	-14.70	20.39	.011775	.082717	-.024619	85.50	.311	.715	8.34
264	-14.70	22.70	.016655	.099564	-.031915	85.04	.309	.714	9.73
265	5.15	8.04	.000190	.031504	.003993	85.08	.309	.714	2.73
266	5.16	10.18	.000393	.077564	.008169	85.22	.310	.714	6.92
267	5.17	12.91	.002874	.103930	.007634	85.22	.310	.714	7.07
268	5.16	19.51	.016624	.133622	-.002425	85.08	.309	.714	11.66

TEST 151 11-FOOT ROTOR

RUN 6 μ = .30 $M_{(1.0,\ 90)}$ = .80 RPM = 534 θ_1 = -10°

PT	ALPHA	THETAO	CJ/SIG	CLP/SIG	CDP/SIG	VFS	V/VMAX	Q TIP	α1
156	.01	9.80	.001879	.021338	.000133	7.03	.023	.626	.01
157	.01	7.95	.001398	.021568	.001156	90.53	.296	.796	2.01
158	.01	9.28	.001497	.042033	.001135	90.89	.298	.795	2.84
159	.01	10.84	.002110	.063887	.000890	90.62	.295	.795	4.43
160	.01	12.52	.003292	.085020	.000327	90.49	.296	.795	5.81
161	-.01	16.09	.009399	.112097	-.004081	91.01	.298	.796	9.22
162	-5.01	11.61	.002940	.040852	-.003011	89.93	.292	.796	5.13
163	-5.01	11.57	.002931	.040866	-.002963	90.86	.295	.795	4.92
164	-5.01	13.18	.004259	.062236	-.005537	91.12	.298	.796	6.35
165	-5.01	15.27	.006190	.084557	-.008062	91.25	.297	.796	8.34
166	-5.01	15.03	.006072	.083114	-.008359	90.98	.296	.796	8.36
167	-3.92	17.77	.010682	.098040	-.015913	90.57	.294	.795	8.84
168	-10.13	14.68	.004737	.044297	-.008130	90.57	.294	.795	8.83
169	-10.13	16.60	.006841	.067674	-.012737	91.22	.297	.796	8.83
170	-10.05	18.59	.009937	.085565	-.018576	92.01	.299	.798	8.86
171	-10.07	20.05	.012958	.094687	-.022467	91.08	.296	.796	8.86
172	-14.63	18.00	.007245	.065584	-.013742	91.87	.299	.797	8.86
173	-14.63	19.76	.010720	.068946	-.021405	92.12	.300	.798	8.87
174	5.20	7.44	.000395	.041872	.005361	91.99	.299	.798	7.55
175	5.20	8.95	.000218	.062740	.007359	91.98	.299	.798	7.55
176	5.21	10.72	.000846	.084289	.008286	92.11	.299	.798	7.55
177	5.21	15.88	.009128	.122267	.009455	91.19	.298	.796	7.56

TEST 151 11-FOOT ROTOR

RUN 7 μ = .30 $M_{(1.0,\ 90)}$ = .87 RPM = 582 θ_1 = -10°

PT	ALPHA	THETAO	CQ/SIG	CLP/SIG	CDP/SIG	VFS	V/OMR	q TIP	dl
178	-3.41	12.38	.003205	.033225	-.001962	99.16	.296	.867	7.49
179	-3.57	13.07	.003783	.050605	-.003560	98.79	.295	.866	7.48
180	-3.72	13.94	.004670	.068565	-.005362	99.51	.297	.867	7.48
181	-3.54	16.62	.008914	.094663	-.012399	98.63	.294	.865	6.13
182	-3.65	13.87	.004736	.068888	-.005391	98.38	.293	.864	5.54

PT	ALPHA	THETAO	CQ/SIG	CLP/SIG	CDP/SIG	VFS	V/OMR	q TIP	dl
185	-.04	9.17	.001593	.035691	.001208	100.90	.301	.871	2.59
186	-.04	10.53	.001932	.053146	.000887	100.63	.300	.869	3.82
187	-.05	11.76	.002525	.071116	.000777	100.63	.300	.869	4.91
188	-.04	13.33	.004058	.088501	-.000436	99.18	.296	.866	6.37
189	-.06	16.76	.009775	.130614	-.005071	99.04	.295	.866	10.14
190	5.11	6.93	.000559	.034583	.003565	99.84	.298	.867	1.75
191	5.11	8.29	.000358	.052585	.000272	99.59	.297	.866	2.77
192	5.11	9.56	.000533	.070383	.001309	99.34	.296	.866	4.24
193	5.12	11.01	.001540	.088729	.001996	99.33	.296	.866	5.49
194	5.09	15.45	.008619	.115369	.005007	99.92	.298	.867	10.55
195	-9.80	13.70	.003917	.037197	-.006282	99.29	.296	.866	4.46
196	-9.80	15.29	.005604	.055228	-.010083	99.76	.298	.867	5.36
197	-9.80	16.96	.007699	.073565	-.014283	100.20	.299	.867	6.50
198	-9.76	17.91	.009677	.085317	-.017369	100.18	.299	.867	7.37
199	-14.59	15.98	.005168	.038282	-.009582	99.20	.296	.865	4.94
200	-14.59	17.72	.007527	.056249	-.013208	99.92	.298	.866	5.86
201	-14.59	19.29	.010495	.074355	-.020928	100.28	.299	.867	7.13

TEST 151 11-FOOT ROTOR

RUN 8 μ = .29 $M_{(1.0,\ 90)}$ = .91 RPM = 617 θ_1 = -10°

PT	ALPHA	THETA0	CD/SIG	CLP/SIG	CUP/SIG	VFS	V/VMR	M TIP	B1
202	.01	8.73	.001722	.031585	.001029	103.98	.293	.914	2.51
203	.01	9.75	.001897	.047064	.000905	103.62	.292	.913	3.26
204	.01	10.99	.002421	.063255	.000801	103.74	.292	.913	4.49
205	.01	12.10	.003409	.079609	.000293	104.08	.293	.914	5.34
206	.01	14.84	.007394	.098254	-.002744	104.52	.294	.915	5.34
207	-4.96	10.96	.002700	.030425	-.001917	103.70	.292	.913	3.30
208	-4.96	11.00	.002685	.029879	-.001928	103.80	.292	.913	3.26
209	-4.96	12.18	.003501	.046674	-.003717	104.26	.293	.914	4.34
210	-4.96	13.32	.004549	.062076	-.005395	104.37	.294	.914	5.37
211	-4.96	14.54	.005995	.078049	-.007305	104.47	.294	.914	5.28
212	-4.97	16.02	.007845	.098379	-.009390	103.88	.292	.913	7.28
213	-4.97	13.12	.004517	.052175	-.005196	103.76	.292	.912	3.29
214	-10.07	13.37	.003915	.034013	-.005426	104.20	.293	.913	4.37
215	-10.06	14.72	.005337	.049790	-.008859	105.00	.295	.915	5.15
216	-10.06	15.94	.007024	.065836	-.012245	105.11	.295	.915	5.97
217	-10.06	15.95	.008126	.074770	-.014088	105.33	.296	.915	5.47
218	-14.62	15.44	.004810	.034165	-.007772	104.63	.294	.914	4.02
219	-14.62	17.08	.006873	.050448	-.012853	104.97	.295	.915	5.08
220	-14.63	17.72	.008024	.058500	-.015504	105.08	.296	.915	5.05
221	5.11	6.39	.000881	.031076	.004444	104.83	.295	.914	1.55
222	5.12	7.54	.000569	.047054	.000093	104.94	.295	.915	2.43
223	5.12	8.70	.000547	.062852	.007412	105.17	.296	.915	3.52
224	5.12	9.56	.000934	.078506	.008529	105.05	.295	.915	4.03
225	5.13	13.44	.001178	.110241	.006337	104.93	.295	.915	6.55

TEST 151 11-FOOT ROTOR

RUN 9 μ = .29 $M_{(1.0, 90)}$ = .96 RPM = 652 θ_1 = -10°

PT	ALPHA	THETAC	CD/SIG	CLP/SIG	CDP/SIG	VFS	V/VMAX	M TIP	θ_1
226	5.13	6.19	.001672	.028114	.000823	110.74	.295	.964	1.39
227	5.14	7.17	.001268	.042134	.000597	110.85	.295	.964	2.19
228	5.13	8.19	.001139	.056134	.000627	110.83	.295	.964	2.86
229	5.13	9.11	.001203	.070367	.000872	109.86	.293	.962	3.72
230	5.14	11.76	.000543	.096839	.000785	110.07	.293	.963	5.07
231	.02	8.34	.002248	.028175	.001888	109.83	.292	.962	1.92
232	.02	9.34	.002393	.042469	.002019	110.70	.295	.964	2.85
233	.02	10.35	.002717	.056452	.002064	110.80	.295	.964	3.75
234	.02	11.42	.003376	.070756	.001790	110.90	.295	.964	4.60
235	.02	13.35	.005832	.098720	.000169	111.33	.295	.964	5.43
236	-5.02	10.73	.003165	.027075	-.000950	110.35	.294	.962	3.10
237	-5.03	10.80	.003081	.026008	-.000850	110.56	.294	.963	3.08
238	-5.03	11.79	.003784	.041235	-.002404	109.24	.291	.960	3.94
239	-5.03	12.85	.004715	.055733	-.003802	109.46	.291	.960	4.82
240	-5.03	12.79	.004637	.055409	-.003783	109.35	.291	.960	5.53
241	-5.04	13.78	.005766	.069597	-.005234	109.68	.292	.961	5.36
242	-5.03	14.12	.006135	.072965	-.005331	111.09	.296	.964	5.48
243	-5.98	12.94	.004108	.030572	-.003930	109.76	.292	.961	4.01
244	-5.99	13.87	.005233	.044278	-.006017	109.76	.292	.961	4.46
245	-5.99	15.06	.006555	.057528	-.009395	109.98	.293	.961	5.13
246	-14.00	15.10	.004861	.030527	-.006177	109.20	.291	.960	4.53
247	-14.00	16.26	.006624	.044960	-.010498	109.63	.292	.961	5.10
248	-14.07	13.83	.003304	.016430	-.001785	108.75	.290	.959	3.57

TEST 151 11-FOOT ROTOR

RUN 10 μ = .30 $M_{(1.0, 90)}$ = .72 RPM = 478 θ_1 = 0°

PT	ALPHA	THETA0	CT/SIG	CLP/SIG	CDP/SIG	VFS	V/OMR	M TIP	B1
280	.04	3.45	.002046	.052363	.000492	82.65	.300	.718	3.81
281	.05	6.71	.003131	.079010	.000167	81.63	.297	.716	5.14
282	.04	10.00	.007174	.105110	-.003115	79.70	.289	.712	7.75
283	.03	14.13	.014769	.117038	-.010489	74.72	.271	.702	11.98
284	-4.89	5.19	.003703	.051140	-.004354	77.56	.282	.708	4.16
285	-4.98	6.85	.003939	.065875	-.004287	81.93	.298	.717	5.36
286	-4.88	10.09	.006384	.077532	-.007930	83.95	.305	.721	6.36
287	-4.91	13.40	.012530	.103943	-.015321	84.22	.306	.722	9.78
288	-4.89	13.38	.012885	.103608	-.015308	84.22	.306	.722	10.89
289	-9.96	10.54	.006369	.055037	-.010650	84.22	.306	.722	5.70
290	-9.96	12.77	.010369	.081900	-.017565	83.78	.304	.721	7.66
291	-9.95	15.16	.015574	.100426	-.024880	83.58	.304	.720	9.88
292	-14.66	10.54	.004792	.029732	-.007270	83.29	.303	.719	4.74
293	-14.62	12.67	.008604	.056527	-.016232	83.57	.304	.720	6.31
294	-14.62	15.14	.013688	.082145	-.025939	83.86	.305	.720	8.31
295	5.08	2.03	.000284	.031684	.005904	83.71	.304	.720	2.79
296	5.08	3.22	.000752	.073581	.007532	83.99	.305	.720	4.53
297	5.09	8.06	.004196	.105283	.006638	83.56	.304	.720	7.25
298	5.08	11.64	.012037	.127440	.001098	83.41	.303	.719	11.75

TEST 151 11-FOOT ROTOR

RUN 11 μ = .30 $M_{(1.0, 90)}$ = .79 RPM = 534 θ_1 = 0°

PT	ALPHA	THETA0	CD/SIG	CLP/SIG	CDP/SIG	VFS	V/VMR	M TIP	31
301	-.01	3.09	.001699	.041744	.000652	91.55	.298	.796	2.91
302	-.01	4.71	.002506	.064063	-.000057	91.81	.299	.796	4.59
303	-.01	7.82	.003931	.084019	-.001234	91.67	.298	.796	5.01
304	-.02	10.76	.009158	.106035	-.005041	92.00	.299	.796	8.93
305	-.02	11.42	.010856	.111502	-.006385	91.20	.297	.794	10.06
306	-4.88	5.13	.003247	.040664	-.004109	91.04	.296	.794	4.17
307	-4.88	5.14	.003252	.040894	-.004123	91.16	.296	.794	5.08
308	-4.89	8.19	.004646	.061811	-.006573	91.55	.298	.795	5.20
309	-4.91	10.28	.007039	.082990	-.009733	91.67	.298	.795	5.87
310	-4.90	10.36	.007214	.083609	-.010147	91.89	.299	.795	8.07
311	-4.91	12.57	.011739	.100529	-.014841	91.75	.298	.795	9.33
312	-9.89	9.11	.005036	.044041	-.009369	91.33	.297	.794	4.98
313	-9.89	10.95	.007360	.054960	-.014098	91.19	.297	.793	5.05
314	-9.87	12.92	.011060	.086226	-.019894	91.71	.298	.795	8.05
315	-14.73	11.30	.006600	.044724	-.013218	90.78	.295	.793	5.37
316	-14.74	13.19	.010035	.065851	-.020388	91.43	.297	.794	5.64
317	-14.75	14.70	.013194	.080868	-.025990	91.43	.297	.794	7.96
318	5.13	.75	.000305	.041389	.004243	89.91	.292	.790	2.49
319	5.14	2.34	.000305	.062860	.006074	89.37	.291	.789	3.36
320	5.15	3.72	.000990	.084011	.007339	89.36	.291	.789	4.84
321	5.16	7.79	.004345	.103409	.005946	89.08	.290	.789	7.52
322	5.15	10.77	.010389	.122449	.002631	89.21	.290	.789	11.02

TEST 151 11-FOOT ROTOR

RUN 12 μ = .29 $M_{(1.0, 90)}$ = .86 RPM = 582 θ_1 = 0°

PT	ALPHA	THETA0	CD/SIG	CLP/SIG	CDP/SIG	VFS	V/OMR	M TIP	B1
323	5.14	-.17	.000325	.035253	.003935	98.17	.293	.862	1.87
324	5.14	2.16	.000291	.053107	.005321	97.92	.292	.861	2.96
325	5.14	2.56	.000462	.070796	.006829	97.30	.291	.860	4.02
326	5.14	4.30	.001680	.088825	.007191	97.04	.289	.859	5.65
327	5.14	10.25	.009717	.113646	.003503	98.14	.293	.862	11.08
328	-.65	3.01	.001648	.035549	-.000420	98.59	.294	.861	2.81
329	-.64	3.49	.002125	.053630	-.000674	98.70	.294	.861	3.90
330	-.65	5.80	.003060	.071305	-.001496	99.06	.295	.862	5.21
331	-.66	8.30	.005072	.089803	-.002984	98.93	.295	.861	6.75
332	-.65	10.05	.008225	.108439	-.005295	98.80	.295	.861	8.65
333	-4.96	4.10	.002788	.034501	-.003581	98.30	.293	.860	3.64
334	-4.96	4.12	.002805	.034098	-.003581	98.30	.293	.860	4.71
335	-4.96	5.40	.003685	.051978	-.005612	98.42	.294	.860	4.83
336	-4.96	8.69	.005460	.070066	-.007941	99.02	.295	.862	5.96
337	-4.95	8.78	.005433	.069847	-.007920	98.90	.295	.861	7.11
338	-4.96	10.58	.008288	.088370	-.010957	99.01	.295	.861	7.80
339	-9.78	7.71	.004252	.037430	-.007482	98.51	.294	.861	4.83
340	-9.80	9.91	.006073	.055310	-.011590	98.39	.294	.860	5.59
341	-9.80	11.37	.008513	.073296	-.015918	99.00	.295	.861	6.72
342	-9.80	12.28	.010525	.083916	-.018615	99.09	.295	.861	7.64
343	-14.82	10.58	.005635	.037660	-.010596	98.34	.293	.859	5.24
344	-14.82	12.04	.008230	.056325	-.016640	98.08	.293	.859	5.93
345	-14.81	12.63	.009530	.064033	-.019182	98.33	.293	.859	6.44

TEST 151 11-FOOT ROTOR

RUN 13 μ = .29 $M_{(1.0, 90)}$ = .91 RPM = 617 θ_1 = 0°

PT	ALPHA	THETA0	CQ/SIG	CLP/SIG	CDP/SIG	VFS	V/OMR	M TIP	B1
346	.62	2.28	.001499	.031101	.000210	104.81	.295	.912	2.79
347	.63	3.03	.001814	.047269	.000149	104.81	.295	.912	3.44
348	.64	3.76	.002448	.063629	-.000017	105.27	.295	.913	4.72
349	.62	5.07	.003515	.078718	-.000576	105.83	.298	.914	5.86
350	.62	7.32	.005279	.097928	-.003181	104.90	.295	.911	7.57
351	-5.11	3.95	.002622	.063322	-.002929	104.66	.295	.911	3.42
352	-5.11	5.59	.004028	.080320	-.004853	103.73	.292	.909	4.76
353	-5.10	5.36	.003813	.080498	-.004792	104.08	.293	.910	5.04
354	-5.10	7.09	.005032	.098979	-.006761	104.08	.293	.910	5.55
355	-5.10	7.54	.005429	.103615	-.006453	103.96	.293	.909	5.36
356	-5.10	9.42	.006721	.078545	-.008903	104.30	.294	.910	5.60
357	-5.10	10.43	.008514	.083153	-.010930	104.30	.293	.910	7.56
358	-10.03	7.12	.005979	.083360	-.006243	106.34	.299	.914	4.57
359	-10.04	9.27	.007805	.099446	-.010054	104.28	.293	.910	5.42
360	-10.04	10.63	.007630	.065307	-.013678	105.64	.297	.913	5.32
361	-9.99	11.87	.009842	.073600	-.016797	105.41	.297	.912	7.39
362	-14.83	10.15	.008148	.084286	-.008964	105.29	.296	.912	4.91
363	-14.83	11.18	.007242	.050136	-.013926	104.48	.294	.910	5.72
364	-14.84	12.71	.009900	.055585	-.018913	104.94	.295	.911	6.78
365	5.21	-.59	.000429	.031398	.003945	104.01	.293	.910	1.75
366	5.20	.90	.000288	.049625	.005375	104.59	.294	.911	2.61
367	5.20	2.24	.000311	.062437	.006804	104.70	.295	.911	3.57
368	5.20	2.66	.000899	.078639	.007630	104.36	.294	.910	4.86
369	5.19	8.94	.007463	.113602	.005254	104.00	.293	.910	9.91

TEST 151 11-FOOT ROTOR

RUN 14 μ = .29 $M_{(1.0, 90)}$ = .96 RPM = 652 θ_1 = 0°

PT	ALPHA	THETA0	CD/SIG	CLP/SIG	CDP/SIG	VFS	V/OMR	M TIP	B1
370	5.18	-1.05	.000673	.027971	.004004	109.89	.293	.961	1.41
371	5.19	.44	.000578	.042039	.005157	109.23	.291	.959	2.26
372	5.19	2.04	.000547	.056115	.006525	108.45	.289	.958	3.00
373	5.19	2.43	.000785	.070121	.007765	108.45	.289	.958	3.91
374	5.19	6.84	.004701	.098197	.007385	108.89	.290	.959	7.35
375	.06	1.75	.001573	.028150	.000931	108.99	.290	.959	2.09
376	.06	2.87	.001878	.042154	.000886	108.88	.290	.959	2.95
377	.07	3.33	.002306	.056458	.000771	109.10	.291	.959	3.67
378	.06	4.69	.003074	.070608	.000547	109.75	.292	.961	4.80
379	.06	9.02	.007000	.093983	-.001583	109.41	.291	.960	7.55
380	-5.02	3.81	.002697	.026730	-.001887	109.82	.292	.960	3.01
381	-5.02	3.84	.002721	.026722	-.001907	110.04	.293	.960	4.09
382	-5.02	4.77	.003449	.040897	-.003342	109.82	.292	.960	3.91
383	-5.02	6.71	.004503	.055240	-.004753	109.93	.293	.960	4.73
384	-5.02	6.77	.004500	.055403	-.004780	110.14	.293	.960	5.58
385	-5.01	8.65	.005880	.069739	-.006491	110.14	.293	.960	5.48
386	-9.92	6.57	.003876	.030230	-.004970	110.02	.293	.960	4.11
387	-9.91	8.72	.005329	.044472	-.008039	110.46	.294	.961	4.81
388	-9.90	9.73	.006582	.056674	-.010519	110.02	.293	.960	5.30
389	-14.78	8.12	.003333	.016802	-.003049	111.74	.298	.964	3.79
390	-14.78	10.08	.005100	.031004	-.007571	110.98	.296	.962	4.76
391	-14.78	11.24	.006916	.044714	-.011858	110.98	.296	.962	5.42

TEST 151 11-FOOT ROTOR

RUN 15 μ = .32 $M_{(1.0, 90)}$ = .87 RPM = 581 θ_1 = 0°

PT	ALPHA	THETAC	CQ/SIG	CLP/SIG	CDP/SIG	VFS	V/OMR	M TIP	B1
393	.06	2.85	.001520	.035446	.000508	105.29	.315	.869	3.03
394	.06	3.26	.001918	.053075	.000435	105.29	.315	.869	3.95
395	.07	5.30	.002778	.071114	-.000058	105.40	.315	.869	5.27
396	.08	8.19	.004941	.088545	-.001624	105.85	.316	.870	7.20
397	.09	10.60	.009400	.103155	-.004786	105.62	.316	.870	9.91
398	-4.94	4.27	.002949	.033627	-.002929	105.27	.315	.869	4.12
399	-4.94	4.25	.002984	.034249	-.003163	105.95	.317	.870	5.00
400	-4.95	6.76	.004043	.051682	-.004995	104.36	.312	.867	5.19
401	-4.95	9.12	.005671	.069550	-.007247	105.38	.315	.869	6.27
402	-4.96	9.18	.005679	.069364	-.007264	105.50	.315	.869	7.38
403	-4.99	11.09	.008954	.087501	-.010725	105.95	.317	.870	9.37
404	-4.99	11.74	.010502	.092903	-.012171	105.27	.315	.869	9.04
405	-10.03	8.27	.004389	.037255	-.006784	104.24	.311	.867	4.90
406	-10.03	10.21	.006406	.055618	-.011007	104.92	.314	.868	5.82
407	-9.99	12.17	.009833	.077166	-.016426	105.49	.315	.869	7.57
408	-14.75	9.51	.003670	.020830	-.004417	104.12	.311	.867	4.44
409	-14.75	11.16	.006015	.038742	-.010110	105.14	.314	.869	5.31
410	-14.76	13.18	.010063	.063428	-.018353	105.82	.316	.870	7.16
411	4.98	-.26	.000355	.034586	.004291	105.82	.316	.870	1.95
412	4.99	1.72	.000197	.052813	.005961	105.82	.316	.870	3.11
413	4.99	2.61	.000522	.070214	.007054	106.16	.317	.871	4.55
414	5.00	4.59	.001882	.088320	.007284	105.37	.315	.869	6.36
415	4.99	7.88	.005173	.103299	.005982	105.71	.316	.870	8.57

TEST 151 11-FOOT ROTOR

RUN 16 μ = .34 $M_{(1.0, 90)}$ = .81 RPM = 525 θ_1 = 0°

PT	ALPHA	THETAC	CD/SIG	CLP/SIG	CDP/SIG	VFS	V/OMR	M TIP	B1
418	.01	3.08	.001733	.044054	.001160	96.73	.329	.794	3.28
419	.00	5.19	.002711	.066404	.000994	103.56	.342	.808	5.29
420	-.01	8.82	.005383	.088922	-.001050	103.65	.343	.806	7.51
421	.01	11.22	.010375	.102881	-.004917	105.36	.348	.811	10.78
422	-5.07	6.58	.003812	.042543	-.003251	105.00	.347	.810	5.14
423	-5.06	6.39	.003703	.041963	-.003505	101.74	.336	.804	5.01
424	-5.07	9.51	.005720	.063931	-.006301	104.29	.345	.809	8.75
425	-5.09	11.59	.009379	.085071	-.010623	103.12	.341	.806	8.88
426	-5.09	11.60	.009486	.086739	-.010555	103.80	.343	.807	9.90
427	-5.09	12.51	.011306	.092144	-.012171	103.33	.342	.806	9.68
428	-9.97	10.13	.005779	.065054	-.008111	103.67	.343	.807	5.65
429	-9.99	12.24	.009083	.068401	-.013687	104.46	.345	.808	7.76
430	-9.93	14.44	.013566	.087012	-.019924	104.11	.344	.808	9.85
431	-14.62	10.72	.004562	.025443	-.004821	103.52	.342	.807	5.04
432	-14.62	12.64	.007675	.047301	-.012219	104.09	.344	.808	6.57
433	-14.61	15.07	.012605	.069450	-.020668	104.77	.346	.809	8.75
434	5.19	.55	.000089	.043659	.005870	104.30	.345	.808	2.78
435	5.19	2.42	.000184	.066066	.007715	103.95	.344	.807	4.42
436	5.20	4.76	.001748	.087291	.008150	104.98	.347	.809	6.51
437	5.19	8.83	.006569	.103402	.005700	104.96	.347	.809	10.32

TEST 151 11-FOOT ROTOR

RUN 17 μ = .36 $M_{(1.0, 90)}$ = .91 RPM = 591 θ_1 = 0°

PT	ALPHA	THETAC	CD/SIG	CLP/SIG	CDP/SIG	VFS	V/VMAX	M TIP	B1
438	-.06	2.90	.001607	.034715	.001084	121.00	.355	.915	3.36
439	-.05	3.46	.002234	.052114	.000793	121.09	.355	.915	5.08
440	-.04	5.79	.003277	.069450	.000549	121.40	.357	.915	6.47
441	-.06	9.21	.006655	.086039	-.001942	121.68	.357	.915	8.98
442	-.07	10.20	.008734	.093247	-.003357	121.38	.357	.915	10.45
443	-4.96	3.88	.002228	.035737	-.000643	120.76	.355	.914	3.32
444	-4.97	4.99	.003285	.052966	-.002482	121.04	.356	.914	4.79
445	-4.97	4.98	.003259	.052968	-.002451	120.83	.355	.914	5.71
446	-4.97	7.72	.004588	.070014	-.004459	120.82	.355	.914	6.19
447	-4.97	9.96	.006747	.087630	-.006931	120.81	.355	.914	7.76
448	-4.98	9.80	.006626	.087367	-.006939	121.01	.355	.913	8.62
449	-5.01	12.03	.010852	.084314	-.010959	121.20	.356	.914	10.15
450	-9.99	5.74	.003080	.018924	-.002061	121.57	.357	.914	4.54
451	-9.99	9.59	.005018	.037435	-.006287	121.99	.358	.915	6.98
452	-10.00	11.10	.007467	.056908	-.010363	121.71	.358	.913	7.25
453	-10.01	12.64	.010451	.072199	-.014715	121.40	.357	.913	8.66
454	-14.76	10.64	.004129	.021143	-.003704	120.99	.355	.912	6.57
455	-14.76	12.09	.006844	.038823	-.009451	120.98	.355	.912	7.12
456	-14.76	13.67	.010143	.057018	-.015553	121.37	.357	.913	8.08
457	5.20	-.80	.000240	.033980	.004853	120.74	.355	.911	2.72
458	5.21	1.21	.000066	.051498	.005687	121.43	.357	.913	3.64
459	5.21	2.45	.000422	.068339	.007742	121.52	.357	.913	5.31
460	5.22	4.87	.002668	.085712	.007236	121.71	.358	.913	7.71
461	5.21	7.63	.005233	.096517	.006651	121.99	.358	.914	9.58

TEST 151 11-FOOT ROTOR

RUN 18 μ = .41 $M_{(1.0, 90)}$ = .95 RPM = 597 θ_1 = 0°

PT	ALPHA	THETAO	CD/SIG	CLP/SIG	CDP/SIG	VFS	V/OMR	% TIP	B1
462	-.05	3.05	.001977	.033153	.001582	139.40	.405	.952	4.03
463	-.05	3.73	.002630	.050981	.001622	140.01	.407	.953	5.74
464	-.04	7.08	.004408	.068450	.000783	140.26	.408	.954	7.67
465	-.04	10.29	.008655	.084756	-.002188	138.78	.404	.951	10.86
466	15.66	44.48	.092537	-1.315696	-1.322195	138.26	.402	.950	4.34
467	-4.89	5.87	.003743	.031407	-.001807	137.83	.401	.949	5.45
468	-4.89	5.94	.003711	.031384	-.001873	137.32	.399	.948	6.56
469	-4.89	9.11	.005369	.048310	-.003500	139.30	.405	.952	7.23
470	-4.88	11.02	.008092	.065194	-.005754	139.86	.407	.953	9.19
471	-4.88	11.06	.008074	.065022	-.005841	140.46	.408	.954	10.08
472	-4.90	11.89	.009542	.069816	-.007221	139.95	.407	.953	13.05
473	-9.95	8.93	.003873	.021211	-.001970	139.43	.406	.952	11.39
474	-9.99	10.68	.005942	.038195	-.005526	138.64	.403	.951	12.71
475	-9.98	12.70	.009258	.056973	-.010031	139.50	.406	.952	12.97
476	-14.82	12.06	.005126	.022990	-.002683	139.58	.406	.953	12.97
477	-14.82	13.52	.008059	.035765	-.007991	139.74	.406	.953	12.97
478	-14.82	14.34	.009688	.047394	-.010604	139.81	.407	.953	12.97
479	5.10	-1.12	.000287	.033130	.005767	138.54	.403	.951	5.02
480	5.11	1.19	.000170	.049544	.007251	140.15	.408	.954	7.79
481	5.11	2.65	.000942	.066347	.008018	140.39	.408	.954	10.31
482	5.13	5.34	.003449	.083591	.007974	139.95	.407	.953	12.83
483	5.19	7.88	.005783	.092354	.007185	140.04	.407	.954	13.05

TEST 151 11-FOOT ROTOR

RUN 19 μ = .39 $M_{(1.0, 90)}$ = .84 RPM = 530 θ_1 = 0°

PT	ALPHA	THETAC	CW/SIG	CLP/SIG	CDP/SIG	VFS	V/OMR	M TIP	B1
487	-.02	3.40	.002042	.043610	.000802	118.61	.389	.845	4.63
488	-.02	6.24	.003343	.065532	.000157	118.70	.389	.846	6.52
489	-.03	9.70	.007105	.086166	-.002354	119.32	.391	.846	9.40
490	-.04	11.30	.010735	.096521	-.005096	119.30	.391	.846	11.61
491	-4.97	7.30	.004241	.041800	-.003810	117.67	.385	.843	5.72
492	-4.97	7.20	.004127	.040812	-.003633	117.76	.386	.843	5.56
493	-4.97	10.13	.006390	.062042	-.006534	118.14	.387	.844	7.05
383	R3+88	+1+86	+9-838	+97333-	R+9-1196	117.94	+275	+731	10.97
495	-4.99	12.61	.011273	.083482	-.011386	118.13	.387	.843	11.72
496	-9.94	8.39	.003815	.024541	-.003703	117.70	.386	.842	4.81
497	-9.97	11.19	.006723	.046914	-.008709	118.28	.387	.843	5.99
498	-9.97	13.27	.010604	.068466	-.014358	119.09	.390	.844	9.18
499	-9.93	14.62	.013232	.078160	-.017486	119.38	.391	.845	10.48
500	-14.66	11.80	.005236	.025894	-.005050	118.65	.389	.843	5.89
501	-14.66	13.90	.009120	.047980	-.012551	118.84	.389	.843	7.96
502	-14.66	15.53	.014860	.069323	-.021114	119.53	.392	.845	10.50
503	5.19	-1.05	.000206	.030411	.004237	118.59	.388	.843	1.97
504	5.19	.26	.000062	.042681	.005353	119.72	.392	.844	2.92
505	5.19	2.42	.000185	.053586	.007043	120.01	.393	.845	4.98
506	5.19	5.41	.002715	.085462	.006674	120.10	.393	.845	7.92
507	5.18	8.49	.006396	.100065	.005130	120.48	.395	.846	10.48

TEST 151 11-FOOT ROTOR

RUN 20 μ = .43 $M_{(1.0, 90)}$ = .90 RPM = 556 θ_1 = 0°

PT	ALPHA	THETA0	CD/SIG	CLP/SIG	CDP/SIG	VFS	V/OMR	M TIP	B1
508	5.18	-1.02	.000140	.031694	.004519	136.24	.425	.906	2.38
509	5.17	-.31	.000033	.038335	.005190	138.31	.432	.910	3.02
510	5.16	2.33	.000154	.059414	.006704	135.57	.423	.905	5.17
511	5.16	4.51	.002599	.077657	.006306	138.05	.431	.909	6.35
512	5.15	7.33	.005021	.088776	.005884	136.78	.427	.905	10.10
513	-.12	1.61	.001518	.020343	.000617	136.03	.425	.904	2.97
514	-.13	3.34	.001981	.039847	.000777	136.45	.426	.905	4.77
515	-.13	5.66	.003245	.058934	.000120	135.60	.427	.905	7.25
516	-.13	9.71	.007247	.079515	-.002117	137.10	.428	.906	10.37
517	-.14	10.31	.008237	.081470	-.002814	137.08	.428	.906	11.00
518	-5.06	4.55	.002401	.016265	-.001393	136.81	.427	.905	4.85
519	-5.07	7.76	.004326	.037179	-.003413	137.14	.428	.905	7.53
520	-5.07	7.84	.004341	.038744	-.003475	137.48	.429	.906	7.55
521	-5.07	10.58	.006826	.056600	-.005965	137.32	.429	.905	9.84
522	-5.07	13.27	.012087	.076381	-.010380	137.29	.429	.905	11.80
523	-5.06	13.35	.011703	.078535	-.009994	137.45	.429	.905	12.55
524	-9.04	8.09	.003161	.015592	-.001759	136.89	.427	.904	5.32
525	-9.05	9.45	.004139	.023951	-.003252	136.87	.427	.904	5.83
526	-9.07	11.66	.006315	.042907	-.007411	137.76	.430	.905	6.92
527	-9.08	13.73	.010575	.063311	-.012421	137.32	.429	.902	10.09
528	-14.79	12.45	.005327	.024501	-.003964	136.62	.426	.900	5.84
529	-14.80	14.72	.009312	.044468	-.010535	136.84	.427	.901	4.95
530	-14.71	15.79	.011616	.053319	-.014057	137.29	.429	.901	4.99

TEST 151 11-FOOT ROTOR

RUN 21 μ = .43 $M_{(1.0, 90)}$ = .80 RPM = 493 θ_1 = 0°

PT	ALPHA	THETA	CD/SIG	CL/SIG	CDP/SIG	VFS	V/VAR	M TIP	M
531	-.03	2.07	.001569	.026972	.000276	123.09	.434	.803	9.1[illegible]
532	-.04	3.73	.002339	.030065	.000356	122.70	.432	.801	9.09
533	-.03	8.51	.004457	.037815	-.001051	121.49	.428	.802	9.07
534	-.02	12.16	.011744	.043762	-.005503	123.36	.434	.803	12.[illegible]
535	-5.03	3.13	.002974	.022245	-.002453	122.78	.432	.801	9.[illegible]
536	-5.03	7.91	.005215	.047621	-.004870	121.06	.428	.802	8.[illegible]
537	-5.03	9.59	.006208	.057330	-.005039	122.36	.433	.801	9.09
538	-5.03	12.21	.009401	.072093	-.008981	122.66	.431	.8[illegible]	10.[illegible]
539	-5.02	14.65	.014294	.084336	-.013243	122.44	.433	.801	10.[illegible]
540	-5.02	12.33	.009559	.072059	-.008855	122.[illegible]	.433	.801	11.[illegible]
541	-10.18	10.52	.004939	.029717	-.005033	122.92	.433	.801	9.09
542	-10.18	12.49	.006856	.039012	-.010659	123.19	.434	.802	9.[illegible]
543	-10.16	15.05	.014750	.070188	-.018042	123.59	.435	.802	12.[illegible]
544	-14.85	13.42	.009524	.053979	-.006455	123.48	.435	.802	7.[illegible]
545	-14.84	16.31	.011971	.056603	-.015212	123.27	.434	.801	10.[illegible]
546	5.07	-1.23	.000036	.032370	.004215	122.77	.432	.800	2.1[illegible]
547	5.08	1.15	-.003119	.049582	.005689	122.76	.432	.800	5.[illegible]
548	5.08	3.05	.001103	.074418	.006915	123.62	.435	.802	5.[illegible]
549	5.08	8.03	.006276	.098747	.009517	124.10	.437	.803	10.[illegible]

TEST 151 11-FOOT ROTOR

RUN 22 μ = .44 $M_{(1.0, 90)}$ = .86 RPM = 528 θ_1 = 0°

PT	ALPHA	THETAJ	CJ/SIG	CLP/SIG	CDP/SIG	VFS	V/UMR	M TIP	J1
550	5.08	-1.10	-.000036	.034022	.004682	134.49	.442	.862	2.60
551	5.08	.18	-.000052	.043254	.005410	134.48	.442	.862	3.57
552	5.08	2.55	.000316	.064241	.007012	134.02	.441	.862	5.95
553	5.08	6.14	.003714	.085489	.006606	134.36	.442	.862	9.36
554	-.09	1.48	.001428	.022232	.000658	133.38	.439	.859	2.93
555	-.08	3.48	.002014	.044153	.000661	132.55	.436	.858	5.17
556	-.07	6.81	.003702	.065731	.000143	134.42	.442	.862	7.68
557	-.07	11.04	.009600	.087354	-.003395	133.95	.440	.861	11.96
558	-4.92	4.25	.002712	.018925	-.001352	133.02	.437	.859	4.53
559	-4.91	8.77	.004667	.040308	-.003857	133.55	.439	.860	7.10
560	-4.91	8.75	.004351	.040527	-.003737	133.72	.440	.859	7.06
561	-4.92	11.17	.007592	.062445	-.006430	132.90	.437	.859	9.37
562	-4.92	13.95	.012857	.078507	-.010584	133.77	.440	.860	12.14
563	-4.92	11.31	.007652	.062316	-.006482	134.34	.442	.861	10.75
564	-10.01	10.20	.004472	.026270	-.003703	133.24	.439	.858	5.27
565	-9.99	12.67	.007811	.047950	-.008753	133.40	.439	.859	8.81
566	-9.99	15.25	.012886	.069425	-.014769	133.56	.439	.859	11.32
567	-14.78	13.08	.005899	.027258	-.004491	133.45	.439	.859	7.35
568	-14.78	15.55	.010522	.049461	-.011911	134.11	.441	.859	9.51
569	-14.80	16.44	.012327	.055763	-.014833	133.19	.438	.858	10.55

TEST 151 11-FOOT ROTOR

RUN 23 μ = .44 $M_{(1.0, 90)}$ = .77 RPM = 474 θ_1 = 0°

PT	ALPHA	THETAO	CQ/SIG	CLP/SIG	CDP/SIG	VFS	V/OMR	M TIP	B1
570	-.06	2.57	.001617	.027449	.000307	119.12	.435	.769	3.41
571	-.04	4.64	.002657	.054522	.000188	119.53	.438	.771	6.08
572	-.04	9.30	.005974	.081400	-.001525	119.95	.439	.771	9.05
573	.00	13.01	.013512	.101961	-.006672	119.78	.439	.771	13.06
574	-5.01	5.40	.003201	.024316	-.002306	118.58	.434	.769	5.03
575	-5.01	10.09	.005833	.051189	-.005259	119.30	.437	.771	7.90
576	-5.00	10.05	.005808	.051164	-.005199	119.00	.436	.770	8.83
577	-4.97	13.38	.011328	.078270	-.010411	118.82	.435	.770	11.35
578	-4.97	13.44	.011142	.077335	-.010613	118.92	.436	.770	12.39
579	-5.01	14.52	.013862	.084142	-.012575	119.01	.436	.770	12.51
580	-9.91	10.75	.005152	.031221	-.003736	118.71	.436	.770	6.57
581	-9.92	13.59	.009709	.058594	-.011423	119.52	.438	.771	9.44
582	-9.84	16.03	.014717	.075710	-.017645	119.53	.438	.771	12.13
583	-14.74	13.75	.007136	.033867	-.007053	118.93	.436	.770	8.02
584	-14.76	15.70	.013487	.060561	-.016924	119.03	.436	.770	10.94
585	5.22	-1.14	.000097	.031504	.004985	119.13	.435	.770	2.04
586	5.24	1.88	0.000000	.052844	.006525	119.34	.437	.771	4.41
587	5.23	4.44	.001841	.080539	.007609	119.75	.439	.772	7.52
588	5.22	8.51	.005807	.097427	.006105	119.75	.439	.772	10.60

TEST 151 11-FOOT ROTOR

RUN 24 μ = .49 $M_{(1.0, 90)}$ = .80 RPM = 474 θ_1 = 0°

PT	ALPHA	THETA0	CD/SIG	CL²/SIG	CDP/SIG	VFS	V/OMR	M TIP	B1
591	.02	3.07	.001678	.028006	.001785	133.68	.490	.798	3.83
592	.02	5.95	.003635	.054551	.001910	133.76	.490	.798	7.10
593	.04	10.89	.008605	.084049	-.000773	134.29	.492	.799	11.36
594	-5.04	7.23	.003607	.023720	-.000876	133.83	.490	.798	5.13
595	-5.04	7.23	.003666	.023732	-.000980	134.37	.492	.799	7.09
596	-5.04	7.37	.003711	.024069	-.000995	134.39	.492	.799	7.18
597	-5.04	11.37	.006895	.051251	-.003670	134.03	.491	.798	9.40
598	-5.04	11.41	.006951	.051210	-.003665	133.93	.491	.798	10.51
599	-5.05	14.14	.011299	.067920	-.007631	134.46	.493	.799	12.35
600	-9.89	11.68	.005792	.032405	-.003600	133.56	.489	.797	7.82
601	-9.90	13.75	.008414	.045297	-.007034	133.47	.489	.797	9.85
602	-9.90	15.68	.011644	.059031	-.010425	133.57	.489	.797	11.83
603	-14.78	15.33	.007829	.038197	-.004935	132.94	.487	.796	9.23
604	-14.78	17.07	.011183	.047315	-.009731	133.20	.488	.797	11.27
605	5.14	-1.20	.000671	.031386	.004801	133.27	.488	.797	2.56
606	5.14	2.28	-.000013	.053878	.006749	133.64	.490	.798	5.06
607	5.15	5.37	.002508	.080541	.007592	134.36	.492	.799	8.52

TEST 151 11-FOOT ROTOR

RUN 25 μ = .48 $M_{(1.0, 90)}$ = .85 RPM = 508 θ_1 = 0°

PT	ALPHA	THETAC	CD/SIG	CLP/SIG	CDP/SIG	VFS	V/VMR	M TIP	M1
608	5.13	-1.27	.000009	.032758	.005171	140.48	.480	.848	2.36
609	5.13	.01	-.000162	.043800	.006507	139.79	.473	.847	3.79
610	5.13	2.91	.000417	.060517	.007892	141.47	.484	.850	7.03
611	5.14	4.76	.002356	.076943	.008692	140.97	.482	.849	9.81
612	-.05	2.29	.001545	.024457	.001400	140.80	.481	.849	5.24
613	-.05	3.36	.001948	.035790	.001321	140.72	.481	.849	6.49
614	-.05	4.31	.002507	.043066	.001353	140.88	.482	.849	8.30
615	-.04	5.83	.003603	.059625	.001137	140.62	.481	.848	7.97
616	-.05	8.97	.005310	.071955	.000524	140.87	.481	.849	9.26
617	-5.09	4.48	.002345	.038349	.000155	141.04	.482	.849	3.91
618	-5.08	5.04	.003273	.021176	-.000937	140.61	.481	.848	5.48
619	-5.08	5.12	.003270	.021175	-.000923	140.53	.481	.848	5.57
620	-5.08	10.20	.005980	.044041	-.002883	141.05	.482	.849	8.65
621	-5.08	10.27	.005827	.044560	-.003059	140.87	.481	.849	9.78
622	-5.07	13.93	.011353	.063727	-.007457	141.03	.482	.849	12.05
623	-10.07	10.25	.003738	.017987	-.000985	140.34	.480	.848	5.54
624	-10.08	11.47	.005268	.023038	-.003261	140.34	.480	.846	7.44
625	-10.07	12.77	.007176	.040848	-.005813	140.34	.480	.848	8.86
626	-10.09	14.10	.009274	.052412	-.008580	140.18	.479	.847	10.27
627	-14.78	13.29	.004708	.013956	-.000349	140.00	.478	.847	7.44
628	-14.79	14.64	.006922	.033629	-.003792	140.15	.479	.847	8.70
629	-14.78	16.73	.010720	.045729	-.009313	140.50	.480	.848	10.92

TEST 151 11-FOOT ROTOR

RUN 26 μ = .49 $M_{(1.0, 90)}$ = .90 RPM = 535 θ_1 = 0°

PT	ALPHA	THETA0	CD/SIG	CLP/SIG	CDP/SIG	VFS	V/OMR	M TIP	B1
630	-.06	1.83	.001526	.022181	.001401	151.13	.490	.898	3.16
631	-.05	3.17	.001779	.032907	.001631	150.49	.488	.897	4.66
632	-.05	3.79	.002266	.043330	.001754	151.13	.490	.898	5.99
633	-.05	6.11	.003203	.054302	.001633	150.56	.489	.897	7.71
634	-.04	8.50	.004771	.063783	.000801	151.36	.491	.899	9.40
635	-5.02	4.50	.002256	.005286	.000572	151.20	.491	.899	4.06
636	-5.03	5.93	.003208	.018147	-.000334	151.03	.490	.898	5.66
637	-5.04	5.83	.003163	.018175	-.000515	151.25	.491	.899	5.53
638	-5.04	8.30	.004206	.029827	-.001268	151.17	.491	.899	7.11
639	-5.03	10.04	.005333	.039341	-.002206	151.95	.493	.900	8.35
640	-5.03	10.12	.005322	.039339	-.002186	151.87	.493	.900	9.41
641	-5.04	11.52	.007284	.051036	-.003685	151.87	.493	.900	9.95
642	-10.07	10.30	.003792	.017727	-.000567	152.11	.494	.900	5.33
643	-10.08	11.55	.005225	.027759	-.002294	152.17	.494	.901	7.53
644	-10.08	12.90	.007103	.038648	-.004762	151.92	.493	.900	9.21
645	-10.09	14.17	.009137	.048550	-.007063	152.32	.494	.901	10.64
646	-14.81	13.50	.004601	.018250	.000586	152.01	.493	.900	7.69
647	-14.81	15.06	.007018	.029867	-.002871	151.85	.493	.900	9.06
648	-14.81	16.48	.009744	.040785	-.006267	152.88	.496	.902	10.51
649	5.19	-1.20	0.000000	.034457	.005197	151.44	.491	.899	2.52
650	5.18	-.01	-.000137	.042295	.005934	151.43	.491	.899	3.83
651	5.19	2.61	.000593	.063037	.007385	152.15	.494	.901	5.63
652	5.20	3.12	.001637	.071027	.007297	152.38	.495	.901	8.00

TEST 151 11-FOOT ROTOR

RUN 27 μ = .49 $M_{(1.0, 90)}$ = .95 RPM = 566 θ_1 = 0°

PT	ALPHA	THETAO	CQ/SIG	CLP/SIG	CDP/SIG	VFS	V/OMR	M TIP	B1
653	5.18	-1.30	.000239	.033642	.005702	158.84	.487	.947	2.95
654	5.18	-.71	.000212	.037831	.006155	158.99	.488	.947	3.27
655	5.18	.82	.000158	.047246	.006854	159.44	.489	.948	4.04
656	5.19	2.26	.000406	.056955	.007772	160.18	.491	.950	5.64
657	5.19	2.79	.001347	.064793	.007716	160.16	.491	.950	7.31
658	.02	1.48	.001819	.019302	.001758	159.08	.488	.948	3.05
659	.02	3.09	.002030	.028783	.001871	159.08	.488	.948	4.45
660	.04	3.56	.002304	.038106	.001991	157.98	.485	.945	5.65
661	.02	4.50	.002971	.048446	.002040	158.64	.487	.947	7.09
662	.02	6.72	.004051	.057280	.001693	159.22	.488	.948	8.38
663	-4.97	4.46	.002548	.006030	.001026	159.59	.490	.948	4.12
664	-4.97	5.36	.003238	.015553	.000208	159.74	.490	.948	5.47
665	-4.98	5.36	.003333	.016430	.000161	159.89	.490	.948	6.50
666	-4.98	7.33	.004058	.025531	-.000568	159.67	.490	.948	6.55
667	-4.98	9.48	.005195	.035070	-.001504	159.75	.490	.948	8.15
668	-4.98	9.48	.005196	.035075	-.001393	160.12	.491	.949	8.93
669	-4.98	11.10	.007026	.047151	-.002783	160.10	.491	.949	9.67
670	-10.09	10.15	.003814	.015134	.000389	159.65	.490	.948	6.55
671	-10.10	11.29	.005036	.024837	-.001394	159.43	.489	.947	7.47
672	-10.12	12.23	.006680	.034972	-.003570	159.13	.488	.947	8.58
673	-10.12	13.46	.008526	.044630	-.005609	159.51	.489	.948	9.85
674	-10.12	14.57	.010237	.051688	-.007424	159.82	.490	.948	10.95
675	-14.82	13.09	.004522	.016566	.001088	159.36	.489	.947	7.17
676	-14.82	14.45	.006590	.026524	-.001383	159.34	.489	.947	8.75
677	-14.84	15.34	.008523	.035301	-.004307	159.26	.489	.947	9.57
678	-14.82	15.33	.010365	.042915	-.006617	159.50	.489	.948	10.53

TEST 151 11-FOOT ROTOR

RUN 28 μ = .58 $M_{(1.0, 90)}$ = .80 RPM = 449 θ_1 = 0°

PT	ALPHA	THETA0	CQ/SIG	CLP/SIG	CDP/SIG	VFS	V/UMR	M TIP	B1
679	.09	1.24	.001572	.016881	.001296	148.43	.574	.795	2.74
680	.09	3.46	.001951	.031388	.001619	147.77	.571	.794	4.96
681	.09	5.61	.002888	.045064	.002163	149.74	.579	.798	7.45
682	.10	9.65	.005173	.059494	.002022	150.29	.581	.799	10.49
683	-5.09	7.26	.003145	.012221	.000949	149.16	.577	.797	5.99
684	-5.09	10.72	.004869	.027100	-.000162	149.72	.579	.798	8.50
685	-5.08	10.67	.004789	.027056	.000144	149.47	.578	.797	9.52
686	-5.08	12.32	.006704	.040504	-.001058	147.64	.571	.794	10.68
687	-5.10	12.94	.007261	.040723	-.000933	150.42	.582	.799	12.15
688	-5.10	13.75	.008391	.046786	-.001858	149.30	.577	.797	12.12
689	-9.93	12.83	.005047	.022970	.000830	149.15	.577	.797	8.53
690	-9.93	15.52	.008315	.039785	-.002079	149.86	.579	.798	11.51
691	5.07	-1.30	-.000079	.034767	.005177	149.28	.577	.797	2.80
692	5.08	.72	-.000172	.045162	.006155	149.28	.577	.797	4.43
693	5.08	2.66	.000502	.059593	.006971	149.52	.578	.797	6.59
694	5.08	3.88	.001544	.068571	.007147	149.93	.580	.798	8.46

TEST 151 11-FOOT ROTOR

RUN 29 μ = .58 $M_{(1.0, 90)}$ = .85 RPM = 478 θ_1 = 0°

PT	ALPHA	THETA0	CD/SIG	CLP/SIG	CDP/SIG	VFS	V/OMR	M TIP	B1
695	5.06	-1.31	-.000044	.034870	.005685	159.14	.578	.848	3.06
696	5.06	2.35	.000127	.053013	.007002	158.99	.578	.848	5.69
697	5.08	2.95	.000905	.063254	.007384	159.37	.579	.848	7.46
698	.02	.16	.001531	.011131	.001470	159.00	.578	.848	2.09
699	.02	3.21	.001778	.027757	.002065	159.01	.578	.848	4.52
700	.02	4.52	.002488	.040773	.002451	159.46	.579	.849	6.80
701	.03	8.24	.004096	.054134	.002742	159.54	.579	.849	9.32
702	-4.96	5.93	.002703	.006010	.001626	159.84	.581	.849	5.43
703	-4.96	9.95	.004367	.022649	.000899	159.60	.580	.849	7.99
704	-4.96	9.88	.004298	.022947	.000787	160.04	.581	.850	8.91
705	-4.96	12.13	.006250	.036039	.000035	159.20	.578	.848	10.47
706	-4.96	12.01	.006328	.036603	-.000324	159.73	.580	.849	11.33
707	-4.96	13.80	.008856	.048831	-.001630	159.12	.578	.848	12.10
708	-10.16	13.04	.005005	.022104	.001497	158.92	.577	.848	8.90
709	-10.17	14.88	.007454	.035594	-.000808	159.14	.578	.848	10.93
710	-10.17	16.19	.009301	.042754	-.002528	159.14	.578	.848	12.32
711	-14.79	16.73	.005892	.022558	.004088	159.38	.579	.848	10.56

TEST 151 11-FOOT ROTOR

RUN 30 μ = .55 $M_{(1.0, 90)}$ = .91 RPM = 513 θ_1 = 0°

PT	ALPHA	THETAO	CQ/SIG	CLP/SIG	CDP/SIG	VFS	V/OMR	M TIP	B1
714	-.03	2.64	.001677	.013417	.001571	162.94	.551	.910	3.44
715	-.03	3.69	.001910	.025032	.001770	161.60	.547	.908	4.76
716	-.02	5.23	.002571	.036862	.001964	162.06	.548	.908	6.58
717	-.04	8.44	.003736	.048134	.002174	162.48	.550	.908	8.70
718	5.18	-1.02	.000142	.027149	.004657	162.69	.551	.909	2.59
719	5.18	.47	-.000076	.036993	.005567	162.26	.549	.908	3.71
720	5.18	2.61	.000115	.048208	.006409	162.47	.550	.908	5.58
721	5.18	3.42	.001164	.059852	.006818	163.05	.552	.910	7.66
722	-4.96	7.08	.002826	.006448	.001125	161.54	.547	.906	5.63
723	-4.96	9.63	.003840	.017255	.000441	162.86	.551	.908	7.12
724	-4.96	9.67	.003900	.017988	.000217	162.92	.551	.909	8.20
725	-4.97	11.57	.005306	.029589	-.000298	162.14	.549	.907	9.87
726	-4.97	13.36	.007849	.043184	-.002003	161.32	.546	.905	11.45
727	-4.97	13.42	.007623	.041165	-.001542	162.77	.551	.908	12.27
728	-9.89	12.45	.004174	.015758	.001379	162.68	.551	.908	7.70
729	-9.90	14.42	.006309	.027717	-.000867	163.03	.552	.908	9.94
730	-9.91	15.95	.008690	.039263	-.003034	163.67	.554	.909	11.60
731	-14.58	15.92	.004820	.016164	.003612	163.01	.552	.908	9.90
732	-14.59	18.05	.008058	.028869	-.000095	163.15	.552	.908	11.44

TEST 151 11-FOOT ROTOR

RUN 31 μ = .56 $M_{(1.0,\ 90)}$ = .96 RPM = 542 θ_1 = 0°

PT	ALPHA	THETA0	CQ/SIG	CLP/SIG	CDP/SIG	VFS	V/OMR	M TIP	B1
733	.02	1.62	.001972	.011398	.001717	172.96	.554	.959	2.84
734	.03	3.41	.002134	.020982	.002085	173.41	.556	.960	4.42
735	.02	4.15	.002554	.031424	.002375	173.36	.555	.959	6.10
736	.02	6.62	.003397	.042204	.002642	173.63	.556	.959	8.03
737	5.09	-.97	.000632	.025878	.004698	173.34	.555	.959	2.88
738	5.10	-.83	.000397	.030706	.005464	173.11	.555	.958	2.88
739	5.09	1.23	.000416	.040838	.006444	174.11	.558	.960	4.73
740	5.08	3.04	.001146	.054310	.006898	173.49	.556	.959	7.18
741	-4.94	6.98	.003179	.005050	.001753	174.09	.558	.960	5.83
742	-4.95	9.36	.004069	.015702	.001064	173.93	.557	.960	7.27
743	-4.94	9.41	.004083	.014934	.001103	173.79	.557	.960	8.43
744	-4.94	11.12	.005317	.025982	.000696	173.46	.556	.959	9.89
745	-4.94	12.49	.006991	.036104	-.000319	173.39	.555	.959	10.84
746	-4.94	12.48	.006990	.036366	-.000173	173.37	.555	.959	11.77
747	-9.89	12.79	.004816	.017496	.001943	174.14	.558	.960	8.54
748	-9.91	14.06	.006529	.027816	.000069	173.75	.557	.960	9.85
749	-9.93	16.24	.009092	.038219	-.001882	173.63	.556	.959	12.15
750	-14.68	16.46	.005891	.019852	.003822	173.63	.556	.959	9.64
751	-14.68	18.02	.008388	.029871	.001079	174.37	.559	.960	11.59

TEST 151 11-FOOT ROTOR

RUN 32 μ = .63 $M_{(1.0, 90)}$ = .91 RPM = 492 θ_1 = 0°

PT	ALPHA	THETAO	CJ/SIG	CLP/SIG	CJP/SIG	VFS	V/OMR	M TIP	B1
752	.04	2.41	.001703	.013128	.001607	176.29	.622	.906	3.23
753	.05	3.97	.001994	.025295	.002359	177.07	.625	.908	5.45
754	.05	7.18	.002980	.038132	.003197	176.95	.624	.907	8.15
755	.06	8.22	.003346	.040946	.002999	175.74	.620	.905	9.09
756	5.12	-1.22	.000077	.024251	.004895	176.65	.623	.907	2.76
757	5.13	.14	-.000042	.036629	.005692	176.04	.621	.905	3.92
758	5.13	2.73	.000247	.048496	.006289	177.47	.626	.908	5.27
759	-4.89	9.61	.003271	.006384	.002899	178.42	.630	.909	7.24
760	-4.89	12.10	.004805	.019932	.003065	177.95	.628	.908	9.83
761	-4.87	12.10	.004781	.019396	.002861	178.02	.628	.909	10.94
762	-4.87	14.28	.005886	.030884	.002353	178.15	.629	.909	12.16
763	-4.88	14.25	.005988	.031771	.002420	178.60	.630	.910	12.94
764	-9.93	15.24	.005321	.020922	.004200	177.61	.627	.908	10.56
765	-9.94	17.72	.008330	.034597	.001946	177.26	.625	.907	13.05

TEST 151 11-FOOT ROTOR

RUN 33 μ = .62 $M_{(1.0, 90)}$ = .96 RPM = 521 θ_1 = 0°

PT	ALPHA	THETA..	CD/SIG	CLP/SIG	CDP/SIG	VFS	V/OMR	M TIP	β1
768	.06	1.87	.002126	.013012	.003584	186.15	.620	.956	3.02
769	.05	3.88	.002547	.023449	.004210	187.97	.626	.961	5.69
770	.08	5.41	.003057	.034293	.005201	186.70	.622	.961	7.51
771	.09	8.90	.004504	.046113	.005552	186.81	.623	.962	9.65
772	-4.84	13.76	.005757	.005184	.005822	186.76	.622	.963	5.83
773	-4.91	15.10	.007301	.013090	.004908	186.04	.620	.962	8.16
774	-4.97	15.08	.007244	.017804	.004897	186.11	.620	.962	8.90
775	-4.94	16.26	.009250	.029329	.003427	185.96	.620	.961	9.79
776	-4.94	15.65	.008414	.025812	.003986	185.53	.618	.960	9.66
777	-10.04	14.74	.005590	.020661	.006291	186.95	.623	.963	10.47
778	-10.07	16.50	.007868	.030563	.004863	186.33	.621	.961	12.12
779	5.14	-1.17	.000375	.034223	.008070	186.62	.622	.962	2.90
780	5.14	1.17	.000439	.044744	.008859	186.27	.621	.961	4.96
781	5.14	2.82	.001058	.055419	.009481	186.14	.620	.961	7.18

TEST 151 11-FOOT ROTOR

RUN 34 μ = .67 $M_{(1.0, 90)}$ = .86 RPM = 451 θ_1 = 0°

PT	ALPHA	THETAO	CQ/SIG	CLP/SIG	CDP/SIG	VFS	V/OMR	M TIP	B1
782	5.16	-1.20	-.000065	.034741	.007405	173.25	.667	.855	2.87
783	5.17	.86	-.000227	.044747	.007937	173.93	.670	.857	4.46
784	5.16	3.25	.000772	.061087	.009461	173.87	.669	.856	7.60
785	.06	3.42	.001755	.017359	.003486	172.80	.665	.854	3.89
786	.07	5.85	.002464	.032216	.004592	173.47	.668	.856	7.10
787	.06	10.25	.004289	.044188	.005908	173.31	.667	.856	10.53
788	-4.94	11.81	.003768	.039018	.005959	173.80	.669	.857	8.88
789	-4.94	14.51	.006023	.023339	.006288	173.47	.668	.856	12.00
790	-4.94	14.45	.005989	.023015	.006116	174.15	.670	.858	12.90
792	-9.53	17.15	.006030	.024128	.007813	173.47	.668	.856	12.13

TEST 151 11-FOOT ROTOR

RUN 35 μ = .72 $M_{(1.0, 90)}$ = .91 RPM = 466 θ_1 = 0°

PT	ALPHA	THETAO	CQ/SIG	CLP/SIG	CDP/SIG	VFS	V/OMR	M TIP	B1
793	.09	3.54	.001971	.015183	.004370	192.02	.715	.910	4.41
794	.09	6.73	.002686	.029480	.006183	191.41	.713	.909	7.96
795	.10	8.26	.003147	.033143	.007211	191.42	.713	.909	8.88
796	5.09	-1.25	.000191	.033791	.007627	192.85	.719	.911	2.96
797	5.08	1.02	.000184	.042219	.008375	191.80	.715	.909	4.78
798	5.08	3.10	.000809	.052074	.009340	191.98	.715	.909	7.39
799	-4.91	12.89	.004022	.006435	.009408	191.72	.714	.912	10.34
800	-4.91	15.86	.006126	.019441	.010923	191.81	.715	.912	13.07
801	-4.89	14.34	.005039	.013030	.010082	191.92	.715	.911	12.89

TEST 151 11-FOOT ROTOR

RUN 36 μ = .72 $M_{(1.0, 90)}$ = .96 RPM = 493 θ_1 = 0°

PT	ALPHA	THETAO	CJ/SIG	CLP/SIG	CDP/SIG	VFS	V/OMR	M TIP	B1
802	-.06	3.74	.002638	.013394	.005747	4.01	.718	.966	5.10
803	-.07	7.03	.003398	.027340	.008116	03.59	.717	.965	8.80
804	-.06	10.96	.005243	.037917	.010347	203.56	.717	.965	12.43

TEST 151 11-FOOT ROTOR

RUN 361 μ = .65 $M_{(1.0, 90)}$ = .93 RPM = 493 θ_1 = 0°

PT	ALPHA	THETAO	CJ/SIG	CLP/SIG	CDP/SIG	VFS	V/OMR	M TIP	B1
807	-.03	3.59	.002231	.015904	.004247	190.95	.672	.945	4.84
808	-.02	5.35	.002803	.028758	.005410	189.92	.669	.943	7.53
809	-.01	9.95	.004625	.041587	.006783	189.31	.667	.942	11.04
810	-5.00	11.27	.003948	.006520	.006954	189.99	.669	.943	9.02
811	-4.98	12.89	.005418	.019336	.005577	184.98	.651	.934	11.08
812	-4.97	13.13	.005507	.018465	.006357	187.43	.660	.939	12.17
813	-4.97	15.46	.008164	.031455	.005674	184.08	.648	.932	13.06
814	5.14	-1.05	.000212	.031509	.006707	182.95	.644	.930	3.18
815	5.14	2.05	.000377	.043681	.007461	183.00	.644	.930	5.64
816	5.13	3.31	.001284	.056634	.008525	181.34	.639	.926	8.07
817	5.14	5.12	.002382	.064106	.009063	178.28	.628	.920	9.46

TEST 151 11-FOOT ROTOR

RUN 37 μ = .70 $M_{(1.0, 90)}$ = .86 RPM = 442 θ_1 = 0°

PT	ALPHA	THETA0	CQ/SIG	CLP/SIG	CDP/SIG	VFS	V/OMR	M TIP	B1
818	5.16	-1.24	.000110	.036937	.008221	193.11	.759	.890	3.14
819	5.15	4.34	.001456	.061095	.009229	174.76	.686	.853	8.80
820	.09	4.02	.002076	.021420	.003964	175.31	.689	.854	5.40
821	.10	9.16	.003582	.037447	.006073	175.47	.689	.855	9.47
822	.10	10.61	.004525	.043179	.007612	179.77	.706	.863	11.08
823	-4.79	12.15	.003968	.007306	.006847	175.60	.690	.855	9.53
824	-4.79	14.24	.005895	.020293	.007302	174.28	.685	.852	11.91
825	-4.79	14.31	.005780	.019311	.006893	174.87	.687	.853	12.93

TEST 151 11-FOOT ROTOR

RUN 38 μ = .73 $M_{(1.0, 90)}$ = .92 RPM = 468 θ_1 = 0°

PT	ALPHA	THETA0	CQ/SIG	CLP/SIG	CDP/SIG	VFS	V/OMR	M TIP	B1
826	-4.81	13.47	.004155	.002744	.011963	198.10	.735	.929	11.70
827	-4.82	15.54	.005329	.011880	.014270	200.16	.743	.934	13.05
828	.05	3.79	.002072	.018176	.005339	197.45	.733	.928	5.38
829	.05	9.09	.003570	.033883	.008210	195.02	.724	.923	9.93
830	4.92	-.23	.000275	.039526	.008052	192.72	.715	.919	4.34
831	4.93	2.95	.000863	.054469	.009696	192.06	.713	.917	7.52
832	4.93	3.92	.001076	.058134	.010366	193.10	.716	.919	8.94

TEST 151 11-FOOT ROTOR

RUN 39 μ = .44 $M_{(1.0, 90)}$ = .62 RPM = 375 θ_1 = 0°

PT	ALPHA	THETAO	CQ/SIG	CLP/SIG	CDP/SIG	VFS	V/OMR	M TIP	BI
833	-.02	3.92	.002398	.044756	.001928	96.40	.445	.622	5.25
834	-.01	11.14	.008237	.085795	-.001380	94.30	.437	.618	10.92
835	-4.99	9.06	.004610	.040860	-.001996	93.82	.434	.617	5.70
836	-4.98	11.65	.007544	.062537	-.004911	93.06	.431	.616	9.21
837	-4.97	11.65	.007535	.062524	-.005233	92.81	.430	.615	10.41
838	-10.03	12.54	.007247	.043879	-.006229	93.63	.434	.617	8.12
839	-10.05	15.48	.011626	.063149	-.010987	94.79	.439	.620	11.16
840	5.12	1.42	.000144	.046852	.006775	95.94	.444	.622	3.87
841	5.11	3.19	.000822	.068569	.008401	95.95	.444	.622	5.41
842	5.13	7.66	.003721	.089692	.008038	96.20	.445	.622	9.27

TEST 151 11-FOOT ROTOR

RUN 40 μ = .61 $M_{(1.0, 90)}$ = .54 RPM = 294 θ_1 = 0°

PT	ALPHA	THETAO	CQ/SIG	CLP/SIG	CDP/SIG	VFS	V/OMR	M TIP	BI
843	5.12	5.93	.002444	.073072	.005952	91.30	.539	.519	8.77
846	.03	5.81	.002496	.033145	.001133	103.17	.609	.543	7.03
847	.04	13.46	.009751	.070125	.000484	103.66	.612	.544	13.06
848	-4.92	13.06	.005940	.027893	-.000328	103.93	.614	.545	10.95
849	-4.92	16.53	.011127	.049917	-.002508	103.47	.611	.544	13.07
850	5.13	5.79	.001972	.067644	.005748	103.40	.611	.544	8.98
851	5.13	10.80	.007906	.088168	.005585	103.30	.610	.544	13.06
852	5.13	.16	.000117	.034839	.003919	103.19	.609	.544	3.22

TEST 151 11-FOOT ROTOR

RUN 41 μ = .83 $M_{(1.0, 90)}$ = .47 RPM = 224 θ_1 = 0°

PT	ALPHA	THETAO	CQ/SIG	CLP/SIG	CDP/SIG	VFS	V/OMR	M TIP	B1
853	5.13	6.82	.003225	.051992	.006769	107.56	.834	.473	11.11
854	.06	11.70	.004003	.021897	.007642	107.68	.835	.473	12.23

TEST 151 11-FOOT ROTOR

RUN 42 μ = .35 $M_{(1.0, 90)}$ = .82 RPM = 528 θ_1 = 0°

PT	ALPHA	THETAO	CQ/SIG	CLP/SIG	CDP/SIG	VFS	V/OMR	M TIP	B1
855	.06	5.45	.002725	.064974	.000261	105.10	.346	.817	5.25
856	.07	7.30	.003743	.064468	-.002371	105.69	.348	.818	7.48
857	.07	8.80	.004905	.064928	-.004847	106.15	.349	.819	9.77
858	.07	10.18	.006627	.065650	-.008442	105.92	.348	.819	12.09

Unclassified

Security Classification

DOCUMENT CONTROL DATA - R & D

(Security classification of title, body of abstract and indexing annotation must be entered when the overall report is classified)

1. ORIGINATING ACTIVITY *(Corporate author)*

Bell Helicopter Company
Fort Worth, Texas

2a. REPORT SECURITY CLASSIFICATION

Unclassified

2b. GROUP

3. REPORT TITLE

WIND-TUNNEL INVESTIGATION OF A QUARTER-SCALE TWO-BLADED HIGH-PERFORMANCE ROTOR IN A FREON ATMOSPHERE

4. DESCRIPTIVE NOTES *(Type of report and inclusive dates)*

Final Technical Report

5. AUTHOR(S) *(First name, middle initial, last name)*

Charles D. Lee
Bruce D. Charles
David L. Kidd

6. REPORT DATE	7a. TOTAL NO. OF PAGES	7b. NO. OF REFS
February 1971	168	10

8a. CONTRACT OR GRANT NO.	9a. ORIGINATOR'S REPORT NUMBER(S)
DA 44-177-AMC-292(T)	USAAVLABS Technical Report 70-58
b. PROJECT NO. Task 1F162204A13903	
c.	9b. OTHER REPORT NO(S) *(Any other numbers that may be assigned this report)*
d.	BHC Report 575-099-004

10. DISTRIBUTION STATEMENT

This document is subj[ect to] Approved for public release; distribution unlimited each transmittal to foreign governments or foreig[n] prior approval of Eustis Directorate, U.S. Arr[y] Air Mobility R&D Laboratory, Fort Eustis, Virginia 23604.

11. SUPPLEMENTARY NOTES	12. SPONSORING MILITARY ACTIVITY
	Eustis Directorate U.S. Army Air Mobility R&D Laboratory Fort Eustis, Virginia

13. ABSTRACT

A joint USAAVLABS/NASA-Langley/Bell Helicopter Company experimental investigation of a quarter-scale two-bladed teetering rotor system was conducted in the NASA-Langley Transonic Dynamics Tunnel using Freon as a test medium. Rotors tested were a dynamically similar Bell 540 rotor having -10-degree twist, and a thin-tipped rotor having 0-degree twist. Aerodynamic and loads data were obtained at advance ratios from 0.30 to 0.72 in combination with advancing-tip Mach numbers varying from 0.70 to 0.96. These data were compared to full-scale data and theory. In general, the aerodynamic test data followed predicted trends and correlated well with full-scale tunnel data in the area of low blade loading at low advance ratio and low advancing-tip Mach numbers. The blade loads data followed the expected trends, but their magnitudes could not be readily compared to existing flight test data due to the differences between the flight test conditions, model test conditions attained, and hub impedance differences.

DD FORM 1 NOV 68 1473 REPLACES DD FORM 1473, 1 JAN 64, WHICH IS OBSOLETE FOR ARMY USE.

Unclassified

Security Classification

14. KEY WORDS	LINK A		LINK B		LINK C	
	ROLE	WT	ROLE	WT	ROLE	WT
Freon Tests Rotor Performance Rotor Loads High-Advance Ratio High Advancing-Tip Mach Number Thin-Tipped Main Rotor Blades						